UNIVERSITY OF STRATHCLYDE
DEPARTMENT OF ELECTRONIC AND ELECTRICAL ENGINEERING

PRECODING AND EQUALISATION FOR BROADBAND MIMO SYSTEMS

by

Chi Hieu Ta

A thesis submitted in fulfilment
of the requirements for the degree of
Doctor of Philosophy

Supervisor: Dr. Stephan Weiss
Reader in Communications and Signal Processing

2008

COPYRIGHT STATEMENT

Abstract

Joint precoding and equalisation can help to effectively exploit the advantages of multi-input multi-output (MIMO) wireless communications systems. For broadband MIMO channels with channel state information (CSI) such techniques to date generally rely on block transmission where guard intervals are applied to mitigate inter-block (IBI) and inter-symbol interference (ISI) but reduce spectral efficiency. Therefore, this thesis investigates novel MIMO transceiver designs to improve the transmission rate and error performance.

Firstly, a broadband MIMO precoding and equalisation design is proposed which combines a recently proposed broadband singular value decomposition (BSVD) algorithm for MIMO decoupling with conventional block transmission techniques to address the remaining broadband SISO subchannels. It is demonstrated that the BSVD not only helps to remove co-channel interference within a MIMO channel, but also reduces ISI at a very small loss in channel energy, leading to an improved error performance and transmission rate.

Secondly, a design for jointly optimal precoding and block decision feedback equalisation (BDFE) that can operate at low redundancy is proposed and demonstrated to outperform existing similar design approaches.

Thirdly, an approach to improve error performance in block transmission systems is proposed. This approach involves a modification of the precoder and an elimination of IBI either by sharing the guard interval between transmitter and receiver or by employing a BDFE.

Lastly, in order to assess the proposed BSVD methods in more realistic communications scenarios, an order reduction of matrices within the BSVD is proposed in order to contain the system complexity. It is shown that the introduced error can be controlled and confined below a pre-set threshold. The effect of such an error — which can also arise from non-perfect CSI — on the BSVD-based system design is investigated. Simulation results show that the proposed BSVD-based designs are more robust to estimation or truncation errors than state-of-the-art block-based transmission system.

Acknowledgements

First and foremost, I would like to express my sincere gratitude to my supervisor, Dr. Stephan Weiss for his excellent guidance, outstanding support and constant encouragement throughout my PhD study. Without his exceptional contributions and invaluable advices, this work would not have been completed.

I would like to express my special thank to Prof. Jonathon A. Chambers for his valuable discussion at the DSP 2007 conference and for his willingness to act as my external examiner.

More thanks go to my colleagues and friends in the Institute for Communications and Signal Processing; Chunguang Liu, Adel Daas, Samir Bendoukhar, Muhammad Zeeshan Shakir. It was delightful to share the ideas with them and have fun together during conference trips.

I would like to acknowledge the financial support of the Ministry of Education and Training of Vietnam. This scholarship provided me a precious chance to pursue my PhD in the United Kingdom. I am grateful to the Institute for Communications and Signal Processing and the Electronic and Electrical Engineering Department at the University of Strathclyde for their supplemental financial support in terms of bursaries.

A special thank goes to my wife, Ngo Cam Thanh, who sacrificed a lot taking care of the family and looking after our two sons while I am away for my study. I am also thankful to my sons, Ta Nhat Anh and Ta Nhat Minh, for being my source of joy and encouragement.

Finally, I wish to express my gratitude to my parents, my mother-in-law and all family members for their love and constant support. I could not have been where I am today without their love and encouragement.

List of Publications

Publications Directly Related to the Thesis

1. **Chi Hieu Ta and Stephan Weiss**, "Design of Precoding and Equalization for Broadband MIMO Transmission," *2nd IEE/EURASIP Conference on DSPenabledRadio*, Southampton, UK, September, 2005.

2. **Chi Hieu Ta and Stephan Weiss**, "A Design of Precoding and Equalisation for Broadband MIMO Systems," *15th International Conference on Digital Signal Processing*, Cardiff, UK, July, 2007.

3. **Chi Hieu Ta and Stephan Weiss**, "A Jointly Optimal Precoder and Block Decision Feedback Equaliser Design with Low Redundancy," *15th European Signal Processing Conference (EUSIPCO)*, Poznan, Poland, September, 2007.

4. **Chi Hieu Ta and Stephan Weiss**, "A Design of Precoding and Equalisation for Broadband MIMO Systems," *41st Asilomar Conference on Signals, Systems, and Computers*, Pacific Grove, CA, November, 2007.

5. **Chi Hieu Ta and Stephan Weiss**, "Shortening the Order of Paraunitary Matrices in SBR2 Algorithm," *6th International Conference on Information, Communications & Signal Processing*, Singapore, December, 2007.

6. **Chi Hieu Ta, Chunguang Liu and Stephan Weiss**, "An Approach for Block Transmission based Precoding and Equalisation with Improved Perfor-

mance," *12th IEEE International Symposium on Power Line Communications and Its Applications (ISPLC)*, Jeju, Korea, April, 2008.

Other Publications

1. **Chunguang Liu, Chi Hieu Ta, Mahmoud Hadef and Stephan Weiss**, "A Coding and Equalisation Approach for Dispersive Channels with Structured Additive Noise," *2nd IEE/EURASIP Conference on DSPenabledRadio*, Southampton, UK, September, 2005.

2. **Chunguang Liu, Chi Hieu Ta and Stephan Weiss**, "A Precoding and Equalisation Design Based on Oversampled Filter Banks for Dispersive Channels with Correlated Noise," *41st Asilomar Conference on Signals, Systems, and Computers*, Pacific Grove, CA, November, 2006.

3. **Stephan Weiss, Chi Hieu Ta and Chunguang Liu**, "A Wiener Filter Approach to the Design of Filter Bank Based Single-Carrier Precoding and Equalisation," *11th IEEE International Symposium on Power Line Communications and Its Applications (ISPLC)*, Pisa, Italy, March, 2007.

4. **Chunguang Liu, Chi Hieu Ta and Stephan Weiss**, "A Precoding and Equalisation Design Based on Oversampled Filter Banks for Dispersive Channels with Correlated Noise," *15th European Signal Processing Conference (EUSIPCO)*, Poznan, Poland, September, 2007.

5. **Chunguang Liu, Chi Hieu Ta and Stephan Weiss**, "Joint Precoding and Equalisation Design using Oversampled Filter Banks for Dispersive Channels with Correlated Noise," *IEEE Workshop on Signal Processing Systems*, Shanghai, China, October, 2007.

6. **Waleed Al-Hanafy, Andrew Millar, Chi Hieu Ta and Stephan Weiss**, "Broadband SVD and Non-Linear Precoding and Equalisation Applied to

Broadband MIMO Channels," accepted for *42nd Asilomar Conference on Signals, Systems, and Computers*, Pacific Grove, CA, October, 2008.

Contents

Chapter 1

Introduction

1.1 Motivation

Recent years have witnessed a substantial growth of wireless communication systems. Today one can see systems such as cellular mobile networks, wireless local area networks, wireless metropolitan area networks being deployed throughout the world. By the end of 2007, the total number of mobile subscribers in the world had reached 3.3 billions, which is half of the world's population [1]. The revolution in wireless communication has been fuelled by two main factors [2], the significant progress in semiconductor technologies and the advances in digital communications. These factors allow mobile terminals to have much smaller size and more functions than just a voice call. They also help to reduce the cost of a handset and the system as a whole. This in turn has boosted the number of mobile users as people now can call from almost anywhere at an often reasonable price. In order to provide more high quality services to users and therefore attract more people to mobile services and increase the market share, the manufacturers now are focusing on the development of systems that can provide high quality multimedia services and can even allow the communication between human and machines over wireless channels. These services are known to require very high data rates and thus contributing to the development

of wireless systems and devices that can provide high data rate at low cost is a major focus of the manufacturers.

There exists, however, a contradiction between the growing demand for high data rate wireless services and the scarcity of the available radio spectrum. High data rate services are known to require high bandwidth and high link reliability, while the electromagnetic spectrum available for wireless communication is limited. Therefore, spectral efficiency is of primary concern in the design of future wireless communication systems.

In addition to the spectral scarcity, the transmit power needs to be constrained in order to extend battery life, limit concerns about harmful influence to human health and reduce interference to other users. Paulraj [3] identifies the limited average Signal-to-Interference-and-Noise-Ratio (SINR) in practical receivers of less then 35 dB have as an obstacle that makes it generally impossible to implement Non-Line-of-Sight (NLOS) wireless links that can provide data rates of 1 Gbit/s and beyond based on using only conventional approaches [3].

A very promising method to increase capacity and link reliability of wireless communications systems without bandwidth expansion is to exploit the spatial diversity in a wireless system. In current cellular systems, frequency reuse and cell sectorization can be considered as a simple method to exploit spatial diversity. The use of multiple antennas, especially adaptive antenna arrays or smart antennas, is considered an active and more effective way to exploit spatial diversity. In many scenarios, multiple antennas are exploited on either receiver or transmitter side to combat fading, delay spread and co-channel interference (CCI) [4, 5, 6, 7, 8, 9].

In the case where multiple antennas are used at both sides of the link, a multiple input multiple output (MIMO) channel arises. MIMO channels have a number of potential advantages over single-input single-output (SISO) channels such as array gain, diversity gain, multiplexing gain and interference reduction capability [3, 10].

Array gain is the improvement in average receive Signal-to-Noise ratio (SNR)

obtained by coherently combining the signals on transmit and receive arrays. Whether the maximum array gain at the transmitter and receiver can be realised or not depends on the availability of the channel status information (CSI) at the transmitter and receiver, respectively. The transmit/receive array gain also depends on the number of transmit and receive antennas.

Diversity gain is the improvement in the link reliability resulting from transmission of the same information over independently fading paths or dimensions. The purpose of this transmission is to ensure with high probability that at least one or more paths will not be in a fade at any given time instance. Thus the diversity gain will result in smaller fluctuation of the received signal power. Some forms of diversity that are exploited in wireless communications systems are temporal diversity, frequency diversity and spatial diversity. Among these forms, the spatial diversity is the most preferred as it does not require extra bandwidth or transmission time.

Multiplexing gain is the improvement in the capacity of a MIMO channel obtained from the use of multiple antennas at both sides of the link. The exploitation of multiple antennas at both transmitter and receiver sides in conjunction with a richly scattering propagation environment helps to create several parallel subchannels, which also are referred to as channel eigenmodes, within a MIMO channel. This leads to a capacity that linearly increases with the number of transmit or receive antennas — whichever is the smaller — with out any requirement for extra bandwidth or transmit power. Note that while the array gain and diversity gain can be obtained when multiple antennas are used at either transmit or receive side, multiplexing gain can only be exploited in MIMO channels where multiple antennas are used at both sides of the link.

The above mentioned advantages lead to significant improvements in terms of *spectral efficiency* and *link reliability* which in turn have made MIMO technology an exciting component of future wireless communications systems that can provide data rates claimed to be potentially as high as 1 Gbit/s [3], 2.5 Gbit/s [11] or even 5 Gbit/s [12].

To exploit the above mentioned leverages of MIMO channels, different approaches to signal processing for MIMO communications have been proposed. They can be generally divided into two groups, which either maximise the diversity gain or the multiplexing gain.

Approaches to maximise the diversity gain aim to perform transmission of a single data stream, as in a SISO system but at an increased SNR. Such approaches usually involve an appropriate combining of the received signals, such as selection combining, maximal ratio combining and equal-gain combining (see, for example [13]), and require the knowledge of the CSI at the receiver (CSIR). In the case that CSI is available at the transmitter (CSIT), approaches to achieve the transmit diversity involve the transmission of judiciously weighted signals from different transmit antennas such that they arrive in phase at the receive antenna, which can be accomplished by, for example, beamsteering at the transmitter [14, 15]. In case the CSI is not known at the transmitter, space-time coding approaches can be applied. The two main coding techniques are space-time trellis coding (STTC) [9] and space-time block coding (STBC) [8, 16]. The STTC can provide not only full diversity gain, but also coding gain [17], however it requires a multidimentional Viterbi algorithm for decoding and thus the complexity of the decoder increases exponentially with the diversity level and transmission rate [18]. STBC was proposed to address the drawback of STTC; it is based on the transmission of orthogonal vectors and therefore the decoder can use a simple maximum likelihood algorithm based on only linear processing at the receiver. STBC can provide full diversity gain, however it does not provide coding gain [17]. STBC also suffers from a loss in capacity when the number of receive antennas is greater than one [19, 17].

Approaches that aim to maximise the multiplexing gain increase the transmission rate by transmitting independent streams of information over multiple parallel subchannels within a MIMO channel. In the case of no CSIT, the input data stream is demultiplexed into independent substreams, which are passed to the various antennas. At the receiver, the individual symbol streams can be separated and detected by

different types of receivers, such as maximum-likelihood (ML) or near ML receivers [3, 20], linear receivers with ML detection [3], successive cancellation receiver [21], or ordered successive cancellation or Vertical Bell Labs Space-Time (V-BLAST) receivers [22, 23]. In case CSIT is available, spatial multiplexing is often performed by a precoder. Precoding helps to significantly improve the system performance and reduce the receiver complexity. An attractive approach to exploit CSI when both CSIT and CSIR are available is the joint transmit and receive processing, which will be referred hereafter as joint precoding and equalisation. In a number of designs proposed in the literature, joint precoding and equalisation is based on the standard singular value decomposition (SVD) to decompose a MIMO channel into a number of independent subchannels. Thereafter joint optimal precoders and equalisers are designed under different criteria, such as to minimise the system mean square error (MSE) [24, 25], maximise the receive SNR [26], maximise the information rate [27] or minimise the system bit-error-rate (BER) [28, 29]. Another approach is based on equal diagonal QR decomposition [30] or geometric mean decomposition [31] of the channel matrix where a linear precoder can be used in combination with an ML detector, V-BLAST receiver or can be jointly designed with a decision-feedback equaliser [32].

One can see that a large number of contributions in the literature focus on frequency-flat or narrowband MIMO channels where the standard SVD or QR decompositions can be appied directly and offer optimality in various respects [33]. For the broadband case, due to the frequency selectivity of the channel one cannot apply the SVD and QR decomposition directly. A straightforward and quite popular approach is to apply Orthogonal Frequency-Division Multiplexing (OFDM) [10] or block transmission schemes [25] where the guard intervals in the form of cyclic-prefix or zero-padding intervals are used to remove the effect of channel frequency selectivity and render the channel back to flat form such that the optimisation techniques for flat MIMO channels can be applied. The use of guard intervals in OFDM or block transmission systems restricts the spectral efficiency and therefore limits

the performance of the system [1]. Especially when the length of input block or the number of subcarriers is not much higher than the channel order.

Therefore, this thesis will focus on maximising the multiplexing gain in case of broadband MIMO channels by proposing joint precoding and equalisation approaches that can to a certain extent avoid the drawback of spectral inefficiency found in block transmission systems and therefore can exploit the channel more efficiently, leading to an improvement in multiplexing gain or BER performance.

1.2 Thesis Contributions

The following contributions contained in this thesis are believed to be novel:

- **Joint precoding and equalisation design for broadband MIMO with improved performance [34, 35, 36]**

  To reduce the effect of the guard periods on the spectral efficiency an approach to joint precoding and equalisation that contains two steps has been proposed. In a first step, with the help of a broadband singular value decomposition (BSVD) algorithm a pair of precoders and equalisers which decompose the original broadband MIMO channel into a number of independent frequency selective (FS) SISO subchannels was designed. Due to the spectral majorisation property of the BSVD algorithm, some of the resulting subchannels are less dynamic and have much higher gain than the remaining subchannels. In a second step, standard approaches for joint precoding and equalisation for FS SISO channels are applied to the decoupled subchannels resulting from the previous step. A water-filling algorithm can be performed over all the SISO subchannels in order to maximise the channel capacity. In this process, subchannels that are highly frequency selective and have low gains are discarded,

[1] It is appreciated that in, for example, IEEE 802.11x with 1024 subcarriers and cyclic prefix length of 10, spectral efficiency is not a problem.

which can be considered to be equivalent to a removal of a part of the ISI in the original MIMO channel at a very small loss in channel power gain or channel energy. Also, since the SISO subchannels that are used for transmission are less dynamic and have low order, more transmit power can be directed to the strong eigenmodes of the channel. These factors lead to improvement in system BER performance and data throughput.

The use of the BSVD to decompose broadband MIMO channels has been initially proposed in [34], in [36] the BSVD is combined with linear precoding and equalisation approaches for SISO subchannels and in [35] the BSVD is combined with a nonlinear joint precoding and equalisation method.

- **Joint optimal precoding and block decision feedback equalisation (BDFE) design with low redundancy [37]**

  The use of guard intervals makes it difficult for block transmission to be applied to channels with long impulse responses. Therefore a joint optimal precoding and block decision feedback equalisation (BDFE) design with low redundancy is proposed. This approach is based on two reported ideas, one for interblock interference (IBI) elimination and the other for joint optimal precoding and BDFE for flat MIMO channels. The proposed design can work with low redundancy by relying on guard intervals that are shorter than the channel order. The design is shown to outperform the analogous state-of-the-art designs.

- **Block transmission based precoding and equalisation design with improved performance [38]**

  Further, the thesis focuses on the system performance rather than on the redundancy and analyses the loss in channel energy caused by the guard interval in block transmission methods. Several designs that can exploit channel energy more efficiently and therefore can provide a better BER performance than the conventional block transmission based designs under the same code rate are proposed. These designs can work for both frequency selective SISO

and MIMO channels. One of the proposed designs is also extended to the broadband MIMO case both directly and in combination with BSVD and the performance of the two designs is compared.

- **Reduction the order of paraunitary matrices in the SBR2 algorithm [39]**

  The algorithm for BSVD computation, which is also referred to as second order sequential best rotation (SBR2) algorithm, results in paraunitary matrices of rather high order. This reduces the applicability of the BSVD in communications. An approach to reduce the order of the paraunitary matrices produced by the SBR2 algorithm is proposed. Simulation results show that the proposed approach can help to significantly reduce the order of the paraunitary matrices at very low loss in their paraunitarity by introducing a low and controllable deviation from paraunitarity. This helps to greatly simplify the design of the precoders and equalisers that are required to decompose broadband MIMO channels.

  The convergence of SBR2 when the matrix being diagonalised is based on pseudo-circulant matrices is also investigated. The simulation results show that in such cases SBR2 converges much slower than in the case of non-circulant matrices, which has important ramifications for selecting time-multiplexing as a technique to increase the number of virtual MIMO subchannels.

- **Evaluation of the effect of non-perfect CSI on BSVD based design**

  In practical systems, it is difficult to obtain perfect CSI. Therefore the evaluation of the effect of non-perfect CSI on the performance of the BSVD based precoding and equalisation design is considered. The simulation results show that in case of small channel estimation errors the proposed BSVD based design is more robust than a bench-mark block transmission based design. However, in the presence of strong channel estimation errors, the robustness of the BSVD based design suffers and attains a performance comparable to

that of the block transmission based design.

1.3 Organisation of the Thesis

The remainder of the thesis is organised as follows:

- **Chapter 2** provides an overview of joint optimal precoding and equalisation for different channels including frequency selective SISO channel, narrowband point-to-multipoint MIMO channels and broadband MIMO channels.

- **Chapter 3** proposes a design for precoding and equalisation for broadband MIMO channels. The design is based on BSVD and standard joint optimal precoding and equalisation methods for SISO channels. First, the BSVD is applied to decompose the broadband MIMO channel into a number of time-dispersive SISO subchannels. Second, either linear or nonlinear precoding and equalisation schemes proposed in the literature are applied to the SISO subchannels mentioned above. The spectral majorisation property of BSVD is exploited by applying a water-filling algorithm to all the SISO subchannels. This helps to eliminiate part of the ISI in the original MIMO channel at a very low loss in channel power gain. Thus the loss caused by ISI elimination can be reduced. The simulation results show that compared with the block transmission based benchmark systems, the proposed design can achieve a better performance in terms of error probability, mutual information and data throughput.

- **Chapter 4** considers several designs of block based precoding and equalisation schemes. First, the design of joint optimal precoding and BDFE with low redundancy will be addressed. Based on a combination of two reported ideas, one on ISI removal with low redundancy, the other on joint optimal precoding and BDFE, an optimal precoding and equalisation scheme using guard intervals that are shorter than the channel order is proposed. Second, the loss in

channel power gain caused by the use of guard intervals in block transmission schemes is analised and several designs with improved performance are proposed. In these designs the input redundancy, which is the difference between the input block length and the transmit block length, is exploit in such a way that the loss in channel power gain can be reduced and the strong eigenmodes of the channel can be selected, leading to a higher performance compared with the standard block transmission designs. Third, one of the proposed designs is extended to the broadband MIMO scenario and the performance in two cases is compared. The first case is a stand-alone system using the proposed design, wherease the second case incorporates the BSVD for the decoupling of the MIMO subchannels.

- **Chapter 5** briefly describes the BEVD computation algorithm and proposes an approach to reduce the order of paraunitary matrices resulting from the algorithm. The evaluation of the influence of imperfect CSI to the performance of the design proposed in Chapter 3 is also given in this chapter.

- **Chapter 6** summarises the main results of the thesis and outlines proposed future research topics.

Chapter 2

Theoretical Background

In this chapter, some precoding and equalisation techniques proposed in the literature are discussed. They include joint precoding and equalisation for single input single output frequency selective channels, joint precoding and equalisation for narrowband MIMO systems and linear precoding for broadband MIMO channels.

2.1 Channel model

In the following, a general discrete-time noise free model of baseband MIMO system with T transmit and R receive antennas as shown in Figure 2.1 is considered. In general case, the channel can be considered to be frequency selective with finite impulse response (FIR). The channel transfer function $\mathbf{C}(z) \in \mathbb{C}^{R\times T}(z)$ can be written as

$$\mathbf{C}(z) = \sum_{l=0}^{L} \mathbf{C}[l]\ z^{-l} \tag{2.1}$$

The maximum support length of the channel impulse responses (CIRs) between each pair of transmit and receive antennas is $L+1$. The matrix $\mathbf{C}[l] \in \mathbb{C}^{R\times T}$ contains the lth time slice of these CIRs. In general case, it can be further assumed that each of the T MIMO inputs emerges from a time multiplex of P input lines. Similarly, each of the R outputs can be demultiplexed into P signals. With the input symbol

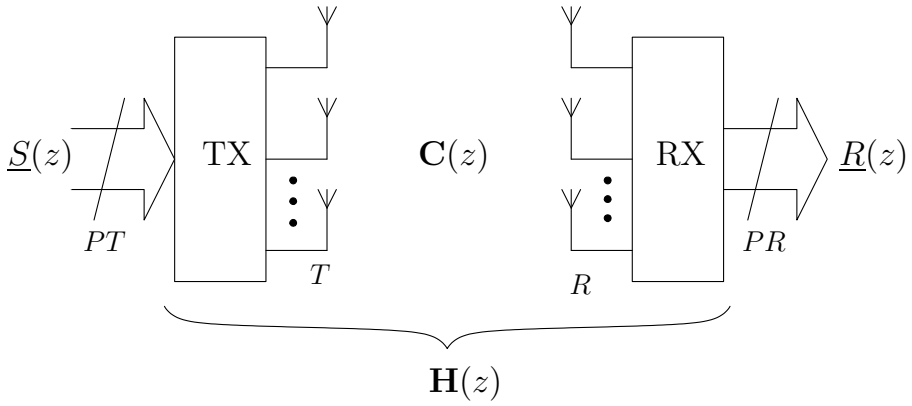

Figure 2.1: General MIMO channel model

vector $\boldsymbol{u}[n] \in \mathbb{C}^{PT}$ and output symbol vector $\boldsymbol{r}[n] \in \mathbb{C}^{PR}$ at discrete time instance n defined as

$$\boldsymbol{u}[n] := \begin{bmatrix} u_1[nP] \\ \vdots \\ u_T[nP] \\ u_1[nP+1] \\ \vdots \\ u_T[nP+1] \\ \vdots \\ u_1[nP+P-1] \\ \vdots \\ u_T[nP+P-1] \end{bmatrix}, \qquad \boldsymbol{r}[n] := \begin{bmatrix} r_1[nP] \\ \vdots \\ r_R[nP] \\ r_1[nP+1] \\ \vdots \\ r_R[nP+1] \\ \vdots \\ r_1[nP+P-1] \\ \vdots \\ r_R[nP+P-1] \end{bmatrix},$$

where $u_i[n],\ (i = \{1, \ldots, T\})$ is the signal sent to the ith transmit antenna and $r_j[n],\ (j = \{1, \ldots, R\})$ is the signal received on the jth receive antenna, the resulting spatio-temporal MIMO system can be written as

$$\underline{R}(z) = \mathbf{H}(z)\underline{U}(z)\ , \tag{2.2}$$

whereby $\underline{U}(z) \bullet\!\!-\!\!\circ\, \boldsymbol{u}[n]$, $\underline{R}(z) \bullet\!\!-\!\!\circ\, \boldsymbol{r}[n]$ and the spatio-temporal MIMO matrix takes the block-pseudo-circulant form

$$\mathbf{H}(z) = \begin{bmatrix} \mathbf{C}_0(z) & z^{-1}\mathbf{C}_{P-1}(z) & \cdots & z^{-1}\mathbf{C}_1(z) \\ \mathbf{C}_1(z) & \mathbf{C}_0(z) & \cdots & z^{-1}\mathbf{C}_2(z) \\ \vdots & & \ddots & \vdots \\ \mathbf{C}_{P-1}(z) & \mathbf{C}_{P-2}(z) & \cdots & \mathbf{C}_0(z) \end{bmatrix}. \tag{2.3}$$

The matrices $\mathbf{C}_p(z)$, $p = 0, 1, \ldots P-1$, are the P polyphase components of $\mathbf{C}(z)$ such that

$$\mathbf{C}(z) = \sum_{p=0}^{P-1} \mathbf{C}_p(z^P)\, z^{-p} \tag{2.4}$$

or alternatively $\mathbf{C}_p(z) = \sum_n \mathbf{C}[nP + p]\, z^{-n}$.

In the following, based on the above general channel model, several joint precoding and equalisation schemes will be reviewed.

2.2 Precoding and equalisation for SISO channels

In this section, a linear joint optimal precoding and equalisation design for block transmission over frequency selective channel, which was proposed in [26] by Scaglione *et al.* is discussed. Similar to other block transmission schemes, this approach also utilises transmit redundancy in the form of zero padding intervals to mitigate the inter-block interference (IBI) caused by the channel frequency selectivity, then the joint optimal precoder and equaliser filter banks are designed to remove the intrablock interference and combat noise. The optimal criteria are maximum output SNR (MaxSNR), minimum mean square error under constrained transmit power(MMSE/CP) [26] and maximum information rate (MaxIR) [27].

The discrete-time system model is illustrated in Figure 2.2. The channel in this case is a SISO frequency selective channel, corresponding to the model presented in Section 2.1 with $T = R = 1$.

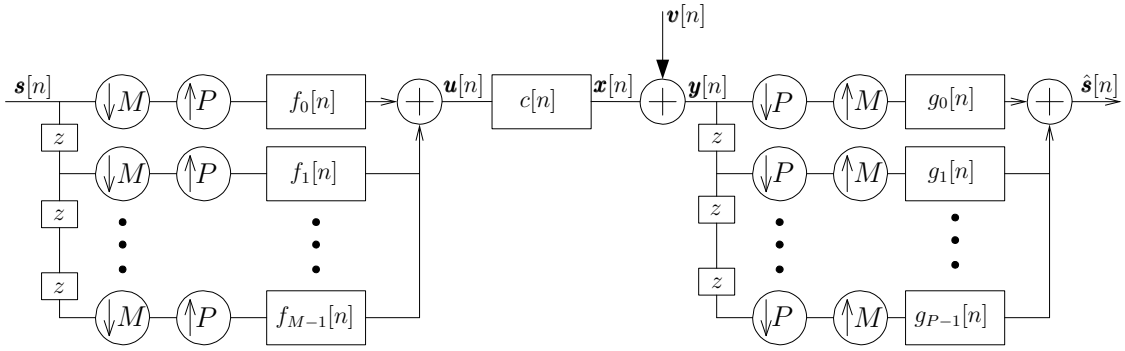

Figure 2.2: Precoding and equalisation for SISO frequency selective channel

The input symbol stream is converted into a sequence of blocks of size M. A guard interval is inserted to mitigate IBI through the upsamplers by P where $P > M$. Thus, the input blocks of size M are mapped into blocks of size P by the precoder filter bank. After being transmitted through frequency selective channel with impulse response $c[n]$, the received blocks of size P are mapped back to a sequence of blocks of size M by the equaliser filter bank. The input and output signal vectors are defined as

$$\boldsymbol{s}[n] := \begin{bmatrix} s[nM] \\ s[nM+1] \\ \vdots \\ s[nM+M-1] \end{bmatrix}, \qquad \hat{\boldsymbol{s}}[n] := \begin{bmatrix} \hat{s}[nM] \\ \hat{s}[nM+1] \\ \vdots \\ \hat{s}[nM+M-1] \end{bmatrix},$$

the output vector of the precoder and the noise-free output of the channel as

$$\boldsymbol{u}[n] := \begin{bmatrix} u[nP] \\ u[nP+1] \\ \vdots \\ u[nP+P-1] \end{bmatrix}, \qquad \boldsymbol{x}[n] := \begin{bmatrix} x[nP] \\ x[nP+1] \\ \vdots \\ x[nP+P-1] \end{bmatrix}$$

and the received vector with noise and the corresponding noise vector as

$$\boldsymbol{y}[n] := \begin{bmatrix} y[nP] \\ y[nP+1] \\ \vdots \\ y[nP+P-1] \end{bmatrix}, \qquad \boldsymbol{v}[n] := \begin{bmatrix} v[nP] \\ v[nP+1] \\ \vdots \\ v[nP+P-1] \end{bmatrix}.$$

In the general case where there is no constraint on the length of precoding filters, channel and equalisers, the relation between input and output vectors of precoder, equaliser and channel can be written as

$$\boldsymbol{u}[n] = \sum_{i=-\infty}^{\infty} \mathbf{F}_i \boldsymbol{s}[n-i] \tag{2.5}$$

$$\hat{\boldsymbol{s}}[n] = \sum_{j=-\infty}^{\infty} \mathbf{G}_j \boldsymbol{y}[n-j] \tag{2.6}$$

$$\boldsymbol{y}[n] = \sum_{l=-\infty}^{\infty} \mathbf{H}_l \boldsymbol{u}[n-l] + \boldsymbol{v}[n] \tag{2.7}$$

where

$$\mathbf{F}_i = \begin{bmatrix} f_0[iP] & f_1[iP] & \cdots & f_{M-1}[iP] \\ f_0[iP+1] & f_1[iP+1] & \cdots & f_{M-1}[iP+1] \\ \vdots & \vdots & \ddots & \vdots \\ f_0[iP+P-1] & f_1[iP+P-1] & \cdots & f_{M-1}[iP+P-1] \end{bmatrix} \tag{2.8}$$

$$\mathbf{G}_j = \begin{bmatrix} g_0[jM] & g_1[jM] & \cdots & g_{P-1}[jM] \\ g_0[jM+1] & g_1[jM+1] & \cdots & g_{P-1}[jM+1] \\ \vdots & \vdots & \ddots & \vdots \\ g_0[jM+M-1] & g_1[jM+M-1] & \cdots & g_{P-1}[jM+M-1] \end{bmatrix} \tag{2.9}$$

$$\mathbf{H}_l = \begin{bmatrix} c[lP] & \cdots & c[lP-P+1] \\ \vdots & \ddots & \vdots \\ c[lP+P-1] & \cdots & c[lP] \end{bmatrix} \tag{2.10}$$

The relation between input and output blocks of the system is therefore described by the following equation

$$\hat{\boldsymbol{s}}[n] = \sum_{j,l,i=-\infty}^{\infty} \mathbf{G}_j \mathbf{H}_l \mathbf{F}_i \boldsymbol{s}[n-l-i-j] + \sum_{j=-\infty}^{\infty} \mathbf{G}_j \boldsymbol{v}[n-j] \; . \tag{2.11}$$

With the following assumptions

1. The channel is of order L with the CIR $c[n] = \{c[0], ..., c[L]\}$; $(c[0], ..., c[L] \neq 0)$.
2. The parameters P, M, L are chosen so that $P = M + L$.
3. Transmit filters $\{f_m[n]\}_{m=0}^{M-1}$ are causal ($f_m[n] = 0$ for $n < 0$) and have maximal length of P ($f_m[n] = 0$ for $n > P$), and receive filters are causal and of length M. The matrix $\mathbf{F}_0$ is selected so that $\text{rank}(\mathbf{F}_0) = M$.

the matrix $\mathbf{H}_l$ now can be simplified to

$$\mathbf{H}_l = \mathbf{H}_0 \delta[l] + \mathbf{H}_1 \delta[l-1] \tag{2.12}$$

where

$$\mathbf{H}_0 = \begin{bmatrix} c[0] & 0 & 0 & \cdots & 0 \\ \vdots & c[0] & 0 & \cdots & 0 \\ c[L] & \cdots & \ddots & \cdots & \vdots \\ \vdots & \ddots & \cdots & \ddots & 0 \\ 0 & \cdots & c[L] & \cdots & c[0] \end{bmatrix} \tag{2.13}$$

$$\mathbf{H}_1 = \begin{bmatrix} 0 & \cdots & c[L] & \cdots & c[1] \\ \vdots & \ddots & 0 & \ddots & \vdots \\ 0 & \cdots & \ddots & \cdots & c[L] \\ \vdots & \vdots & \vdots & \ddots & \vdots \\ 0 & \cdots & 0 & \cdots & 0) \end{bmatrix} \; , \tag{2.14}$$

and the transmit and receive filter banks can be modeled as

$$\mathbf{F}_i = \mathbf{F}_0 \delta[i] \tag{2.15}$$

$$\mathbf{G}_j = \mathbf{G}_0 \delta[j] \; . \tag{2.16}$$

Compare with the general channel model in Section 2.1, one can see that the system being considered here is a specific case of the general model in Section 2.1 with $T = R = 1$ and the matrix $\mathbf{H}(z)$ is now given by $\mathbf{H}(z) = \mathbf{H}_0 + \mathbf{H}_1 z^{-1}$.

Equation (2.11) can be rewritten as

$$\hat{\boldsymbol{s}}[n] = \mathbf{G}_0\mathbf{H}_0\mathbf{F}_0\boldsymbol{s}[n] + \mathbf{G}_0\mathbf{H}_1\mathbf{F}_0\boldsymbol{s}[n-1] + \mathbf{G}_0\boldsymbol{v}[n] \; . \tag{2.17}$$

From equation (2.17) one can see that the term $\mathbf{G}_0\mathbf{H}_1\mathbf{F}_0\boldsymbol{s}[n-1]$ represents the IBI and therefore it is necessary to have $\mathbf{G}_0\mathbf{H}_1\mathbf{F}_0 = 0$. With the form of $\mathbf{H}_1$ in (2.14), this condition leads to the following two approaches.

(i) Set the last L components in the impulse responses of the transmit filters to be zero so that $\mathbf{F}_0 = (\mathbf{F}^{\mathrm{T}} \quad \mathbf{0})^{\mathrm{T}}$ where $\mathbf{F}$ is an $M \times M$ matrix and $\mathbf{0}$ is an $L \times M$ block of zeros. This approach is referred to as the *trailing zero* (TZ) approach.

(ii) Set the first L filters in the receive filter bank to be zero, so that $\mathbf{G}_0 = (\mathbf{0} \quad \mathbf{G})$ where $\mathbf{G}$ is an $M \times M$ matrix and $\mathbf{0}$ now is an $M \times L$ block of zeros. This approach is referred to as the *leading zero* (LZ) approach.

With TZ precoder or LZ equaliser, IBI can be eliminated and equation (2.17) is simplified to

$$\hat{\boldsymbol{s}}[n] = \mathbf{GHF}\boldsymbol{s}[n] + \mathbf{G}\boldsymbol{v}[n] \tag{2.18}$$

where in the TZ case $\mathbf{G} = \mathbf{G}_0$ and in the LZ case $\mathbf{F} = \mathbf{F}_0$. In the TZ case, $\mathbf{H}$ is a $P \times M$ matrix defined as

$$\mathbf{H} = \begin{bmatrix} c[0] & 0 & \cdots & 0 \\ \vdots & \ddots & \ddots & \vdots \\ c[L] & \ddots & \ddots & 0 \\ 0 & \ddots & \ddots & c[0] \\ \vdots & \ddots & \ddots & \vdots \\ 0 & \cdots & 0 & c[L] \end{bmatrix} \tag{2.19}$$

and in the LZ case, $\mathbf{H}$ is an $M \times P$ matrix defined as

$$\mathbf{H} = \begin{bmatrix} c[L] & \cdots & c[0] & 0 & \cdots & 0 \\ 0 & \ddots & \ddots & \ddots & \ddots & \vdots \\ \vdots & \ddots & \ddots & \ddots & \ddots & 0 \\ 0 & \cdots & 0 & c[L] & \cdots & c[0] \end{bmatrix} \tag{2.20}$$

After elimination of IBI by applying the TZ or LZ approach, the precoder and equaliser matrices are optimized further under several criteria, such as MaxSNR and MMSE/CP [26] or MaxIR [27]. Here, the input signal $\boldsymbol{s}[n]$ and the noise $\boldsymbol{v}[n]$ are assumed to be mutually uncorrelated, wide-sense stationary with known covariance matrices $\mathbf{R}_{ss}$ and $\mathbf{R}_{vv}$.

The optimal precoder and equaliser under MaxSNR criteria are designed to maximise the SNR at the equaliser output subject to zero-forcing (ZF) constraint $\mathbf{GHF} = \mathbf{I}$. The equaliser is derived as a function of the precoder matrix from the condition of maximising the output SNR, the precoder matrix is then calculated from the ZF constraint.

Based on the following eigendecompositions

$$\begin{aligned} \mathbf{R}_{ss} &= \mathbf{U}\boldsymbol{\Delta}\mathbf{U}^{\mathrm{H}} \\ \mathbf{H}^{\mathrm{H}}\mathbf{R}_{vv}^{-1}\mathbf{H} &= \begin{cases} \mathbf{V}\boldsymbol{\Lambda}\mathbf{V}^{\mathrm{H}} & \text{for TZ case} \\ (\mathbf{V}, \mathbf{V}_n) \begin{pmatrix} \boldsymbol{\Lambda} & \mathbf{0} \\ \mathbf{0} & \mathbf{0} \end{pmatrix} (\mathbf{V}, \mathbf{V_n})^{\mathrm{H}} & \text{for LZ case} \end{cases} \end{aligned} \tag{2.21}$$

where $\mathbf{U}, \mathbf{V}, \mathbf{V}_n$ are unitary matrices and $\boldsymbol{\Delta}, \boldsymbol{\Lambda}$ are diagonal matrices, the optimal precoder and equaliser under the MaxSNR criterion are given by [26]:

$$\begin{aligned} \mathbf{F}_{opt} &= \frac{\sqrt{\mathcal{K}}}{\sigma_v}\mathbf{V}\boldsymbol{\Lambda}^{-(1/2)} \\ \mathbf{G}_{opt} &= \sigma_v\sqrt{\mathcal{K}}\boldsymbol{\Lambda}^{-(1/2)}\mathbf{V}^{\mathrm{H}}\mathbf{H}^{\mathrm{H}}\mathbf{R}_{vv}^{-1} \end{aligned} \tag{2.22}$$

where $\mathcal{K}$ is defined as transmit-amplification gain and depends on the transmit power and σ_v^2 is the variance of noise.

In case the input signal is white with $\mathbf{R}_{ss} = \sigma_s^2\mathbf{I}$ and the transmit power is constrained to be P_0, $\mathcal{K}$ is given by [25]

$$\mathcal{K} = \frac{P_0\sigma_v}{\sigma_s \sum_i \lambda_{ii}^{-1}} \,. \tag{2.23}$$

Under the MMSE/CP criterion, the optimal precoder and equaliser pair is designed to minimise the arithmetic MSE of the system subject to constrained transmit power. Here the equaliser matrix is derived as the Wiener solution and the precoder requires a water-filling algorithm over diagonal elements of $\mathbf{\Lambda}$. The MMSE/CP optimal pair of precoder and equaliser is given by [26]

$$\mathbf{F}_{opt} = \mathbf{V}\mathbf{\Phi}\mathbf{U}^{\mathrm{H}} \tag{2.24}$$

$$\mathbf{G}_{opt} = \mathbf{R}_{ss}\mathbf{F}_{opt}^{\mathrm{H}}\mathbf{H}^{\mathrm{H}}(\mathbf{R}_{vv} + \mathbf{H}\mathbf{F}_{opt}\mathbf{R}_{ss}\mathbf{F}_{opt}^{\mathrm{H}}\mathbf{H}^{\mathrm{H}})^{-1} \tag{2.25}$$

where $\mathbf{\Phi}$ is a diagonal matrix with main diagonal elements obtained by a water-filling algorithm

$$|\phi_{ii}|^2 = \max\left(\frac{P_0 + \sum_{j=1}^{\bar{M}} \lambda_{jj}^{-1}}{\sum_{j=1}^{\bar{M}} (\delta_{jj}/\lambda_{jj})^{1/2}} \frac{1}{\sqrt{\lambda_{ii}\delta_{ii}}} - \frac{1}{\lambda_{ii}\delta_{ii}},\ 0\right). \tag{2.26}$$

For the MaxIR criteria [27], the precoder and equaliser pair is designed to maximise the mutual information between the input and the output signals. The optimal MaxIR precoder can be writen as in (2.24). The maximisation of mutual information is achieved by the power allocation according to a classical water-filling algorithm with single water level [40], which results in the main diagonal elements of $\mathbf{\Phi}$ as

$$|\phi_{ii}|^2 = \max\left(\frac{P_0 + \sum_{j=1}^{\bar{M}} \lambda_{jj}^{-1}}{\bar{M}\delta_{ii}} - \frac{1}{\lambda_{ii}\delta_{ii}},\ 0\right). \tag{2.27}$$

where in both MMSE/CP and MaxIR cases, $\bar{M}$ is the number of positive $|\phi_{ii}|^2$.

The optimal equaliser in this case can be derived under either ZF or MMSE criteria. Given the optimal precoder, the ZF equaliser can be writen as

$$\mathbf{G}_{opt} = \left(\mathbf{R}_{vv}^{-1/2}\mathbf{H}\mathbf{F}_{opt}\right)^{\dagger}\mathbf{R}_{vv}^{-1/2} \tag{2.28}$$

whereby $(.)^{\dagger}$ is the pseudo-inverse operation. The MMSE equaliser in this case has the same form as in (2.25).

The optimal precoder and equaliser pairs mentioned above render a frequency selective SISO channel into a number of flat subchannels. One should note that the water-filling algorithm for MMSE/CP design differs from the water-filling algorithm for MaxIR design. In the former, depending on the value of the water level, the transmit power allocated for each flat subchannel can be a convex function or monotonically decreasing function of λ_{ii} while in the later the transmit power allocated for each flat subchannel is always a monotonically increasing function of λ_{ii}.

2.3 Joint precoding and equalisation for narrowband MIMO systems

This section will discuss a joint precoding and equalisation design proposed in [41, 42] to mitigate multiuser interference (MUI) while maximising the system capacity or allowing power control in multiuser narrowband MIMO systems. The algorithm, which is referred to as block diagonalisation, is based on the SVD of the channel matrices, the precoder is designed to remove the inter-user interference and achieve maximum capacity or allow power control and the equaliser is designed to separate the individual data streams.

Consider a multiuser flat-fading MIMO system with a base station which has T transmit antennas and K users, each with R_i receive antennas. Let the total number of antennas of all receivers to be $R = \sum_{i=1}^{K} R_i$. The MIMO channel between the transmitter and the ith user is represented by matrix $\mathbf{H}_i \in \mathbb{C}^{R_i \times T}$. One can see that this MIMO system is a specific case of the system described in Section 2.1 with $L = 0$, $P = 1$ and $\mathbf{H}(z) = \mathbf{C}_0$ is actually a stacked version of all matrices $\mathbf{H}_i$. For simplicity, the matrix $\mathbf{H}(z)$ is written as $\mathbf{H}(z) = \mathbf{H}$. Let the precoding matrix associated with the ith user be denoted by $\mathbf{B}_i \in \mathbb{C}^{T \times m_i}$ where m_i is the length of the vector of symbols $\boldsymbol{s}_i[n]$ which is destined to this user. The input vector $\boldsymbol{s}_i[n]$

is linearly mapped by the precoder $\mathbf{B}_i$ to vector $\boldsymbol{u}_i[n]$ which is actually broadcast from the transmit antennas. At the input of the ith receiver, the received signal includes the contributions from the signals for all users as well as the noise and can be written as

$$\boldsymbol{y}_i[n] = \sum_{k=1}^{K} \mathbf{H}_i \mathbf{B}_k \boldsymbol{s}_k[n] + \boldsymbol{v}_i[n] \tag{2.29}$$

where $\boldsymbol{v}_i[n]$ denotes the spatially white noise and interference with covariance matrix $\mathcal{E}\{\boldsymbol{v}_i[n]\boldsymbol{v}_i^*[n]\} = \sigma_v^2\mathbf{I}$. To capture the operation of the whole system in matrix form, the received data from all of the receivers are stacked together and represented as

$$\begin{aligned} \boldsymbol{y}[n] &= \begin{bmatrix} \boldsymbol{y}_1[n] \\ \vdots \\ \boldsymbol{y}_K[n] \end{bmatrix} = \begin{bmatrix} \mathbf{H}_1 \\ \vdots \\ \mathbf{H}_K \end{bmatrix} \begin{bmatrix} \mathbf{B}_1 & \cdots & \mathbf{B}_K \end{bmatrix} \begin{bmatrix} \boldsymbol{s}_1[n] \\ \vdots \\ \boldsymbol{s}_K[n] \end{bmatrix} + \begin{bmatrix} \boldsymbol{v}_1[n] \\ \vdots \\ \boldsymbol{v}_K[n] \end{bmatrix} \\ &= \mathbf{HB}\, \boldsymbol{s}[n] + \boldsymbol{v}[n] \end{aligned} \tag{2.30}$$

where the definitions of $\boldsymbol{y}[n], \mathbf{H}, \mathbf{B}, \boldsymbol{s}[n]$ are clear from the equation.

In order to remove inter-user interference, the precoders are designed so that $\mathbf{H}_i\mathbf{B}_i \neq \mathbf{0}$ and $\mathbf{H}_j\mathbf{B}_i = \mathbf{0}$ for $j \neq i$. In other words, $\mathbf{HB}$ is a block-diagonal matrix. Define matrix $\hat{\mathbf{H}}_i \in \mathbb{C}^{(R-R_i)\times T}$ as follow

$$\hat{\mathbf{H}}_i = \left[\mathbf{H}_1^{\mathrm{T}} \cdots \mathbf{H}_{i-1}^{\mathrm{T}} \mathbf{H}_{i+1}^{\mathrm{T}} \cdots \mathbf{H}_K^{\mathrm{T}}\right]^{\mathrm{T}} \tag{2.31}$$

Assume $T > R$ and let $\mathrm{rank}(\hat{\mathbf{H}}_i) = L_i \leq (R - R_i)$, consider the following SVD

$$\hat{\mathbf{H}}_i = \hat{\mathbf{U}}_i\, \hat{\mathbf{\Sigma}}_i \begin{bmatrix} \hat{\mathbf{V}}_{i,1}^{\mathrm{H}} \\ \hat{\mathbf{V}}_{i,0}^{\mathrm{H}} \end{bmatrix} \tag{2.32}$$

where $\hat{\mathbf{V}}_{i,1}^{\mathrm{H}}$ contains the first L_i rows that correspond to the non-zero singular values of $\hat{\mathbf{H}}_i$ and $\hat{\mathbf{V}}_{i,0}^{\mathrm{H}}$ contains the last $T - L_i$ rows. It is clear that the columns of $\hat{\mathbf{V}}_{i,0}$ span the null space of $\hat{\mathbf{H}}_i$ ($\hat{\mathbf{H}}_i\hat{\mathbf{V}}_{i,0} = \mathbf{0}$). Thus, $\hat{\mathbf{V}}_{i,0}$ can help to eliminate MUI and therefore let $\mathbf{B}_i = \hat{\mathbf{V}}_{i,0}$, the precoder matrix $\mathbf{B}$ for all users can be written as

$$\mathbf{B} = \left[\hat{\mathbf{V}}_{1,0} \ \cdots \ \hat{\mathbf{V}}_{K,0}\right]. \tag{2.33}$$

The overall channel transfer matrix preprocessed by $\mathbf{B}$ now becomes

$$\mathbf{HB} = \begin{bmatrix} \mathbf{H}_i \\ \hat{\mathbf{H}}_i \end{bmatrix} \begin{bmatrix} \hat{\mathbf{V}}_{1,0} & \cdots & \hat{\mathbf{V}}_{K,0} \end{bmatrix} = \begin{bmatrix} \mathbf{H}_1\hat{\mathbf{V}}_{1,0} & & \mathbf{0} \\ & \ddots & \\ \mathbf{0} & & \mathbf{H}_K\hat{\mathbf{V}}_{K,0} \end{bmatrix}. \tag{2.34}$$

Further, let $L_i^{'} = \text{rank}(\mathbf{H}_i\hat{\mathbf{V}}_{i,0})$ and consider the SVD

$$\mathbf{H}_i\hat{\mathbf{V}}_{i,0} = \mathbf{U}_i \begin{bmatrix} \mathbf{\Sigma}_i & \mathbf{0} \\ \mathbf{0} & \mathbf{0} \end{bmatrix} \begin{bmatrix} \mathbf{V}_{i,1}^{\text{H}} \\ \mathbf{V}_{i,0}^{\text{H}} \end{bmatrix} \tag{2.35}$$

where $\mathbf{V}_{i,1}$ holds the first $L_i^{'}$ right singular vectors that correspond to the non-zero singular values in diagonal matrix $\mathbf{\Sigma}_i \in \mathbb{C}^{L_i^{'} \times L_i^{'}}$, one can see that

$$\mathbf{U}_i^{\text{H}}\mathbf{H}_i\hat{\mathbf{V}}_{i,0}\mathbf{V}_{i,1} = \mathbf{\Sigma}_i \, . \tag{2.36}$$

This motivates the use of an equaliser $\mathbf{W}_i = \mathbf{U}_i^{\text{H}}$ and setting the precoder as

$$\mathbf{B} = \begin{bmatrix} \hat{\mathbf{V}}_{1,0}\mathbf{V}_{1,1} & \hat{\mathbf{V}}_{2,0}\mathbf{V}_{2,1} & \cdots & \hat{\mathbf{V}}_{K,0}\mathbf{V}_{K,1} \end{bmatrix} \tag{2.37}$$

so that the product

$$\begin{bmatrix} \mathbf{W}_1 & & \mathbf{0} \\ & \ddots & \\ \mathbf{0} & & \mathbf{W}_K \end{bmatrix} \mathbf{HB} = \begin{bmatrix} \mathbf{\Sigma}_1 & & \mathbf{0} \\ & \ddots & \\ \mathbf{0} & & \mathbf{\Sigma}_K \end{bmatrix} \tag{2.38}$$

is a completely diagonal matrix, which means the MUI and the co-channel interference caused by MIMO components is completely eliminated. The overall operation of the system can be described through the following equation

$$\begin{aligned} \hat{\boldsymbol{s}}[n] &= \mathbf{WHB}\boldsymbol{s}[n] + \mathbf{W}\boldsymbol{v}[n] \\ &= \mathbf{\Sigma}\, \boldsymbol{s}[n] + \mathbf{W}\boldsymbol{v}[n] \end{aligned} \tag{2.39}$$

where $\mathbf{W} = \text{diag}\begin{pmatrix} \mathbf{U}_1^{\text{H}} & \cdots & \mathbf{U}_K^{\text{H}} \end{pmatrix}$, $\mathbf{\Sigma} = \text{diag}\begin{pmatrix} \mathbf{\Sigma}_1 & \cdots & \mathbf{\Sigma}_K \end{pmatrix}$ and $\hat{\boldsymbol{s}}[n] = [\hat{\boldsymbol{s}}_1^{\text{T}}[n] \cdots \hat{\boldsymbol{s}}_K^{\text{T}}[n]]^{\text{T}}$ with $\hat{\boldsymbol{s}}_i[n]$ the vector of estimated symbols at the output of equaliser $\mathbf{W}_i$.

In order to maximise the system capacity, a water-filling algorithm with single water level is performed on the diagonal elements of $\mathbf{\Sigma}$ so that the transmit power will be allocated accordingly. Thus the precoder $\mathbf{B}$ now becomes

$$\mathbf{B} = \left[\hat{\mathbf{V}}_{1,0}\mathbf{V}_{1,1} \quad \hat{\mathbf{V}}_{2,0}\mathbf{V}_{2,1} \ \cdots \ \hat{\mathbf{V}}_{K,0}\mathbf{V}_{K,1}\right] \mathbf{\Lambda}^{1/2} \, . \tag{2.40}$$

where $\mathbf{\Lambda}$ is a diagonal matrix with diagonal elements λ_{jj} obtained from the above mentioned water-filling algorithm.

The system capacity is given by [42]

$$C = \log_2 \left| \mathbf{I} + \frac{\mathbf{\Sigma}^2 \mathbf{\Lambda}}{\sigma_v^2} \right| . \tag{2.41}$$

With the precoder matrix defined as in equation (2.40), it can be seen that $m_i = L_i^{'}$ and therefore, it is necessary that $L_i^{'} \geq 1$ so that the transmission for the ith user can take place.

In the case of the power control problem where one have to minimise the transmit power subject to achieving a desired transmission rate for each user, the precoder and equaliser matrices can be derived in similar steps as mentioned above, except that the matrix $\mathbf{\Lambda}$ is defined by performing water-filling separately for each user, where the constrained transmit power for each user is scaled to achieve the required transmission rate.

From the SVD in (2.32), one can see that in order for $\hat{\mathbf{V}}_{i,0}$ to exist, it is required that

$$T > \max\{\text{rank}(\hat{\mathbf{H}}_1), \cdots, \text{rank}(\hat{\mathbf{H}}_K)\}. \tag{2.42}$$

This condition can be violated when $R > T$ and therefore, to loosen the constraint on the number of transmit antennas T, a coordinated transmit-receive beamforming approach was proposed [41, 42]. There the equalisers $\mathbf{W}_i$ were initially set to be the first m_i left singular vectors of $\mathbf{H}_i$, then the above algorithm is applied for matrices $\bar{\mathbf{H}}_i = \mathbf{W}_i^{\mathrm{H}} \mathbf{H}_i$ to yield $\mathbf{B}$ and new $\mathbf{W}_i$, finally the equaliser matrix is calculated as a product between the first m_i singular vectors of $\mathbf{H}_i$ with the new $\mathbf{W}_i$.

The new constraint on the number of transmit antennas now is

$$T \geq \sum_{i=1}^{K} m_i \ . \tag{2.43}$$

2.4 Linear precoding and equalisation for broadband MIMO systems

In this section, an approach for joint precoding and equalisation for frequency selective MIMO systems is discussed. This approach was proposed in [25] and similar to the one in [26], it is also based on block transmission and utilises redundancy in the form of guard intervals to mitigate inter-block interference and exploits the channel eigendecomposition to design the optimal precoders and equalisers. Several design criteria were proposed in [25] which targeted minimum MSE and BER under constraints on the transmit average power or peak power. This section will focus on the optimal designs under constrained transmit average power.

Consider the MIMO channel model in Section 2.1, assume that the channel is stationary or slowly time-varying, the channel with linear precoder and equaliser is illustrated in Figure 2.3.

The blocks of input symbols $\boldsymbol{s}[n] \in \mathbb{C}^N$ are mapped into vectors $\boldsymbol{u}[n] \in \mathbb{C}^{PT}$ by the precoder $\mathbf{F}$ so that

$$\boldsymbol{u}[n] = \mathbf{F}\boldsymbol{s}[n] \ . \tag{2.44}$$

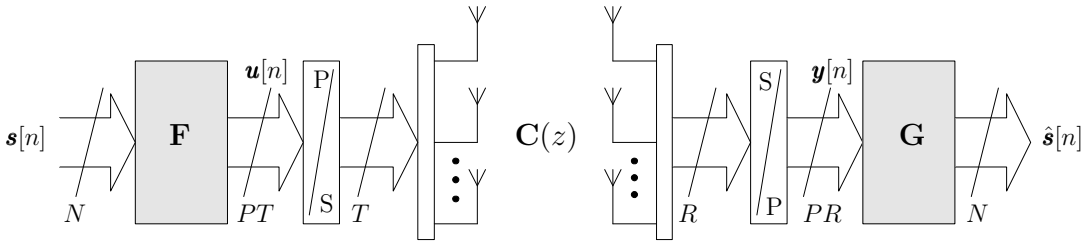

Figure 2.3: Linear precoding and equalisation for broadband MIMO

Through the parallel-to-serial converter, each vector $\boldsymbol{u}[n]$ is divided into P blocks of length T, which will be transmitted through T transmit antennas after pulse shaping. At the receiver, the received symbol blocks of length R from the receive antennas are stacked together by the serial-to-parallel converter to form the vector $\boldsymbol{y}[n] \in \mathbb{C}^{PR}$. The equaliser $\mathbf{G} \in \mathbb{C}^{N \times PR}$ will perform the inverse mapping on $\boldsymbol{y}[n]$ to give the estimated output symbol blocks $\hat{\boldsymbol{s}}[n]$.

The system can be equivalently illustrated as in Figure 2.4 where the MIMO channel is now represented by pseudo-circulant matrix $\mathbf{H}(z)$ as in (2.3). With $P > L$, polynomial matrix $\mathbf{H}(z)$ has unit order and the relation between the input and output blocks can be written as

$$\hat{\boldsymbol{s}}[n] = \mathbf{G}\mathbf{H}_0\mathbf{F}\boldsymbol{s}[n] + \mathbf{G}\mathbf{H}_1\mathbf{F}\boldsymbol{s}[n-1] + \mathbf{G}\boldsymbol{v}[n] \tag{2.45}$$

whereby $\mathbf{H}_0$ and $\mathbf{H}_1$ are two coefficient matrices of $\mathbf{H}(z)$, $\boldsymbol{v}[n]$ is the block of noise samples.

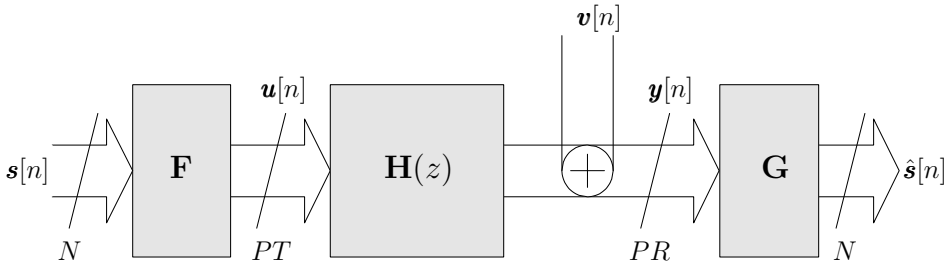

Figure 2.4: Linear precoding for broadband MIMO - simplified scheme

Assume that the channel is stationary or slowly time-varying, one can write $\mathbf{H}_0$ and $\mathbf{H}_1$ in the following form

$$\mathbf{H}_0 = \begin{bmatrix} \mathbf{C}[0] & \mathbf{0} & \cdots & \cdots & \mathbf{0} \\ \vdots & \mathbf{C}[0] & \mathbf{0} & \cdots & \mathbf{0} \\ \mathbf{C}[L] & \cdots & \ddots & \cdots & \vdots \\ \vdots & \ddots & \cdots & \ddots & \mathbf{0} \\ \mathbf{0} & \cdots & \mathbf{C}[L] & \cdots & \mathbf{C}[0] \end{bmatrix} \tag{2.46}$$

$$\mathbf{H}_1 = \begin{bmatrix} \mathbf{0} & \cdots & \mathbf{C}[L] & \cdots & \mathbf{C}[1] \\ \vdots & \ddots & \mathbf{0} & \ddots & \vdots \\ \mathbf{0} & \cdots & \ddots & \cdots & \mathbf{C}[L] \\ \vdots & \vdots & \vdots & \ddots & \vdots \\ \mathbf{0} & \cdots & \mathbf{0} & \cdots & \mathbf{0} \end{bmatrix} \tag{2.47}$$

From equations (2.45) and (2.47), one can see that similar to the case of SISO dispersive channels in Section 2.2, the IBI here can be eliminated by setting the term $\mathbf{GH}_1\mathbf{F}$ to zero, which also leads to either the TZ approach where the last LT rows of precoder matrix are forced to be zero or LZ approach where the first LR columns of equaliser matrix are set to zero. These two approaches are equivalent to the setting of the last L blocks among P transmitted blocks of length T to zero (TZ method) or discarding the first L blocks among P received blocks of length R (LZ method) as mentioned in [25].

With the IBI eliminated and $P = M + L$, equation (2.45) can be simplified as

$$\hat{\boldsymbol{s}}[n] = \mathbf{G}_0\mathbf{H}\mathbf{F}_0\boldsymbol{s}[n] + \mathbf{G}_0\boldsymbol{v}[n] \tag{2.48}$$

whereby in the TZ case $\mathbf{G}_0 \in \mathbb{C}^{N\times PR}$, $\mathbf{F}_0 \in \mathbb{C}^{MT\times N}$ and $\mathbf{H} \in \mathbb{C}^{PR\times MT}$,

$$\mathbf{H} = \begin{bmatrix} \mathbf{C}[0] & 0 & \cdots & 0 \\ \vdots & \ddots & \ddots & \vdots \\ \mathbf{C}[L] & \ddots & \ddots & 0 \\ 0 & \ddots & \ddots & \mathbf{C}[0] \\ \vdots & \ddots & \ddots & \vdots \\ 0 & \cdots & 0 & \mathbf{C}[L] \end{bmatrix}, \tag{2.49}$$

and in the LZ case $\mathbf{G}_0 \in \mathbb{C}^{N\times MR}$, $\mathbf{F}_0 \in \mathbb{C}^{PT\times N}$ and $\mathbf{H} \in \mathbb{C}^{MR\times PT}$,

$$\mathbf{H} = \begin{bmatrix} \mathbf{C}[L] & \cdots & \mathbf{C}[0] & \cdots & 0 \\ \vdots & \ddots & \ddots & \ddots & \vdots \\ 0 & \cdots & \mathbf{C}[L] & \cdots & \mathbf{C}[0] \end{bmatrix}. \tag{2.50}$$

In the case when the channel is time-varying, $\mathbf{H}$ is a block-banded matrix.

Note that in order for the output symbols to be recovered by linear equaliser $\mathbf{G}$, it is necessary that $N \leq \text{rank}(\mathbf{H})$. Therefore in the TZ case, it is required that $N \leq \min(PR, MT)$ and in the LZ case, $N \leq \min(MR, PT)$ is required.

Assume that the transmit symbols are white with the covariance matrix

$$\mathbf{R}_{ss} = \mathcal{E}\{\boldsymbol{s}[n]\boldsymbol{s}[n]^{\text{H}}\} = \sigma_s^2\mathbf{I}\,, \tag{2.51}$$

the noise is Gaussian with positive definite covariance matrix $\mathbf{R}_{vv}$, $\boldsymbol{v}[n]$ and $\boldsymbol{s}[n]$ are mutually uncorrelated. Consider the following eigenvalue decomposition

$$\mathbf{H}^{\text{H}}\mathbf{R}_{vv}^{-1}\mathbf{H} = \hat{\mathbf{V}}\hat{\mathbf{\Lambda}}\hat{\mathbf{V}}^{\text{H}} \tag{2.52}$$

where $\hat{\mathbf{\Lambda}}$ is a $Q^{'} \times Q^{'}$ diagonal matrix, $Q^{'} = \text{rank}(\mathbf{H}^{\text{H}}\mathbf{R}_{vv}^{-1}\mathbf{H})$. Assume that the elements in the diagonal of $\hat{\mathbf{\Lambda}}$ are sorted in decreasing order, denote the top left $N \times N$ block of $\hat{\mathbf{\Lambda}}$ by $\mathbf{\Lambda}$ and denote the coresponding first N columns of $\hat{\mathbf{V}}$ by $\mathbf{V}$.

The optimal precoders and equalisers are also designed under either the MMSE criterion or a criterion similar to maximising the system SNR. Here for simplicity, the latter will be referred to as the MaxSNR criterion.

Under the MMSE criterion, the optimal equaliser which minimises the arithmetic MSE is given by

$$\mathbf{G}_{opt} = \mathbf{R}_{ss}\mathbf{F}_0^{\text{H}}\mathbf{H}^{\text{H}}\left(\mathbf{H}\mathbf{F}_0\mathbf{R}_{ss}\mathbf{F}_0^{\text{H}}\mathbf{H}^{\text{H}} + \mathbf{R}_{vv}\right)^{-1}\,. \tag{2.53}$$

The error covariance matrix can then be written as a function of the precoder matrix $\mathbf{F}_0$ as

$$\mathbf{R}_{ee} = \sigma_s^2(\mathbf{I} + \sigma_s^2\mathbf{F}_0^{\text{H}}\mathbf{H}^{\text{H}}\mathbf{R}_{vv}^{-1}\mathbf{H}\mathbf{F}_0)^{-1} \tag{2.54}$$

In the case of minimising trace($\mathbf{R}_{ee}$) subject to power constraint trace($\mathbf{F}_{opt}\mathbf{F}_{opt}^{\text{H}})\sigma_s^2 = P_0$, the optimal precoder is given by

$$\mathbf{F}_{opt} = \mathbf{V}\mathbf{\Phi} \tag{2.55}$$

where $\mathbf{\Phi}$ is a diagonal matrix with diagonal elements obtained from a water-filling algorithm

$$|\phi_{ii}|^2 = \max\left(\frac{P_0 + \sum_{j=1}^{\bar{N}} \lambda_{jj}^{-1}}{\sigma_s^2 \sum_{j=1}^{\bar{N}} \lambda_{jj}^{-1/2}} \lambda_{ii}^{-1/2} - \frac{1}{\lambda_{ii}\sigma_s^2}\ ,\ 0\right), \tag{2.56}$$

where $\bar{N} \leq N$ is the number of positive $|\phi_{ii}|^2$ ($|\phi_{ii}|^2 > 0$ for $i \in [1, \bar{N}]$ and $|\phi_{ii}|^2 = 0$ for $i \in [\bar{N}+1, N]$).

In the case of minimising the determinant of error covariance matrix $|\mathbf{R}_{ee}|$ subject to power constraint $\text{trace}(\mathbf{F}_{opt}\mathbf{F}_{opt}^{\text{H}})\sigma_s^2 = P_0$, the optimal precoder also has the form $\mathbf{F}_{opt} = \mathbf{V}\mathbf{\Phi}$ where $\mathbf{\Phi}$ is $N \times N$ diagonal matrix with diagonal elements obtained from water-filling algorithm with single water level

$$|\phi_{ii}|^2 = \max\left(\frac{P_0 + \sum_{j=1}^{\bar{N}} \lambda_{jj}^{-1}}{\bar{N}\sigma_s^2} - \frac{1}{\lambda_{ii}\sigma_s^2}\ ,\ 0\right), \tag{2.57}$$

where similar to the previous case, $\bar{N} \leq N$ is the number of positive $|\phi_{ii}|^2$. It has been shown in [25] that this optimal precoder also maximises the mutual information of the system.

The precoder that maximises the output SNR subject to constrained transmit power is also given in the form $\mathbf{F}_{opt} = \mathbf{V}\mathbf{\Phi}$ where $\mathbf{\Phi} \in \mathbb{C}^{N\times N}$ is a digonal matrix with diagonal elements given by

$$|\phi_{ii}|^2 = \frac{P_0}{\sigma_s^2 \sum_j \lambda_{jj}^{-1}} \lambda_{ii}^{-1} \tag{2.58}$$

and the optimal equaliser is written as $\mathbf{G}_{opt} = \mathbf{S}\mathbf{V}^H\mathbf{H}^{\text{H}}\mathbf{R}_{vv}^{-1}$ where $\mathbf{S}$ is $N \times N$ invertible matrix.

2.5 Concluding Remarks

In this chapter some state-of-the-art joint precoding and equalisation designs have been reviewed. The designs considered here exploit the standard SVD as a powerful tool to decompose the channel matrix and eliminate the CCI. In Section 2.3, the property of the SVD is also utilised to eliminate multiple access interference. The

designs for frequency selective channels, either SISO or MIMO, in Section 2.2 and Section 2.4 utilise zero-padding intervals of the length equal to the channel order to eliminate IBI caused by channel frequency selectivity. The use of zero-padding intervals allows the block based transmission over a frequency selective channel to be described in the matrix form, thus the standard SVD can be applied to remove intra-block interference. Zero-padding intervals, however, reduce the spectral efficiency of the system, especially in case of broadband or frequency selective MIMO channels.

The next chapter will consider an approach to reduce the effect of the guard intervals such that the channel can be better exploited in term of spectral efficiency, and a better performance can be achieved.

Chapter 3

BSVD Based MIMO Precoding and Equalisation

The use of guard intervals to eliminate IBI in block transmission systems reduces the spectral efficiency of the system. This chapter will discuss a new approach to precoding and equalisation for frequency selective MIMO channels by applying a recently proposed broadband singular value decomposition (BSVD) to decouple the MIMO channel matrix into approximately independent frequency selective SISO subchannels. In a second step, the remaining ISI in the subchannels is eliminated using methods reported in the literature. This first step helps to remove not only co-channel interference (CCI) but can also eliminate part of the inter-symbol interference with a very small loss in channel power gain as will be demonstrated. A numerical example given in this chapter shows that the proposed method can provide better bit error rate performance than that of a benchmark design. Under a quality of service constraint, the proposed design can achieve higher data throughput and mutual information than that of the benchmark design while maintaining a similar symbol error performance.

3.1 Introduction

In wireless communications MIMO systems arise when multiple antennas are used at both the transmitter and receiver sides. Such systems can offer transmission with increased capacity over SISO channels provided that the transmission paths are uncorrelated [43, 44, 45] and at the same time provide an increase in range and reliability without consuming additional bandwidth.

In many cases, it is assumed that the channel state information (CSI) is available only at the receiver (CSIR). In such cases, either space-time coding [9, 16, 46], the V-BLAST [47, 43] or equalisation techniques [48, 49, 50] can be applied. However, in some scenarios, such as frequency division duplex (FDD) or time division duplex (TDD) systems, the CSI can be made available at the transmitter (CSIT) either through a feedback channel or through the reciprocity of the channel. In such cases, the problem of joint transmit and receive processing or joint precoder and equaliser design [51, 52, 41, 24, 25, 53, 54, 32] becomes very appealing as it can achieve much higher performance than systems with isolated designs.

A large number of research publications focus on the case of narrowband or frequency flat fading MIMO [41, 55, 56], where the channel can be represented by a matrix and the standard singular value decomposition (SVD) plays a central role in the joint design process in order to decouple the MIMO channel into independent flat subchannels.

With the demand for higher transmission rates, the transmission channel can no longer be considered as narrowband and designs for the resulting broadband MIMO systems have attracted attention. In broadband MIMO systems, apart from the elimination of CCI caused by the MIMO components, additionally the elimination of ISI caused by the channel frequency selectivity is required. A widely applied approach is based on block transmission. Firstly, multicarrier modulation can be utilised to decompose the broadband problem into a number of narrowband ones, where the above mentioned powerful SVD-based designs can decouple the MIMO

system. Secondly, single carrier broadband approaches have been formulated for the single-input single-output case in [26, 27], which can be easily extended to the MIMO case [25]. In [53], Palomar *et al.* also assume that the IBI has been eliminated by the use of guard intervals and then generalise the results on joint design of linear precoding and equalisation for flat fading MIMO systems to several criteria using convex optimisation functions. There, the equaliser is first derived as a Wiener filter, then under different optimisation criteria that have been unified in form of Schur-concave or Schur-convex functions, the precoder is determined via the SVD of the whitened channel.

In [54], an iterative algorithm to design joint optimal precoder and equaliser for broadband MIMO channels was proposed. There, the optimal precoder and equaliser in the form of FIR MIMO filters are designed to minimise the system MSE under constrained transmit power and in the presence of near-end crosstalk.

The designs in [26, 25, 53] generally rely on a block-transmission approach, which requires a certain amount of redundancy to eliminate inter-block interference (IBI). This redundancy limits the spectral efficiency of the system. The loss in spectral efficiency can be reduced by increasing transmit block size, however due to the constrained transmit power, the energy per symbol will be decreased and therefore the bit error rate performance becomes poorer. Also, one can see that the use of guard intervals always requires an amount of degrees of freedom (DOF) equal to the channel order to be invested into IBI cancellation only and therefore it cannot be traded-off against ISI and noise amplification unless channel shortening is used. In [54], it is also shown that the use of zero-padding intervals as proposed in [26, 25] is not optimal in terms of SNR performance.

In this chapter, a method for precoding and equalisation for point-to-point broadband MIMO channels is proposed. Different from block transmission based approaches in [25, 53], in the first step a recently proposed broadband singular value decomposition (BSVD) [57, 58] is utilised to decompose the broadband MIMO channel matrix, which is polynomial, into two paraunitary matrices and a polynomial

diagonal matrix and thus the broadband MIMO channel can be decomposed into a number of nearly independent frequency selective (FS) SISO subchannels whose transfer functions correspond to the main diagonal elements of the diagonal polynomial matrix mentioned above. The use of BSVD helps to eliminate not only the CCI in the MIMO channel but also a part of ISI when combined with a water-filling algorithm in the second step. In the second step, the decoupled FS SISO subchannels are precoded and equalised using standard methods such as in [26, 27, 32]. Since ISI has been eliminated partly with the help of the BSVD, this approach loosens the constraint of ISI elimination and provides a possibility to achieve a better spectral efficiency for the decoupled FS SISO subchannels and thus leads to an improved system performance.

This chapter is organised as follows. In Section 3.2, the overall channel and system setup are laid out. Section 3.3 addresses the first step in the proposed design, aiming at CCI cancellation, while Section 3.4 considers the elimination of remaining ISI on FS subchannels. Finally, a numerical example is provided in Section 3.5, while conclusions are drawn in Section 3.6.

3.2 Channel Model and System Set Up

3.2.1 MIMO System Model

Here the precoding and equalisation design for the stationary broadband MIMO channel, whose model has been described in Section 2.1 will be considered. Recall that the channel is of order L and has T inputs and R outputs, the transfer function of the channel is

$$\mathbf{C}(z) = \sum_{l=0}^{L} \mathbf{C}[l]\, z^{-l} \quad . \tag{3.1}$$

It is further assumed that the exact CSI is available to both the transmitter and receiver sides.

In the general case, when one assumes that the signal on each of the T inputs has resulted from a time-multiplexing of P input signals, and each of R outputs is demultiplexed into P signals, the MIMO channel can be represented by the pseudo-circulant matrix $\mathbf{H}(z) \in \mathbb{C}^{RP \times TP}(z)$ as explained in Section 2.1. Recall that $\mathbf{H}(z)$ is given by

$$\mathbf{H}(z) = \begin{bmatrix} \mathbf{C}_0(z) & z^{-1}\mathbf{C}_{P-1}(z) & \cdots & z^{-1}\mathbf{C}_1(z) \\ \mathbf{C}_1(z) & \mathbf{C}_0(z) & \cdots & z^{-1}\mathbf{C}_2(z) \\ \vdots & & \ddots & \vdots \\ \mathbf{C}_{P-1}(z) & \mathbf{C}_{P-2}(z) & \cdots & \mathbf{C}_0(z) \end{bmatrix}, \tag{3.2}$$

where $\mathbf{C}_p(z)$ are the polyphase components of $\mathbf{C}(z)$,

$$\mathbf{C}_p(z) = \sum_{n=-\infty}^{+\infty} \mathbf{C}[nP + p]\, z^{-n} \quad . \tag{3.3}$$

In the following a generic model with precoder $\mathbf{P}(z) \in \mathbb{C}^{K \times PT}(z)$ and equaliser $\mathbf{E}(z) \in \mathbb{C}^{PR \times K}(z)$ and the channel $\mathbf{H}(z)$ as illustrated in Figure 3.1 is considered.

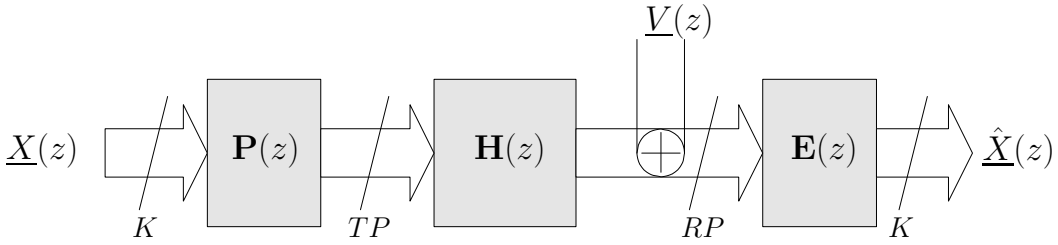

Figure 3.1: MIMO channel $\mathbf{H}(z)$ with precoder $\mathbf{P}(z)$ and equaliser $\mathbf{E}(z)$ including a multiplexing by P.

3.2.2 Block Based Precoder and Equaliser

When $P = 1$, $\mathbf{H}(z) = \mathbf{C}(z)$ is an $R \times T$ polynomial matrix of order L. As the number of polyphase components P increases, the size of $\mathbf{H}(z)$ becomes larger, but its polynomial order reduces in accordance with the shortening polyphase responses. Once $P = L$ is reached, the polyphase components $\mathbf{C}_p(z)$ are constants with no

dependency on z. However, the block-pseudo-circulant form of $\mathbf{H}(z)$ in (2.3) ensures that for all $P > L$, the spatio-temporal MIMO system matrix $\mathbf{H}(z)$ will be a first order polynomial, which means that IBI always exists.

As it has been reviewed in Sections 2.2 and 2.4, to overcome the polynomial order and therefore to eliminate the ISI or IBI, the block transmission based system in [26] for $T = R = 1$ and in [24, 25] for arbitrary T and R rely on a time multiplex that is chosen longer than the channel order, i.e. $P > L$. As a result, $\mathbf{H}(z)$ now becomes a sparse block-pseudo-circulant matrix of only first order in z, as noted earlier. Specifically

$$\mathbf{H}(z) = \mathbf{H}_0 + \mathbf{H}_1 z^{-1} \tag{3.4}$$

whereby $\mathbf{H}_0$ and $\mathbf{H}_1$ are given in (2.13) and (2.14) for the SISO case and in (2.46) and (2.47) for the MIMO case.

The polynomial order of the MIMO system matrix $\mathbf{H}(z)$ can be eliminated by suppressing $\mathbf{H}_1$ through either TZ or LZ approaches as mentioned in Sections 2.2 and 2.4. Thus the polynomial nature of $\mathbf{H}(z)$ has been eliminated and the precoder and equaliser can be selected as non-polynomial matrices. However, one can see again that these TZ or LZ approaches or even the multicarrier approach which uses cyclic prefix always require at least the first L degrees of freedom (DOF) to be used only for the ISI elimination.

3.2.3 Proposed Design

The proposed design has two components. Firstly, the MIMO system matrix $\mathbf{H}(z)$ is decoupled into a number of independent FS subchannels based on a recently proposed broadband singular value decomposition [58, 57]. This allows to factorise $\mathbf{H}(z)$ as

$$\mathbf{H}(z) = \mathbf{U}(z) \begin{bmatrix} \mathbf{S}(z) & \mathbf{0} \\ \mathbf{0} & \mathbf{0} \end{bmatrix} \tilde{\mathbf{V}}(z) \tag{3.5}$$

whereby $\mathbf{S}(z) = \text{diag}\{S_{00}(z), S_{11}(z), \cdots S_{K-1,K-1}(z)\}$ and $\mathbf{U}(z)$ and $\mathbf{V}(z)$ are paraunitary matrices.

The factorisation (3.5) motivates the use of a precoder $\mathbf{P}(z)$ containing the first K columns of $\mathbf{V}(z)$ and an equaliser $\mathbf{E}(z)$ containing the first K rows of $\tilde{\mathbf{U}}(z)$ such that the broadband MIMO channel matrix is decomposed into $K \leq \min(RP, TP)$ independent FS subchannels. One can write

$$\underline{\hat{X}}(z) = \mathbf{E}(z)\mathbf{C}(z)\mathbf{P}(z)\underline{X}(z) + \mathbf{E}(z)\underline{V}(z) \tag{3.6}$$

$$= \mathbf{S}(z)\underline{X}(z) + \mathbf{E}(z)\underline{V}(z) \tag{3.7}$$

where $\underline{X}(z) \in \mathbb{C}^K(z)$ is the signal vector at the input of the precoder $\mathbf{P}(z)$, $\underline{\hat{X}}(z) \in \mathbb{C}^K(z)$ is the signal vector at the output of the equaliser $\mathbf{E}(z)$, and $\underline{V}(z) \in \mathbb{C}^{RP}(z)$ characterises additive white Gaussian noise as illustrated in Figure 3.1.

Although the CCI has been eliminated with the help of $\mathbf{P}(z)$ and $\mathbf{E}(z)$, the decoupled subchannels are still dispersive and cause ISI. Therefore in a second step a precoder and equaliser are designed for each decoupled subchannel so that the remaining ISI is eliminated. These precoders and equalisers can be the linear optimal precoders and equalisers in [26, 27] which are also reviewed in Section 2.2 or nonlinear optimal precoders and equalissers proposed in [32]. One can see that depending on the precoding and equalisation method applied for the SISO FS subchannels, the block transmission might be invoked in the second step, but only for a small portion of the system design. In addition, the second stage design of precoders and equalisers can take the individual properties of each subchannel — such as its SNR — into account.

Note that P is both the number of polyphase components and the block size. For block transmission systems in [26, 25], $P >> 1$, while for the designs proposed here, P is generaly very small and can be equal to 1.

3.3 MIMO System Decomposition Via BSVD

3.3.1 Broadband Singular Value Decomposition

In the following the BSVD described in [58, 59, 57], and the resulting properties of the subchannels are characterised. Different from the standard SVD, which can diagonalise only scalar matrices, the BSVD is applied to diagonalise polynomial matrices. A BSVD can be obtained via two broadband eigenvalue decompositions (BEVD), whereby a parahermitian matrix $\mathbf{R}_1(z) = \mathbf{H}(z)\tilde{\mathbf{H}}(z)$ is decomposed such that

$$\mathbf{R}_1(z) = \mathbf{U}(z)\mathbf{\Gamma}_1(z)\tilde{\mathbf{U}}(z) \quad . \tag{3.8}$$

In an ideal case, besides the diagonality of $\mathbf{\Gamma}_1(z)$, one would demand the paraunitarity or losslessness of $\mathbf{U}(z)$ such that

$$\mathbf{U}(z)\tilde{\mathbf{U}}(z) = \tilde{\mathbf{U}}(z)\mathbf{U}(z) = \mathbf{I} \tag{3.9}$$

and spectral majorisation of $\mathbf{\Gamma}_1(z)$ [60] such that its diagonal elements

$$\Gamma_{00}^{(1)}(z),\ \Gamma_{11}^{(1)}(z),\ \ \ldots\ \ \Gamma_{RP-1,RP-1}^{(1)}(z)$$

are ordered according to

$$\left|\Gamma_{kk}^{(1)}(e^{j\Omega})\right| \geq \left|\Gamma_{k+1,k+1}^{(1)}(e^{j\Omega})\right| \qquad \forall\ \Omega \quad \text{and} \quad k = 0, 1, \ldots, RP-2, \tag{3.10}$$

similar to the ranking of the singular values in a standard singular value decomposition. Note that paraunitariness or losslessness of $\mathbf{U}(z)$ conserves power, which means $\text{trace}\{\mathbf{\Gamma}_1[0]\} = \text{trace}\{\mathbf{R}_1[0]\}$ with $\mathbf{\Gamma}_1[\tau] \circ\!\!-\!\!\bullet\ \mathbf{\Gamma}_1(z)$ and $\mathbf{R}_1[\tau] \circ\!\!-\!\!\bullet\ \mathbf{R}_1(z)$.

In a similar operation, $\mathbf{V}(z)$ can be obtained via BEVD of

$$\mathbf{R}_2(z) = \tilde{\mathbf{H}}(z)\mathbf{H}(z) = \mathbf{V}(z)\mathbf{\Gamma}_2(z)\tilde{\mathbf{V}}(z) \quad . \tag{3.11}$$

An iterative numerical algorithm reported in [58, 59, 57] which employs a sequence of paraunitary operations to yield a close approximation of a diagonal and spectrally majorised polynomial matrices $\mathbf{\Gamma}_1(z)$ and $\mathbf{\Gamma}_2(z)$ will be discussed in more details in Chapter 5.

3.3.2 Precoder and Equaliser for CCI Suppression

Applying the algorithm in Section 3.3.1 to find the decoupling precoder and equaliser according to Section 3.2.3, an approximately diagonalised

$$\mathbf{S}(z) = \mathbf{E}(z)\mathbf{H}(z)\mathbf{P}(z) \tag{3.12}$$

results for the overall system shown in Figure 3.1. Since $\mathbf{S}(z)$ is not absolutely diagonal, there exists a certain amount of CCI at the output of equaliser $\mathbf{E}(z)$ and thus the term that include the noise filtered by $\mathbf{E}(z)$ and the remaining CCI is denoted as $V_i^{'}(z)$. In the following the components of $V_i^{'}(z)$ will be characterised.

Let $R_{v_i'v_i'}(z)$ be the power spectral density of $V_i^{'}(z)$ on the ith subchannel, $S_{ij}(z)$ the element of $\mathbf{S}(z)$ placed in the ith row and jth column. Further, $R_{x_i,x_i}(z)$ is the power spectral density of the ith input in $\underline{X}(z)$, which is assumed to be mutually uncorrelated with all other inputs. Then at the receiver, the remaining CCI components can be characterised by the CCI power spectral density $R_{i,\mathrm{CCI}}(z)$,

$$R_{i,\mathrm{CCI}}(z) = \sum_{j,j\neq i} S_{ij}(z)\; R_{x_j,x_j}(z)\; \tilde{S}_{ij}(z) \quad . \tag{3.13}$$

The channel noise appears in the output $\underline{\hat{X}}(z)$ filtered by the equaliser $\mathbf{E}(z)$, such that its power spectral matrix at the output is

$$\mathbf{R}_{\eta\eta}(z) = \mathbf{E}(z)\mathbf{R}_{vv}(z)\tilde{\mathbf{E}}(z)\ . \tag{3.14}$$

Thus the power spectral density of $V_i^{'}(z)$ is given by

$$R_{v_i'v_i'}(z) = R_{\eta\eta}^{(ii)}(z) + R_{i,\mathrm{CCI}}(z) \tag{3.15}$$

where $R_{\eta\eta}^{(ii)}(z)$ is an element on the main diagonal of $\mathbf{R}_{\eta\eta}(z)$, lying in the intersection of the ith row and the ith column. If the noise power spectral density $\mathbf{R}_{vv}(z) = \sigma_{vv}^2\mathbf{I}$, then due to paraunitariness of $\mathbf{E}(z)$, $\mathbf{R}_{\eta\eta}(z) = \sigma_{vv}^2\mathbf{I}$. Therefore, we obtain

$$R_{v_i'v_i'}(z) = R_{i,\mathrm{CCI}}(z) + \sigma_{vv}^2 \quad . \tag{3.16}$$

Thus the effect of the remaining CCI will be taken into account in the designing of the second stage precoder and equaliser pair, which is designed to remove ISI within the selected subchannels.

3.4 SISO Subchannel Precoding and Equalisation

As it has been mentioned, various methods can be employed to eliminate the remaining ISI from the FS subchannels. This section will consider two approaches, one is the linear joint optimal precoding and equalisation for SISO channels proposed in [26, 27], the other is the joint optimal precoding and block decision feedback equalisation (BDFE) proposed in [32]. The extension of these approaches for the frequency selective MIMO channels will be used as benchmarks to highlight the gain in performance of our proposed method.

3.4.1 Linear Precoding and Equalisation for SISO subchannels

Here the joint linear precoding and equalisation methods proposed in [26, 27], which were also reviewed in Section 2.2, will be applied for decoupled SISO subchannels. The system arrangement for the ith SISO subchannel is shown in Figure 3.2, which is actually a generic version of the system illustrated in 2.2.

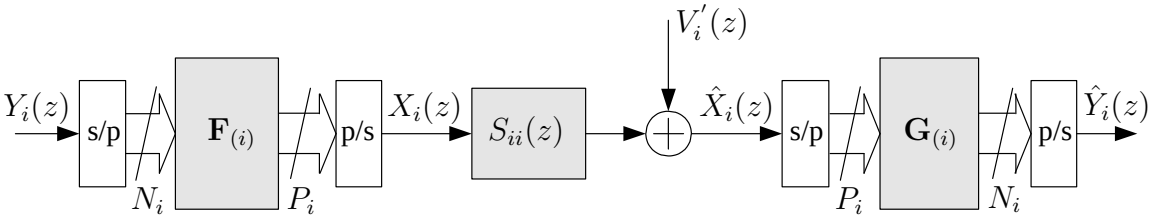

Figure 3.2: Linear joint precoding and equalisation for decoupled SISO frequency selective subchannels

Assuming that the channel has a length of $L_i + 1$, the transmit block length including the redundancy for IBI cancellation P_i is chosen such that $P_i > L_i$. The input block length is $N_i \leq M_i$ where $M_i = P_i - L_i$. Without loss of generality, we assume that the TZ approach mentioned in [26] is used for IBI elimination. This

leads to a precoder of the form

$$\mathbf{F}_{(i)} = \begin{bmatrix} \mathbf{F}_{(i),0} \\ \mathbf{0}_{L_i \times N_i} \end{bmatrix} \quad , \tag{3.17}$$

where $\mathbf{F}_{(i),0} \in \mathbb{C}^{M_i \times N_i}$. The covariance matrix of the input signal $Y_i(z)$ is defined as $\mathbf{R}_{y_i y_i} \in \mathbb{C}^{N_i \times N_i}$ and the noise covariance matrix arising from the signal $V_i^{'}(z)$ is defined as $\mathbf{R}_{v_i' v_i'} \in \mathbb{C}^{P_i \times P_i}$. Note that the latter comprises of the channel noise filtered by $\mathbf{E}(z)$ and the CCI components of the ith subchannel characterised in (3.13). Further, similar to (2.19), with the use of a TZ precoder for IBI elimination, the Toeplitz matrix $\mathbf{S}_{(i)}$ containing the impulse response of length $L_i + 1$ of the ith subchannel, $S_{ii}(z)$, produced by the BSVD in Section 3.3.2 is written as

$$\mathbf{S}_{(i)} = \begin{bmatrix} s^{(i)}[0] & 0 & \dots & 0 \\ \vdots & \ddots & \ddots & \vdots \\ s^{(i)}[L_i] & & \ddots & 0 \\ 0 & \ddots & & s^{(i)}[0] \\ \vdots & \ddots & \ddots & \vdots \\ 0 & \dots & 0 & s^{(i)}[L_i] \end{bmatrix} \quad , \tag{3.18}$$

whereby $S_{ii}(z) = \sum_{n=0}^{L_i} s^{(i)}[n] z^{-n}$.

Based on $\mathbf{R}_{y_i y_i}$, $\mathbf{R}_{v_i' v_i'}$, and $\mathbf{S}_{(i)}$, one can define the following EVD factorisations

$$\mathbf{R}_{y_i y_i} = \mathbf{U}_i \mathbf{\Delta}_i \mathbf{U}_i^{\mathrm{H}} \tag{3.19}$$

$$\mathbf{S}_{(i)}^{\mathrm{H}} \mathbf{R}_{v_i' v_i'}^{-1} \mathbf{S}_{(i)} = \mathbf{V}_i \mathbf{\Lambda}_i \mathbf{V}_i^{\mathrm{H}} \, , \tag{3.20}$$

with the diagonal matrices

$$\mathbf{\Delta}_i = \mathrm{diag}\Big\{ \delta_{00}^{(i)}, \ \delta_{11}^{(i)}, \ \cdots \ \delta_{M_i-1,M_i-1}^{(i)} \Big\} \tag{3.21}$$

$$\mathbf{\Lambda}_i = \mathrm{diag}\Big\{ \lambda_{00}^{(i)}, \ \lambda_{11}^{(i)}, \ \cdots \ \lambda_{M_i-1,M_i-1}^{(i)} \Big\} \quad . \tag{3.22}$$

The non-zero part $\mathbf{F}_{(i),0}$ of the precoder and the equaliser $\mathbf{G}_{(i)}$ will be designed under several optimal criteria as reviewed in Section 2.2. This subsection will consider the MMSE/CP and the MaxIR optimal precoders and equalisers proposed in

[26] and [27], respectively. With $\mathbf{V}_{(Ni)}$ containing the first N_i columns of $\mathbf{V}_i$, the optimal MMSE filterbank pairs in both cases are given by

$$\mathbf{F}_{i,opt} = \mathbf{V}_{(Ni)}\mathbf{\Phi}_i\mathbf{U}_i^{\mathrm{H}} \tag{3.23}$$

$$\mathbf{G}_{i,opt} = \mathbf{R}_{y_iy_i}(\mathbf{F}_{i,opt})^{\mathrm{H}}\mathbf{S}_{(i)}^{\mathrm{H}}\left[\mathbf{R}_{v_i'v_i'} + \mathbf{S}_{(i)}\mathbf{F}_{i,opt}\mathbf{R}_{y_iy_i}(\mathbf{F}_{i,opt})^{\mathrm{H}}\mathbf{S}_{(i)}^{\mathrm{H}}\right]^{-1} \quad , \tag{3.24}$$

where the elements of the diagonal matrix $\mathbf{\Phi}_i$ are determined by the water-filling algorithms as described in [26] and [27]. Note that in the design proposed here, the total transmit power P_0 for the whole MIMO system will be allocated by performing the water-filling algorithm for all $\mathbf{\Lambda}_i$, $(i = 1, \cdots, K)$ at the same time.

The use of the MMSE optimal precoder and equaliser filterbanks given in (3.23) and (3.24) helps to decompose a frequency selective channel into $\overline{M}_i \leq M_i$ flat subchannels with different SNRs, whereby the value of $\overline{M}_i$ is determined by the water-filling algorithm. With the input block size of N_i ($N_i \leq M_i$) and the SNR on each flat subchannel to be ρ_j with $j = 1...N_i$, the normalised mutual information between the output and input of the ith frequency selective SISO subchannel is given by

$$I_i = \frac{1}{N_i}\sum_{j=1}^{N_i}\log_2(1+\rho_j) \quad . \tag{3.25}$$

The water-filling algorithm for the MaxIR case is based on the assumption that the input signal has Gaussian distribution. In practice, however, the transmit symbols come from finite order constellations and practical coding schemes. Thus for practical scenarios, one often has to consider the problem of bit loading which helps to achieve a desired performance while still maximising the data throughput by selecting optimal constellation sizes for each flat subchannel under the quality of service (QoS) constraint that the symbol error probability for the jth FS subchannel $P_{se}^{(j)}$ must be limited by an upper bound $P_{se,\max}$ [27, 25]. Assuming that QAM modulation is used for all flat subchannels, the water-filling algorithm for the MaxIR precoder design is modified accordingly when the QoS constraint $P_{se}^{(i)} \leq P_{se,\max}$ is applied, resulting in a reduction of $\overline{M}_i$ [27].

The maximum constellation size that satisfies QoS constraint on the jth flat subchannel is given by

$$Q_j = \left\lfloor 1 + \frac{\rho_j}{(2/3)\left[\text{erfc}^{-1}\left(P_{se,\max}/2\right)\right]^2} \right\rfloor \tag{3.26}$$

where $\lfloor a \rfloor$ is the foor operation which rounds off a to the nearest integer less than or equals to a.

Therefore the total number of bits that can be transmitted over the ith SISO FS subchannel under a given constraint $P_{se,\max}$ is

$$N_{\text{bit}}^{(i)} = \sum_{j=1}^{N_i} \log_2 Q_j \quad . \tag{3.27}$$

The data throughput, which is the number of information bits transmitted through the channel in one sampling period, for the ith subchannel is equal to

$$D_i = \frac{N_{\text{bit}}^{(i)} N_i}{P_i} \text{ [bits/sampling period]} , \tag{3.28}$$

such that the average data throughput of the overall MIMO system is given by

$$D = \frac{1}{K} \sum_{i}^{K} D_i \text{ [bits/sampling period]} \quad . \tag{3.29}$$

3.4.2 Joint Precoding and Block Decision Feedback Equalisation for SISO subchannels

This subsection considers the application of the joint optimal precoding and block decision feedback equalisation (BDFE) design proposed in [32] for the decoupled SISO FS subchannels. The jointly optimal precoder and BDFE equaliser proposed in [32] are derived so that the mean square error (MSE) between the input and output symbols can achieve its minimised lower bound. Although the derivation of optimal precoder and BDFE in [32] was based on the flat MIMO channel model, the authors have pointed out that the approach can also be applied for FS channels using block based transmission with guard intervals of the length of the channel

order to eliminate IBI as discussed in Sections 2.2 and 2.4. Due to the particular structure and design criteria of the scheme in [32], this approach will be applied to the decoupled SISO FS subchannels with a minor modification.

The system set up of joint precoding and BDFE for the ith SISO subchannel is illustrated in Figure 3.3, where for simplicity the serial-to-parallel and parallel-to-serial converters have been removed. Note that the same input signal $\underline{Y}(z)$ is put into all the SISO subchannels that are used for transmission. The signals at the output of the feed-forward filterbanks are summed together before adding with the feedback signal and then put into the decision device.

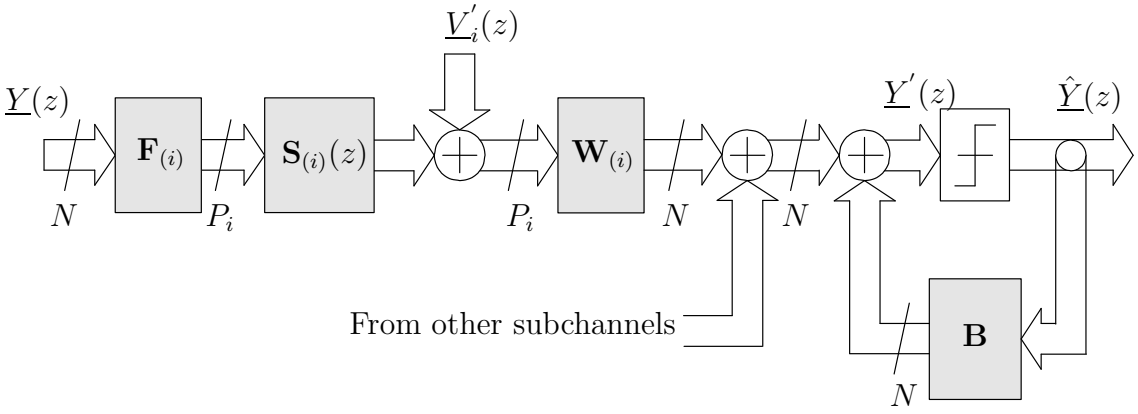

Figure 3.3: Joint precoding and BDFE for decoupled SISO frequency selective subchannels

The input signal $\underline{Y}(z)$ is assumed to be white with unit variance. Similar to the previous subsection, $\mathbf{R}_{v_i'v_i'} \in \mathbb{C}^{P_i \times P_i}$ is defined as the covariance matrix of $V_i'(z)$, which comprises of the channel noise filtered by $\mathbf{E}(z)$ and the CCI components of the ith channel as mentioned in subsection 3.3.2.

As mentioned above, the IBI elimination will be performed by the use of guard intervals, thus similar to the case of linear design, the transmit block length P_i is chosen such that $P_i = M_i + L_i$ where the definitions of M_i, L_i are similar to those in the previous subsection, N is the length of the input symbol block. A TZ precoder

$\mathbf{F}_{(i)} \in \mathbb{C}^{P_i \times N}$ of the form

$$\mathbf{F}_{(i)} = \begin{bmatrix} \mathbf{F}_{(i),0} \\ \mathbf{0}_{L_i \times N} \end{bmatrix} \tag{3.30}$$

is also used to eliminate the IBI on each SISO FS subchannel.

Defining matrices $\mathbf{F} \in \mathbb{C}^{P_\Sigma \times N}$, $\mathbf{W} \in \mathbb{C}^{N \times P_\Sigma}$, $\mathcal{H} \in \mathbb{C}^{P_\Sigma \times M_\Sigma}$, $\mathbf{R}^{-1}_{v'v'} \in \mathbb{C}^{P_\Sigma \times P_\Sigma}$ and the vector $\underline{V}^{'}(z) \in \mathbb{C}^{P_\Sigma}(z)$ as

$$\mathbf{F} = \begin{bmatrix} \mathbf{F}_{(1),0} \\ \vdots \\ \mathbf{F}_{(K),0} \end{bmatrix}, \tag{3.31}$$

$$\mathbf{W} = \begin{bmatrix} \mathbf{W}_{(1)} & \cdots & \mathbf{W}_{(K)} \end{bmatrix}, \tag{3.32}$$

$$\mathcal{H} = \begin{bmatrix} \mathbf{S}_{(1)} & & \mathbf{0} \\ & \ddots & \\ \mathbf{0} & & \mathbf{S}_{(K)} \end{bmatrix}, \tag{3.33}$$

$$\mathbf{R}_{v'v'} = \begin{bmatrix} \mathbf{R}_{v'_1 v'_1} & & \mathbf{0} \\ & \ddots & \\ \mathbf{0} & & \mathbf{R}_{v'_K v'_K} \end{bmatrix}, \tag{3.34}$$

$$\underline{V}^{'}(z) = \begin{bmatrix} \underline{V}^{'}_1(z) \\ \vdots \\ \underline{V}^{'}_K(z) \end{bmatrix}, \tag{3.35}$$

where $P_\Sigma = \sum_{i=1}^{K} P_i$, $M_\Sigma = \sum_{i=1}^{K} M_i$ and $\mathbf{S}_{(i)}$ $(i = [1, \ldots, K])$ is the Toeplitz matrix given by (3.18), one can write the relation between the input signal $\underline{Y}(z)$ and the signal at the input of the decision device as

$$\underline{Y}^{'}(z) = \sum_{i=1}^{K} \mathbf{W}_{(i)} \mathbf{S}_{(i)} \mathbf{F}_{(i),0}\, \underline{Y}(z) + \mathbf{B}\, \hat{\underline{Y}}(z) + \sum_{i=1}^{K} \mathbf{W}_{(i)}\, \underline{V}^{'}_i(z) \tag{3.36}$$

$$= \mathbf{W}\mathcal{H}\mathbf{F}\, \underline{Y}(z) + \mathbf{B}\, \hat{\underline{Y}}(z) + \mathbf{W}\, \underline{V}^{'}(z) \tag{3.37}$$

The joint optimal transceivers proposed in [32] have been designed under either zero-forcing or minimum mean square error criteria, in the proposed design the

MMSE joint optimal precoding and BDFE scheme is applied since it can help to implement a simple and effective water-filling algorithm to allocate transmit power for the whole MIMO channel. Consider the eigenvalue decomposition

$$\mathcal{H}^{\mathrm{H}}\mathbf{R}_{v'v'}^{-1}\mathcal{H} = \mathbf{V}\mathbf{\Lambda}\mathbf{V}^{\mathrm{H}} \tag{3.38}$$

with diagonal matrix

$$\mathbf{\Lambda} = \mathrm{diag}\{\lambda_1,\ \ \lambda_2,\ \ \cdots\ \ \lambda_{M_\Sigma}\} \quad , \tag{3.39}$$

then according to [32], the minimisation of the MSE lower bound will maximise the mutual information between transmitter and receiver for a Gaussian distributed input. Therefore a water-filling algorithm with a single water level is applied to $\mathbf{\Lambda}$ in order to obtain a $(m \times m)$ diagonal matrix $\mathbf{\Phi}$ with

$$|\phi_{kk}|^2 = \frac{P_0 + \sum_{j=1}^{m} \frac{1}{\lambda_j}}{m} - \frac{1}{\lambda_k} \quad , \tag{3.40}$$

whereby $m = \min\{\bar{N}, N\}$, $\bar{N}$ is the maximum integer satisfying

$$\frac{1}{\lambda_{\bar{N}}} < \frac{P_0 + \sum_{j=1}^{\bar{N}} 1/\lambda_j}{\bar{N}} \, . \tag{3.41}$$

With $\mathbf{\Phi}' = [\mathbf{\Phi} \quad \mathbf{0}_{m\times(N-m)}]$ constructed from $\mathbf{\Phi}$, the optimal precoder that minimises the MSE lower bound takes the form

$$\mathbf{F} = \mathbf{V}_m\mathbf{\Phi}'\mathbf{\Theta} \tag{3.42}$$

where matrix $\mathbf{V}_m$ contains the first m columns of $\mathbf{V}$ and $\mathbf{\Theta}$ is a unitary matrix satisfying

$$\left(\mathbf{I}_{N\times N} + \mathbf{\Phi}'^{T}\mathbf{\Lambda}_m\mathbf{\Phi}'\right)^{1/2}\mathbf{\Theta} = \mathbf{U}\mathbf{R} \tag{3.43}$$

whereby $\mathbf{\Lambda}_m$ is the upper left $m \times m$ block of $\mathbf{\Lambda}$, $\mathbf{U}$ is a unitary and $\mathbf{R}$ an upper-triangular matrix with equal diagonal elements. The feedback and feedforward matrices that achieve the minimum MSE lower bound are given by

$$\mathbf{B} = \sigma_e\mathbf{R} - \mathbf{I}_{m\times m} \tag{3.44}$$

$$\mathbf{W} = \sigma_e\mathbf{R}(\mathcal{H}\mathbf{F})^{\mathrm{H}}\left[(\mathcal{H}\mathbf{F})(\mathcal{H}\mathbf{F})^{\mathrm{H}} + \mathbf{R}_{v'v'}\right]^{-1} \tag{3.45}$$

where

$$\sigma_e^2 = m^{m/N} \left(P_0 + \sum_{j=1}^{m} 1/\lambda_j \right)^{-m/N} \prod_{j=1}^{m} (\lambda_j)^{-1/N} \quad . \tag{3.46}$$

whereby P_0 is the constrained transmit power for the MIMO channel. Equation (3.40) shows that the water-filling algorithm is performed simultaneously over all SISO subchannels.

3.5 Simulations and Results

In this section, the proposed approach will be illustrated by means of a numerical example.

3.5.1 Channel Model

The channel is assumed to be a 4×4 broadband MIMO channel whose responses are generated from a Saleh-Valenzuela model [61]. This statistical channel model of an indoor LAN environment describes a series of clustered reflections, whose arrival rate is governed by a Poisson process with an exponentially decaying amplitude. In turn, each cluster contains a number of rays, which are controlled by a second Poisson process in terms of their arrival times and an exponential decay for the rays' amplitudes. This model has been extensively used in the context of broadband communications and is therefore not further elaborated here; instead, the interested reader is referred to the original work by Saleh and Valenzuela [61] and extensive descriptions in [62, 63, 64].

For this set of simulations, the following parameters have been used for the Saleh-Valenzuela model: cluster arrival rate $\Lambda = 1/300$ ns^{-1}, ray arrival rate $\lambda = 0.2$ ns^{-1}, cluster power-decay time constant $\Gamma = 60$ ns, ray power-decay time constant $\gamma = 20$ ns and the observation time is 800 ns. The length of the MIMO channel is limited to $L + 1 = 11$ as the components of the channel CIR with higher indices are

statistically very small and can be neglected. The Frobenius norm of the channel matrix is set to unity. The simulations are performed over 50 random channel realisations. Figure 3.4 shows, as an example, the modulus of the CIR of one single channel realisation.

3.5.2 Performance of the MIMO system with $P = 1$

First consider the case when the number of polyphase components is $P = 1$ leading to $\mathbf{H}(z) = \mathbf{C}(z)$. The diagonalisation of $\mathbf{H}(z)$ leads to a nearly diagonal polynomial matrix $\mathbf{S}(z)$ whose coefficient moduli corresponding to the channel realisation in Figure 3.4 are shown in Figure 3.5. It can be seen from this figure that the off-diagonal elements of $\mathbf{S}(z)$ are very close to zero, which means in this example the matrix $\mathbf{H}(z)$ is pretty well diagonalised. The frequency responses of the subchannels corresponding to the diagonal elements of $\mathbf{S}(z)$ in Figure 3.5 are shown in Figure 3.6. It can be seen from the figure that the spectral majorisation of $\mathbf{H}(z)$ makes these frequency responses ordered in descending value. Defining the channel power gain of an FS subchannel as the square of the norm of the CIR, one can see that the subchannels possess different values for their power gains. In the example of Figure 3.6, power gains of subchannels share, in the order of their indices, 64.2%, 25.2%, 9.6% and 1% of the overall MIMO channel power gain. Furthermore, as it is shown in Section 3.3.1, the BSVD algorithm is obtained from two BEVD algorithms which in turn rely on sequences of delays and rotations, these operations, as it can be seen later in Chapter 5, help to make some subchannels become flatter and have higher gain. Thus one can note from Figure 3.6 that as the subchannel index is increasing, the subchannel becomes more dynamic. This means that the subchannel order as well as the amount of ISI in each FS subchannel are increasing with the channel index. Also one can see that if the transmission is performed only on the subchannels which have high gain then the amount of ISI one has to deal with is smaller than that of the whole original MIMO channel. In other words, by making some SISO subchannels to be less dynamic, the BSVD can help to reduce the amount

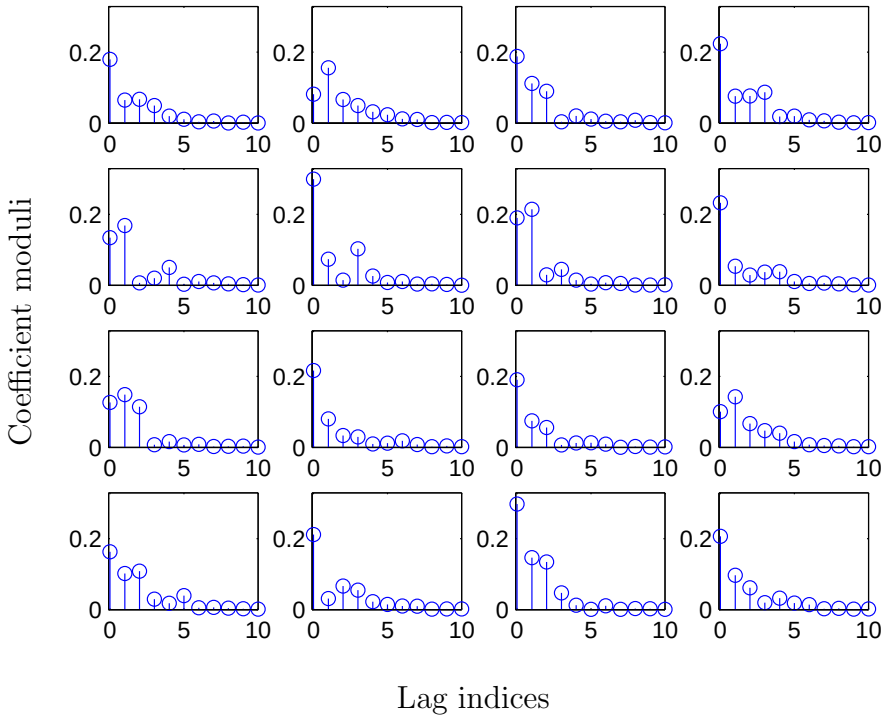

Figure 3.4: Moduli of the coefficients of channel matrix $\mathbf{C}(z)$.

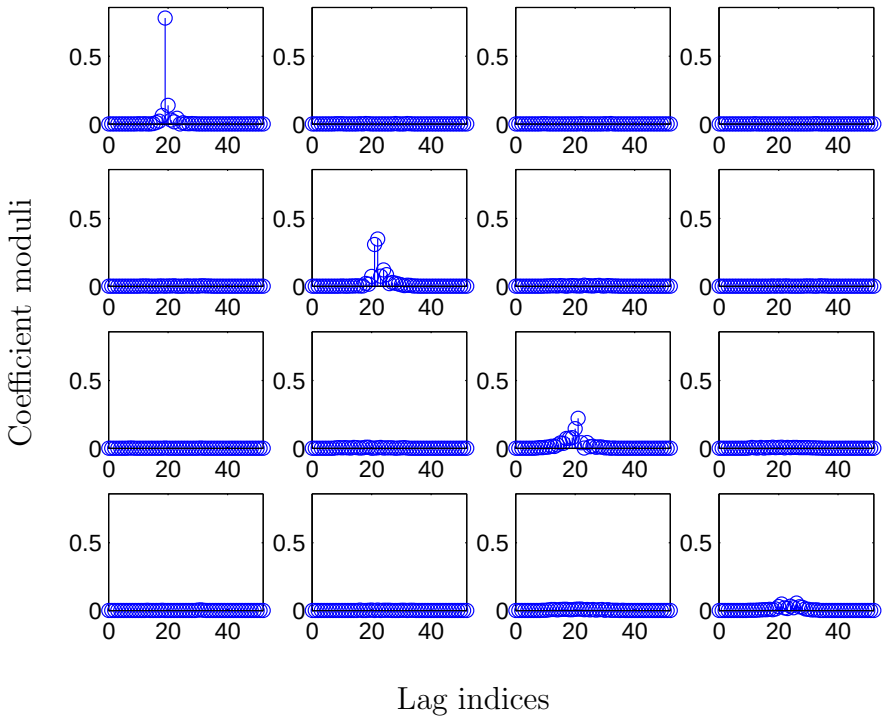

Figure 3.5: Moduli of the coefficients of $\mathbf{S}(z)$.

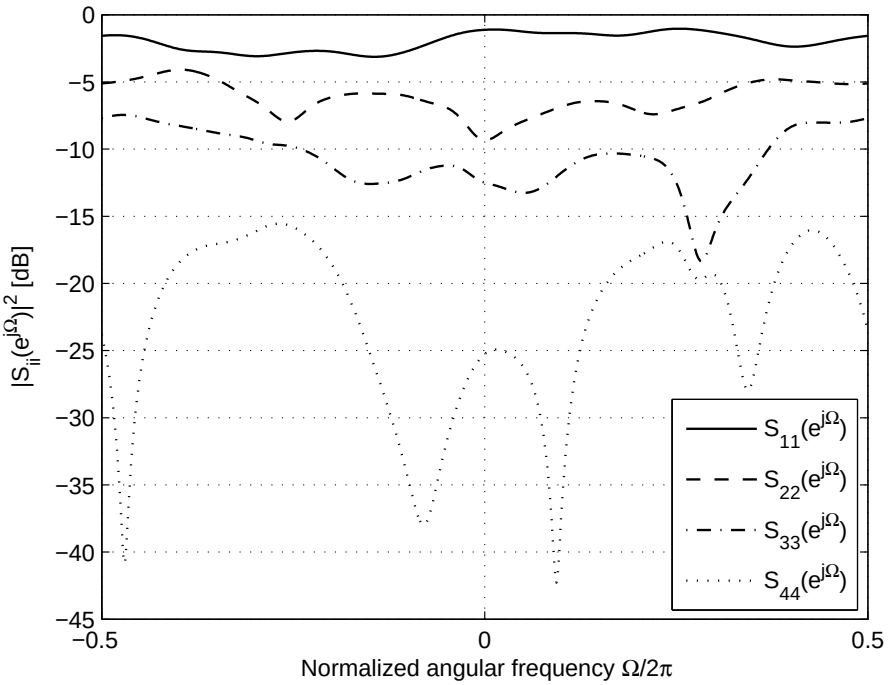

Figure 3.6: Frequency responses $S_{ii}(e^{j\Omega})$ of subchannels after diagonalisation of $\mathbf{H}(z)$.

of ISI in a broadband MIMO channel. For the above example, it can be seen that by discarding the fourth SISO subchannel and only use the first three subchannels for transmission, a part of the ISI in the MIMO dispersive channel can be reduced by sacrifying only 1% of the power gain of the overall MIMO channel.

3.5.2.1 Design with linear precoding and equalisation

First the design based on the BSVD and linear joint optimal precoding and equalisation as mentioned in subsection 3.4 is considered. The designs of MMSE/CP and MaxIR linear precoding and equalisation for MIMO systems proposed in [25] which is an extension of the designs in [26, 27] for MIMO scenarios are taken as benchmarks. Note that these designs have been also reviewed in Section 2.4. In these benchmark designs, a transmitted data block consists of 168 symbols, of which $4L = 40$ symbols redundancy are required for IBI cancellation. The input block size is chosen to be

$N = 96$, which leads to a code rate of 0.57. The loss in channel power gain due to IBI cancellation therefore is $40/168 \approx 24\%$.

For each subchannel in the proposed design, MMSE/CP and MaxIR precoder and equaliser pairs are computed according to subsection 2.2. Since the sampling rate on every FS subchannel must be equal, P_i is chosen such that $P_1 = P_2 = P_3 = P_4$. The parameter M_i will be calculated from $M_i = P_i - L_i$ and since the subchannels have different orders [1], one can have $M_1 > M_2 > M_3 > M_4$ or in other words, the FS subchannel with high gain also has large M_i. The input block size N is chosen so that the code rate is equal to that of the benchmark design.

Transmit power in the proposed design is chosen to be equal to the transmit power in the benchmark design and is allocated according to water-filling algorithms performed across all the FS SISO subchannels. These water-filling algorithms will decide which portion of the bandwidth of each SISO subchannel will be used for transmission. Thus the parameter N_i is decided by water-filling algorithms under the constraint $\sum_i N_i = N$.

The average power gain share over 50 random channel realisations is 64%, 26%, 9%, 1% for the first, the second, the third and the fourth SISO subchannels, respectively. The average orders of the SISO FS subchannels are given as $L_1 = 3,\ L_2 = 5$ and $L_3 = 10$ thus the total loss in channel power gain due to IBI cancellation is

$$(L_1/P_1)0.64 + (L_2/P_2)0.26 + (L_3/P_3)0.09 + 0.01 = 10\%$$

which is obviously less than the loss of 24% in the benchmark design.

In order to assess the result of the MMSE/CP design, which scales the transmit power on the flat subchannels to minimise the sum of MSE on all the flat subchannels, one can measure the average BER in terms of SNR figure suggested in [26], which sets the afforded transmit energy per bit against the channel noise measured

[1] Note that the order of a SISO subchannel mentioned here is the order of a portion of the CIR shown in Figure 3.5 which contains more than 99.9% of the subchannel power gain

at the receiver.

$$\text{SNR} = \frac{P_0}{NK_b\sigma_v^2} \quad . \tag{3.47}$$

where K_b is the number of bits per symbol. In this simulation, the BPSK modulation with $K_b = 1$ is chosen for both designs. It can clearly be noted from Figure 3.7 that with the same transmit power, the proposed design has a better BER performance than that of the benchmark. For example, at the BER of 10^{-3} the proposed design can achieve a gain of about 2 dB in its SNR compared with the benchmark design.

Next, the performance of the proposed design which uses the MaxIR optimal precoding and equalisation is compared with the performance of the linear design under the same optimal criteria in [25] (Lemma 2). The mutual information of the whole MIMO system, which is calculated as

$$I = \frac{1}{N}\sum_{j=1}^{N}\log_2(1+\rho_j) \ , \tag{3.48}$$

is illustrated as a function of SNR in Figure 3.8, highlighting the ability of the proposed design to achieve higher mutual information than that of the benchmark. For example, at the SNR = 15 dB the proposed design can achieve a mutual information of nearly 3.9 bits/sec/Hz while the benchmark design can achieve a mutual information of about 3.1 bits/sec/Hz.

Finally, the data throughput when Gray coded QAM modulation with a bit loading applied for all flat subchannels under the QoS constraint $P_{se} \leq P_{se,\max} = 10^{-5}$ is measured. With the symbol error probability of the two designs vs SNR being well kept under the upper bound $P_{se,\max} = 10^{-5}$ as shown in Figure 3.9, the result in Figure 3.10 underlines that the proposed design can achieve higher data throughput than that of the benchmark design while still satisfying the QoS constraint. For example, at the SNR = 20 dB, the proposed design can achieve a data throughput of about 150 bits/sampling period while the data throughput of the benchmark design is nearly 110 bits/sampling period.

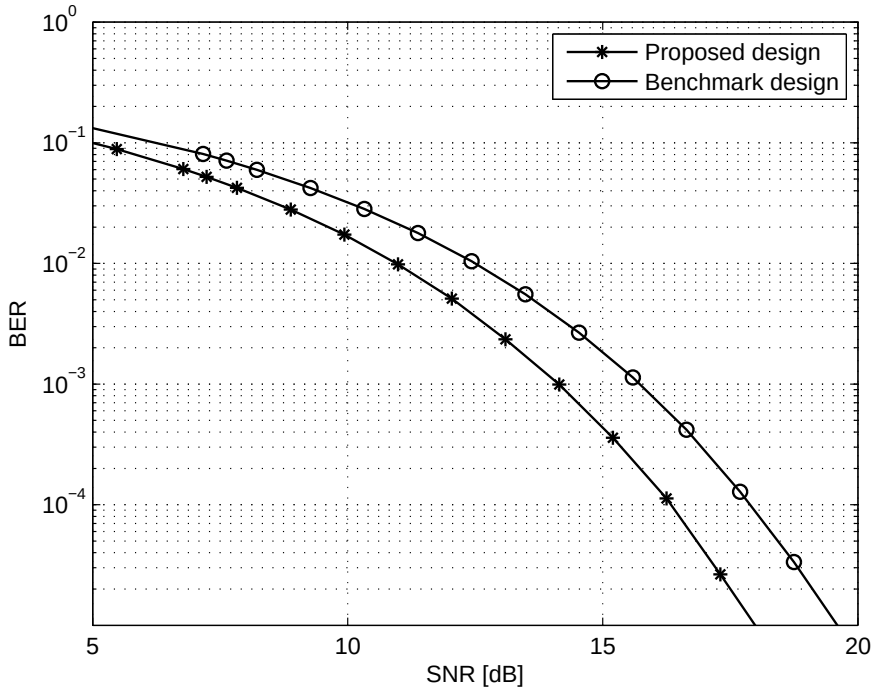

Figure 3.7: BPSK modulated, uncoded BER versus SNR for the proposed design and for the benchmark design in Section 2.4.

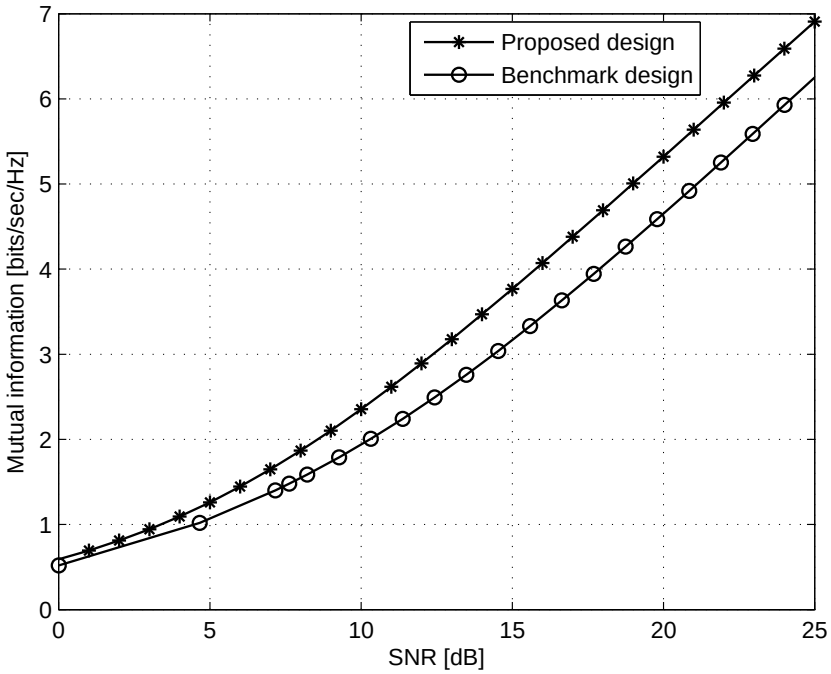

Figure 3.8: Mutual information versus SNR for the proposed design and for the benchmark design in Section 2.4.

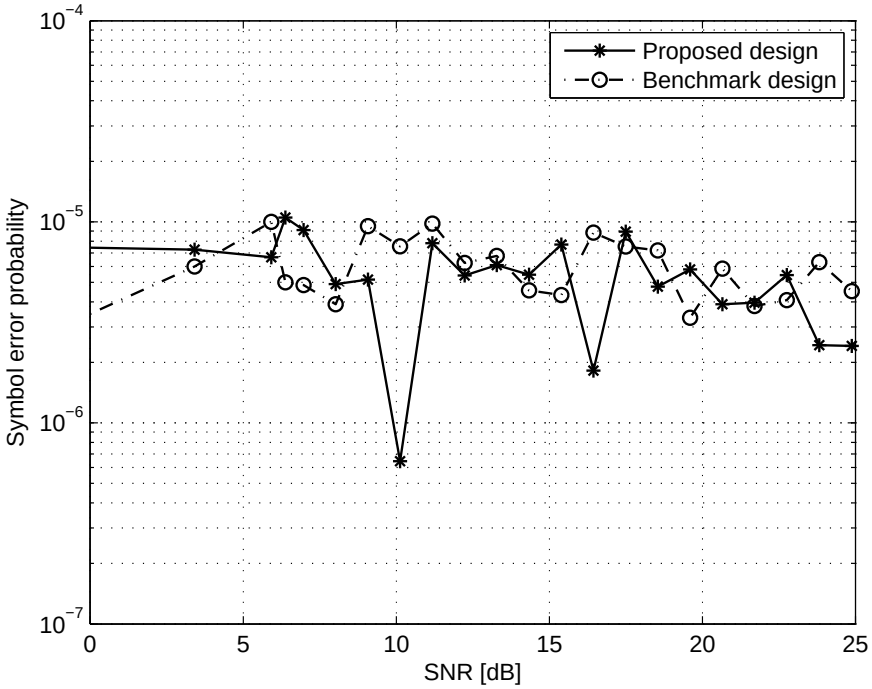

Figure 3.9: Symbol error rate versus SNR for the proposed design and for the benchmark design in Section 2.4.

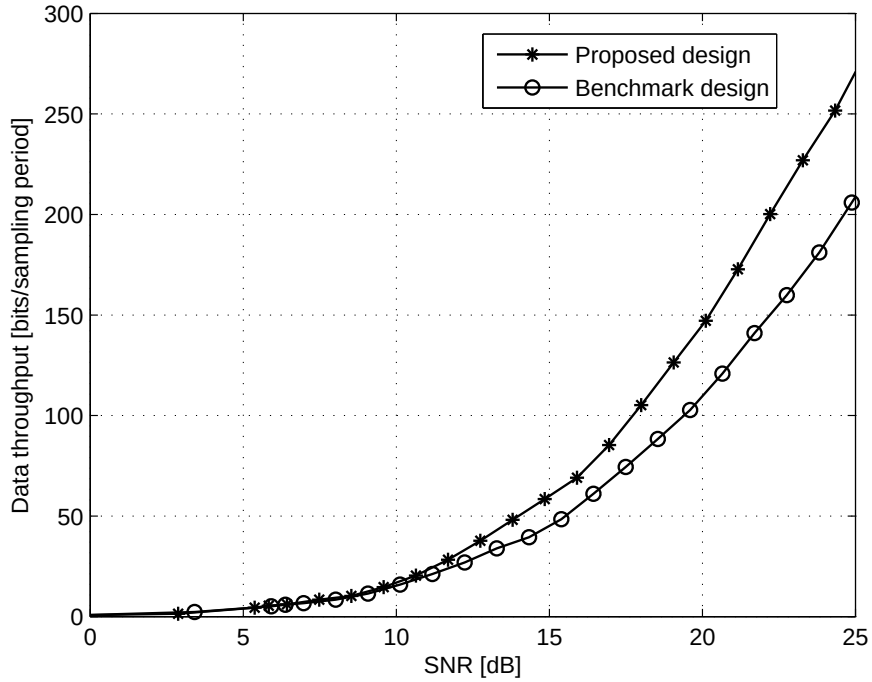

Figure 3.10: Data throughput versus SNR for the proposed design and for the benchmark design in Section 2.4.

3.5.2.2 Design with joint optimal precoding and BDFE

To obtain a more comprehensive view on the proposed approach, the performance of the BSVD approach with joint optimal precoding and BDFE for SISO subchannels as shown in subsection 3.4.2 will be compared with the performance of the MMSE joint optimal precoder and BDFE proposed in [32] applied for broadband MIMO as a benchmark.

The channel model is chosen to be similar to the one used in the previous subsection. The benchmark design also has the transmitted data blocks containing 168 symbols, of which $4L = 40$ symbols are used as redundancy for IBI cancellation. The input block length is also chosen to be $N = 96$ leading to the input code rate of 0.57.

Similar to the case of linear design in the previous subsection, the length of the transmitted blocks on all SISO subchannels is chosen such that $P_1 = P_2 = P_3 = P_4$, and therefore one also can write $M_1 > M_2 > M_3 > M_4$ since the order of the SISO FS subchannels is increasing with the channel index and $M_i = P_i - L_i$.

The transmit power is allocated according to water-filling across all the FS SISO subchannels for a total of $N = \sum_i N_i$ whereby the N_i can vary across subchannels. This ensures that both the benchmark and the proposed design afford the same transmit power and redundancy across the given MIMO channel.

The average BER in terms of SNR figure, which is also given as in (3.47), of the proposed design and of the benckmarker is illustrated on Figure 3.11. In this simulation, Gray coded 4-QAM modulation with $K_b = 2$ is chosen for both designs. Again, one can see from Figure 3.11 that with the same transmit power, the proposed BSVD based design exhibits better BER performance than that of the benchmark. For example, at the BER $= 10^{-3}$, the proposed design can achieve a gain of about 1 dB compared with the benchmark design.

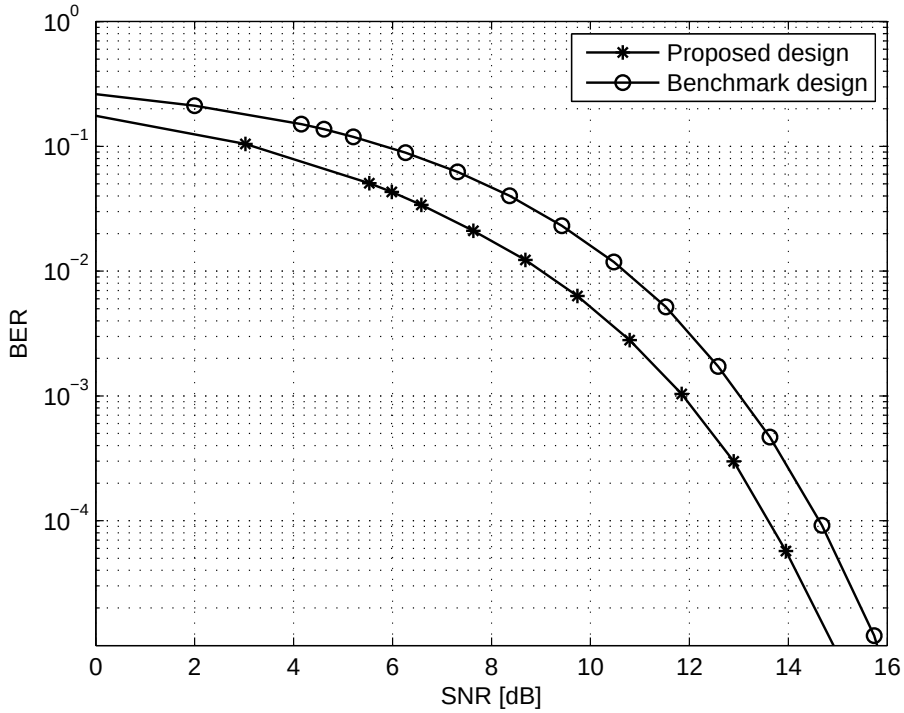

Figure 3.11: Data throughput versus SNR for the proposed design and for the benchmark design in [25].

3.5.3 Performance of the MIMO system with $P > 1$

When $P > 1$, the size of the pseudo-circulant matrix $\mathbf{H}(z)$ increases by a factor P and its order drops to $\lceil \frac{L}{P} \rceil$. From equation (3.2), one can see that the number of elements of $\mathbf{H}(z)$ is $TP \cdot RP \cdot \lceil L/P \rceil \propto P$ thus compared with $\mathbf{C}(z)$, $\mathbf{H}(z)$ can be expected to consume a higher number of iterations to approximate a BSVD.

As an example, let us set $P = 2$ and consider the decomposition of a matrix $\mathbf{H}(z)$ based on the same channel matrix $\mathbf{C}(z)$ which provided the result for $P = 1$ in Figure 3.6. The frequency responses of the decoupled FS SISO subchannels of the approximately diagonalised $\mathbf{S}(z)$ obtained after 800 iterations where no further significant convergence is observed are illustrated in Figure 3.12. One can see from the figure that with $P = 2$, after 800 iterations the BSVD computation algorithm cannot achieve a good spectral majorisation, the resulting subchannels are more

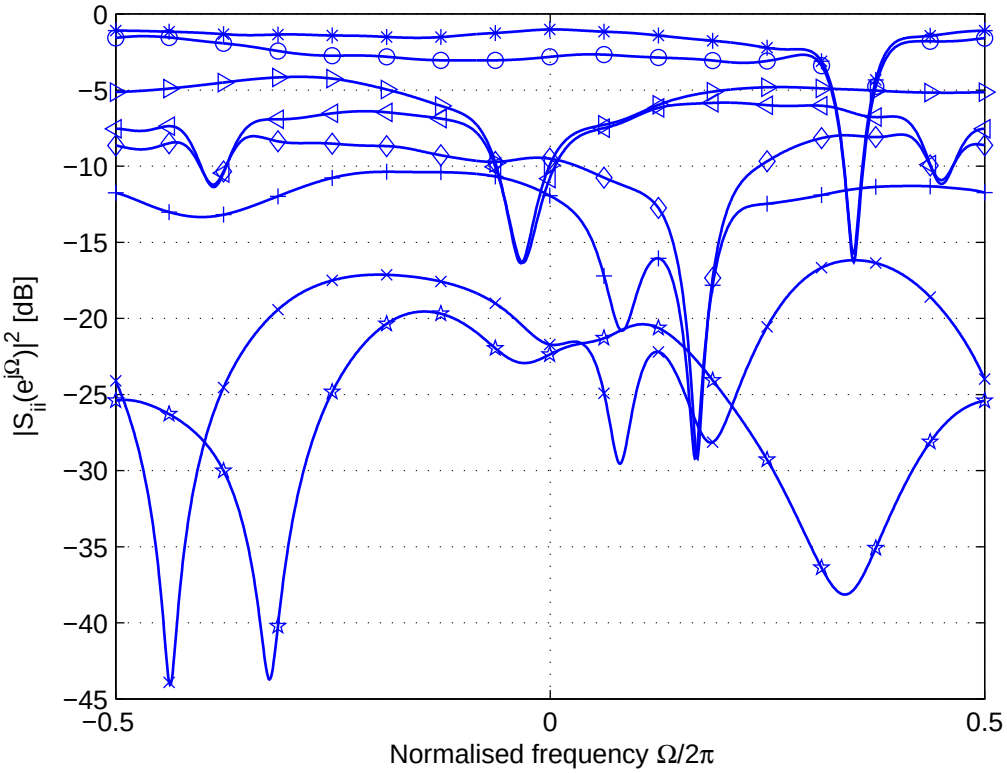

Figure 3.12: Frequency responses of the decoupled SISO subchannels when $P = 2$. $*$: $S_{11}(e^{j\Omega})$, $\circ$: $S_{22}(e^{j\Omega})$, $\triangleright$: $S_{33}(e^{j\Omega})$, $\triangleleft$: $S_{44}(e^{j\Omega})$, $\diamond$: $S_{55}(e^{j\Omega})$, $+$: $S_{66}(e^{j\Omega})$, $\times$: $S_{77}(e^{j\Omega})$, $\star$: $S_{88}(e^{j\Omega})$

dynamic and even the first and the second subchannels also have some deep fades in their frequency responses.

To see how well $\mathbf{S}(z)$ is diagonalised, a matrix $\mathbf{G}_S$ which has the same size as $\mathbf{S}(z)$ and each element of $\mathbf{G}_S$ is equal to the sum of the squares of polynomial coefficients of the corresponding element of $\mathbf{S}(z)$ is considered.

With the matrix $\mathbf{S}(z)$ obtained after 800 iterations, the value of $\mathbf{G}_S$ is given as

$$\mathbf{G}_S = \begin{bmatrix} \mathbf{0.694} & 0.0186 & 0.0000 & 0.0000 & 0.0000 & 0.0000 & 0.0000 & 0.0000 \\ 0.0186 & \mathbf{0.5476} & 0.0000 & 0.0000 & 0.0000 & 0.0000 & 0.0000 & 0.0000 \\ 0.0000 & 0.0000 & \mathbf{0.2907} & 0.0079 & 0.0000 & 0.0000 & 0.0000 & 0.0000 \\ 0.0000 & 0.0000 & 0.0079 & \mathbf{0.1963} & 0.0053 & 0.0000 & 0.0000 & 0.0000 \\ 0.0000 & 0.0000 & 0.0000 & 0.0053 & \mathbf{0.1172} & 0.0023 & 0.0000 & 0.0000 \\ 0.0000 & 0.0000 & 0.0000 & 0.0000 & 0.0023 & \mathbf{0.0627} & 0.0004 & 0.0001 \\ 0.0000 & 0.0000 & 0.0000 & 0.0000 & 0.0000 & 0.0005 & \mathbf{0.0135} & 0.0011 \\ 0.0000 & 0.0000 & 0.0000 & 0.0000 & 0.0000 & 0.0001 & 0.0012 & \mathbf{0.0059} \end{bmatrix} \tag{3.49}$$

The ratio between the sum of the on-diagonal elements and the sum of the off-diagonal elements of $\mathbf{G}_S$ is taken as a measure of how close $\mathbf{S}(z)$ is to a diagonal matrix. From the value of $\mathbf{G}_S$ given above, one can see that this ratio can reach a value of only about 27 after 800 iterations while for the same channel matrix with $P = 1$, this ratio can reach a value of about 323 after only 190 iterations. This means in case $P = 2$, the effectiveness of the BSVD computation algorithm is reduced and the algorithm requires a much higher number of iterations than in the case $P = 1$ to achieve a good diagonalisation of $\mathbf{S}(z)$. The remaining CCI between the decoupled subchannels in the case $P > 1$ is higher than for the case $P = 1$. This is due to the slow convergence of the BEVD computation algorithm in diagonalising the para-Hermitian matrices constructed from the pseudo-circulant matrices. The interested reader is referred to Section 5.1.2 for more details on this particular property of BEVD computation algorithm.

To further investigate the system performance when $P > 1$, the MMSE linear precoding and equalisation design in subsection 3.4.1 is applied to the SISO subchannels and the BER performance for the case $P = 2$ is compared with the BER performance when $P = 1$. To keep the sampling rate on the MIMO channel unchanged, the transmit block size on the subchannels P_i is chosen to be half of that of the case $P = 1$. The input block length N is chosen such that the code rates in

both cases are equal. Figure 3.13 compares the BER performance measured against SNR in the case when $P = 2$ and $P = 1$.

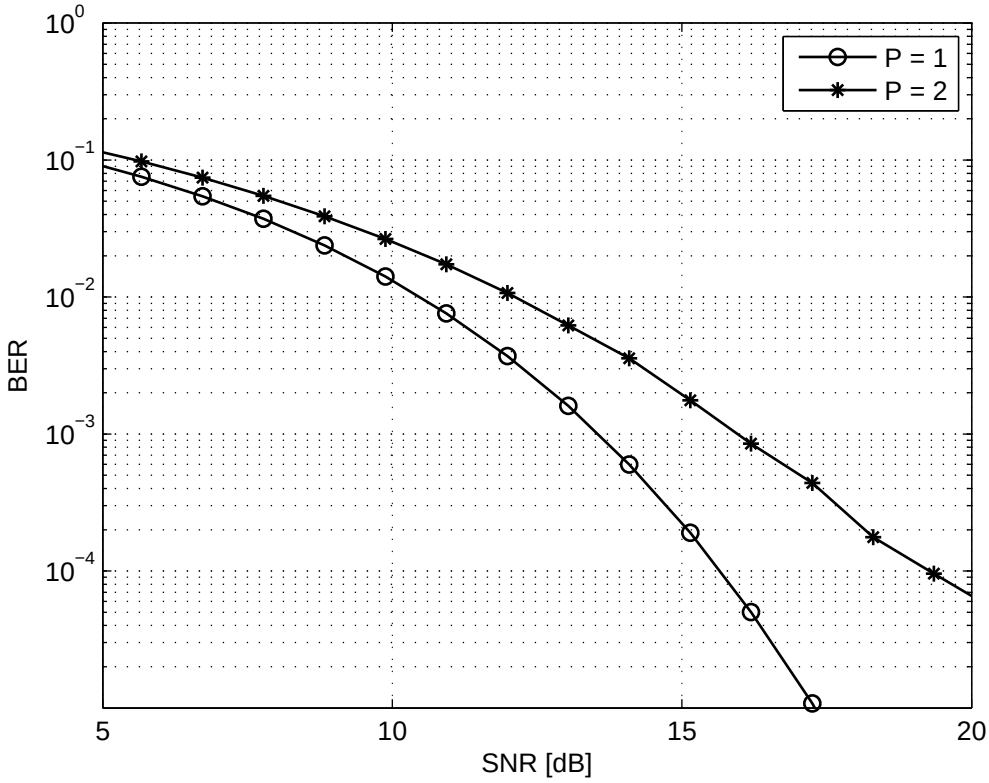

Figure 3.13: Comparison of the BER performance of proposed design when $P = 2$ and $P = 1$.

From Figure 3.13, one can see that the BER performance in case $P = 2$ is poorer than the BER performance in the case $P = 1$. This is due to the higher remaining CCI level as can be seen above. Moreover, the subchannels in this case are more dynamic, which means that the BSVD does not contribute to the elimination of ISI as in case $P = 1$. Also, the system complexity is much higher as the BSVD requires more iterations to decompose $\mathbf{H}(z)$ and subsequently results in precoding and equalising filter banks of higher orders.

3.6 Chapter Summary and Conclusion

In this chapter, a new design of precoding and equalisation for broadband MIMO systems has been discussed. The design is based on two separate steps. First, the CCI imposed by the MIMO transmission system is suppressed by means of a BSVD, analogous to the procedure by which a standard SVD would be employed for a narrowband MIMO channel. However, unlike the standard SVD, the BSVD is applied to a polynomial matrix and provides decoupled but still dispersive subchannels. Second, SISO precoding and equalisation techniques are invoked in order to mitigate the ISI within the decoupled FS subchannels.

The simulation results show that in case $P = 1$ the BSVD can effectively suppress the CCI and produce some SISO FS subchannels which have high power gain and are rather flat in the frequency domain, therefore, one can effectively remove a part of ISI in the system by losing a very small amount of channel power gain. This makes the proposed scheme outperform the linear precoding and equalisation scheme proposed in [25] in term of BER performance, mutual information and data throughput. In the case that the joint optimal precoding and BDFE is applied for the decoupled subchannels, the proposed design also has better BER performance compared with the performance of the benchmark design.

When $P = 2$, however, the number of elements in $\mathbf{H}(z)$ becomes larger and the diagonality of $\mathbf{S}(z)$ is much poorer than that of the case $P = 1$ although the BSVD computation algorithm has used a number of iterations which is about four times higher than that of the case $P = 1$. This leads to a higher amount of remaining CCI and the resulting SISO subchannels are more dynamic, therefore in this case the BSVD cannot help to effectively reduce ISI and CCI, leading to a poorer BER performance compare with that of the previous case when $P = 1$.

In the next chapter, some different precoding and equalisation schemes which can either work with the guard intervals that are shorter than the channel order or can better employ the channel resource so that the error performance of the system can

be improved will be proposed and discussed.

Chapter 4

Advanced Precoding and Equalisation Schemes

As it has been pointed out in previous chapters, although the use of guard intervals in block transmission based precoding and equalisation schemes is very effective in IBI eliminating, it reduces the spectral efficiency of the transmission system. In this chapter, a number of approaches to tackle this drawback will be considered initially for the broadband SISO and later for the broadband MIMO case. Firstly, the Section 4.1 will propose two designs of joint optimal precoding and BDFE with low redundancy which can work when the length of the guard intervals is shorter than the length of the CIR. Secondly, Section 4.2 will suggest some approaches to employ the redundancy in block transmission schemes in a more efficient way so that the system performance can be improved. Finally, the application of one of the approaches mentioned in Section 4.2 for the broadband MIMO case will be considered.

4.1 Jointly Optimal precoder and block decision feedback equaliser design with low redundancy

In this section a filter bank based design for jointly optimal precoding and block decision feedback equalisation is proposed. Precoding and equalisation using filter banks typically is block based, and redundancy needs to be injected into the transmission in order to avoid inter-block interference. Here the case where spectral efficiency demands low levels of redundancy such that some residual IBI remains is targeted. For the proposed system, two recently reported ideas — one on equalisation in the presence of IBI, and one on jointly optimal design of the overall system in the absence of IBI — are combined. The result is a jointly optimal design in terms of both zero-forcing and minimum mean square error criteria that can operate in the presence of IBI, i.e. at low levels of redundancy and with high spectral efficiency. It is shown by means of simulation results, that the proposed system can provide significantly better performance than a benchmark design.

4.1.1 Motivation

Block transmission has been shown to be a very effective method to combat ISI caused by frequency selective channels. However, in order to eliminate IBI, block transmission systems always require an amount of redundancy in the form of either cyclic prefix or zero padded intervals whose length must be equal or larger than the channel order. This requirement makes it difficult for block transmission systems to be applied to channels with a long impulse response since a long guard interval will decrease the bandwidth efficiency.

One approach to cope with long CIR is channel shortening [65], where a time domain equaliser rather than inverting the channel reduces the effective channel length to a very short support. The shortened support permits the deployment of complex detectors such as the Viterbi algorithm, although part of the channel

energy (and therefore capacity) is lost [65]. In [66], an approach to design channel shortening receive filter and joint transmit-receive filters in frequency domain for broadband MIMO channels has been proposed. Compared with time-domain designs, the frequency-domain designs in [66] have much lower complexity and can provide a better BER performance. The problem of long CIRs has also been approached in [67], where a Wiener filter is employed as equaliser and a precoder minimises the mean square error of the system. In [68] Stamoulis *et. al.* have proposed a block decision feedback equaliser for the case where IBI is present, e.g. if the redundancy in the transmission does not allow a guard interval that is longer than the CIR order. These BDFEs can work well even with small transmit redundancy, however the precoder in [68] has been chosen independently from the equaliser and the problem of joint optimisation of precoder and equaliser is still open. In [32], Xu *et. al.* have proposed jointly optimal designs for the precoder and BDFE in the absence of IBI, which can achieve much better performance than linear designs in [25] but still require sufficient redundancy to entirely suppress IBI.

Based on a combination of the designs in [68] and [32], a precoding and BDFE scheme which can work in the case of insufficient redundancy to suppress IBI is proposed in this section. Due to the joint optimisation of the precoder and equaliser, the proposed design can perform better than the designs in [68] even when the latter use optimal linear zero-forcing (ZF) or minimum mean-square error (MMSE) precoders proposed in [25].

The section is organised as follows. In Section 4.1.2, the system model and its components are described. Section 4.1.3 addresses the proposed jointly optimal precoder and BDFE design, while Section 4.1.4 considers the designs of BDFEs as proposed in [68] as well as the optimal linear precoders proposed in [25]. The combination of the latter two designs form the benchmarks for a numerical example provided in Section 4.1.5.

4.1.2 System model

Consider a block transmission system over an FIR channel as illustrated in Figure 4.1.

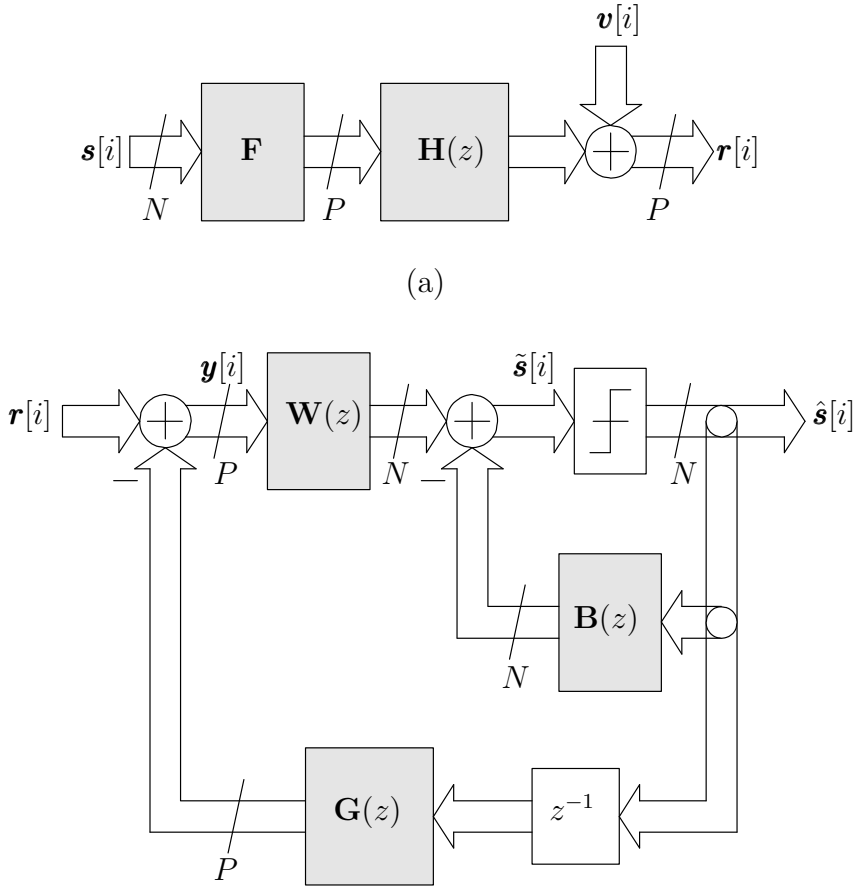

Figure 4.1: System model comprising of (a) precoder, channel and (b) equaliser.

The channel is assumed to be stationary with CIR coefficients $\{c[0], \ldots, c[L]\}$; $(c[0], \ldots, c[L] \neq 0)$, where L is the channel order. With the input symbol stream, $s[n]$, and the sampled version of the received signal, $r[n]$, one can define the input symbol blocks as $\boldsymbol{s}[i] = [s[iN], \ldots, s[iN+N-1]]^{\mathrm{T}}$, the symbol blocks at the receiver input as $\boldsymbol{r}[i] = [r[iP], \ldots, r[iP+P-1]]^{\mathrm{T}}$, the symbol blocks at the input of the feedforward filter bank as $\boldsymbol{y}[i] = [y[iP], \ldots, y[iP+P-1]]^{\mathrm{T}}$, the symbol blocks before the

decision device as $\tilde{\boldsymbol{s}}[i] = [\tilde{s}[iN], \ldots, \tilde{s}[iN+N-1]]^{\mathrm{T}}$, and the output symbol blocks as $\hat{\boldsymbol{s}}[i] = [\hat{s}[iN], \ldots, \hat{s}[iN+N-1]]^{\mathrm{T}}$. Together with $\boldsymbol{x}[i]$, the blocks of noise samples are defined as $\boldsymbol{v}[i] = [v[iP], \ldots, v[iP+P-1]]^{\mathrm{T}}$.

The input symbol blocks $\boldsymbol{s}[i]$ are mapped into transmitted blocks of size P by the precoder $\mathbf{F} \in \mathbb{C}^{P \times N}$, which has the following structure

$$\mathbf{F} = \begin{bmatrix} \mathbf{F}_0 \\ \mathbf{0}_{(P-M)\times N} \end{bmatrix} \quad , \tag{4.1}$$

where $\mathbf{F}_0$ is an $M \times N$ matrix, $P \geq M \geq N$, corresponding to the optimal precoder proposed in [32]. The form of $\mathbf{F}$ in equation (4.1) shows that an amount of redundancy in the form of $P - M$ zeros is inserted into each transmitted block. In the case of low redundancy, defined by $P - M < L$, the redundancy helps to reduce only a part of IBI but not to entirely eliminate it.

As it has been explained in Section 2.1, due to the blocking and unblocking operations at the channel input and output, the channel can be described by a polynomial pseudo-circulant matrix $\mathbf{H}(z) = \sum_{n=0}^{\infty} \mathbf{H}_n z^{-n}$. When $P > L$, the polynomial order of $\mathbf{H}(z)$ is one, and the symbol blocks $\boldsymbol{y}[i]$ at the input of the feed-forward filter bank are given by

$$\boldsymbol{y}[i] = \mathbf{H}_0 \mathbf{F} \boldsymbol{s}[i] + \mathbf{H}_1 \mathbf{F} \boldsymbol{s}[i-1] - \mathbf{G}_1 \hat{\boldsymbol{s}}[i-1] + \boldsymbol{v}[i] \tag{4.2}$$

where $\mathbf{H}_0$ and $\mathbf{H}_1$ are $P \times P$ matrices given by (2.13) and (2.14). With $P > L$, the first feedback filter bank $\mathbf{G}(z) = \sum_{n=1}^{\infty} \mathbf{G}_n z^{-n}$ suffices to be of non-polynomial form and removes the remaining IBI from the received data stream by setting $\mathbf{G}_1 = \mathbf{H}_1 \mathbf{F}$. Assuming that the past decisions are correct, one can re-write (4.2) as

$$\boldsymbol{y}[i] \;=\; \mathbf{H}_0 \mathbf{F} \boldsymbol{s}[i] + \boldsymbol{v}[i] \;=\; \mathbf{H}_M \mathbf{F}_0 \mathbf{s}[i] + \boldsymbol{v}[i] \quad , \tag{4.3}$$

where $\mathbf{H}_M$ contains the first M columns of $\mathbf{H}_0$, and obtain

$$\tilde{\boldsymbol{s}}[i] = \mathbf{W}_0 \mathbf{H}_M \mathbf{F}_0 \mathbf{s}[i] + \mathbf{W}_0 \mathbf{v}[i] - \mathbf{B}_0 \hat{\boldsymbol{s}}[i] \quad . \tag{4.4}$$

In the proposed design, the feed-forward filter is set as $\mathbf{W}(z) = \mathbf{W}_0$ whereby $\mathbf{W}_0$ is given by equation (4.9) or (4.16). Similarly, the inner feedback filter bank is set

to non-polynomial form $\mathbf{B}(z) = \mathbf{B}_0$, $\mathbf{B}_0$ is given by equation (4.8) or (4.15), and aims to cancel the interference between symbols within each block. This interference is referred to as intra-block ISI. The feedback filter bank $\mathbf{B}_0$ works such that the symbols in each block $\tilde{\boldsymbol{s}}[i]$ are detected sequentially, starting from the Nth symbol, whereby the detected symbols are weighted by the feedback filter bank and removed from $\boldsymbol{z}[i]$ prior to the detection of the next symbol. This is referred to as *successive cancellation* [68, 32] and the condition that makes it possible is the feedback filter bank matrix $\mathbf{B}_0$ must be *strictly upper triangular*.

With the assumption that the past decisions are correct, the error between the symbols at the input of the decision device, $\tilde{\boldsymbol{s}}[i]$, and the input symbols, $\boldsymbol{s}[i]$, is

$$\boldsymbol{e}[i] = \tilde{\boldsymbol{s}}[i] - \boldsymbol{s}[i] = (\mathbf{W}_0\mathbf{H}_M\mathbf{F}_0 - \mathbf{B}_0 - \mathbf{I})\boldsymbol{s}[i] + \mathbf{W}_0\mathbf{v}[i]. \tag{4.5}$$

The covariance matrix of the error, $\mathbf{R}_{ee} = E\{\boldsymbol{e}[i]\boldsymbol{e}^{\mathrm{H}}[i]\}$, is given by

$$\mathbf{R}_{ee} = (\mathbf{W}_0\mathbf{H}_M\mathbf{F}_0 - \mathbf{B}_0 - \mathbf{I})(\mathbf{W}_0\mathbf{H}_M\mathbf{F}_0 - \mathbf{B}_0 - \mathbf{I})^H + \mathbf{W}_0\mathbf{R}_{vv}\mathbf{W}_0^H \quad , \tag{4.6}$$

where the input signal $\boldsymbol{s}[i]$ is assumed to be uncorrelated with unit variance, and the noise covariance matrix is given by $\mathbf{R}_{vv}$.

4.1.3 Joint precoding and BDFE with low redundancy

After the remaining IBI has been removed by the first feedback loop, the design of joint optimal precoder and the BDFE proposed in [32] is applied to remove intra-block ISI. With equation (4.2) being exact for the non-IBI case, and together with $\mathbf{H}_M$, one can now derive the precoder matrix $\mathbf{F}_0$ as well as the feed-forward and feedback matrices $\mathbf{W}_0$ and $\mathbf{B}_0$, such that the system MSE can achieve its minimised lower bound.

4.1.3.1 ZF Joint Optimal Precoding and BDFE

The design problem for a precoder and BDFE equaliser that are jointly optimal in the zero-forcing (ZF) sense can be stated as [32]

$$\begin{aligned} \min_{\mathbf{F}_0,\mathbf{W}_0,\mathbf{B}_0} \quad & \operatorname{trace}(\mathbf{R}_{ee}) \\ \text{subject to} \quad & \operatorname{trace}(\mathbf{F}_0\mathbf{F}_0^{\mathrm{H}}) = P_0 \\ & \mathbf{W}_0\mathbf{H}_M\mathbf{F}_0 = \mathbf{B}_0 + \mathbf{I} \\ & \mathbf{B}_0 \text{ is strictly upper triangular,} \end{aligned}$$

where P_0 is the transmit power.

The optimal precoder matrix for this case has the form

$$\mathbf{F}_0 = \sqrt{P_0/N}\,\mathbf{V}_N\mathbf{\Theta} \quad , \tag{4.7}$$

and the feedback and feedforward matrices of the BDFE are given by

$$\mathbf{B}_0 = \left(\prod_{i=1}^{N}\lambda_{ii}\right)^{-\frac{1}{2N}}\mathbf{R} - \mathbf{I} \tag{4.8}$$

$$\mathbf{W}_0 = (\mathbf{B}_0 + \mathbf{I})(\mathbf{H}_M\mathbf{F}_0)^{\dagger} \quad , \tag{4.9}$$

whereby $\mathbf{V}_N$ contains the first N columns of $\mathbf{V}$ obtained from the EVD

$$\mathbf{H}_M^{\mathrm{H}}\mathbf{R}_{vv}^{-1}\mathbf{H}_M = \mathbf{V}\mathbf{\Lambda}\mathbf{V}^{\mathrm{H}} \, , \tag{4.10}$$

$\lambda_{ii},\ (i = 1 \ldots N)$ are the diagonal elements of $\mathbf{\Lambda}$ and $\mathbf{R}$ and $\mathbf{\Theta}$ are obtained from the following geometric mean decomposition

$$\mathbf{\Lambda}^{1/2} = \mathbf{U}\mathbf{R}\mathbf{\Theta}^{\mathrm{H}} \, . \tag{4.11}$$

The details on the derivation of the above optimal precoder and equaliser are provided in appendix A.1.

4.1.3.2 MMSE Joint Optimal Precoding and BDFE

The MSE precoder and BDFE equaliser are required to fulfill the following design problem for the case of joint optimality in the MMSE sense [32]:

$$\begin{aligned} \min_{\mathbf{F}_0,\mathbf{W}_0,\mathbf{B}_0} \quad & \text{trace}(\mathbf{R}_{ee}) \\ \text{subject to} \quad & \text{trace}(\mathbf{F}_0\mathbf{F}_0^{\text{H}}) = P_0 \\ & \mathbf{W}_0 = (\mathbf{B}_0 + \mathbf{I})\mathbf{R}_{sy}\mathbf{R}_{yy}^{-1} \\ & \mathbf{B}_0 \text{ is strictly upper triangular.} \end{aligned}$$

where

$$\mathbf{R}_{sy} = (\mathbf{H}_M\mathbf{F}_0)^{\text{H}} \tag{4.12}$$

$$\mathbf{R}_{yy} = (\mathbf{H}_M\mathbf{F}_0)(\mathbf{H}_M\mathbf{F}_0)^{\text{H}} + \mathbf{R}_{vv} \quad . \tag{4.13}$$

In this case, the optimal precoder that helps to minimise the MSE lower bound and to achieve that bound is then given by

$$\mathbf{F}_0 = \mathbf{V}_q\mathbf{\Phi}'\mathbf{\Theta} \, , \tag{4.14}$$

and the feedback and feedforward filterbanks under MMSE criterion are given by

$$\mathbf{B}_0 = \mathbf{R} - \mathbf{I} \tag{4.15}$$

$$\mathbf{W}_0 = \sigma_e\mathbf{R}\mathbf{R}_{sy}\mathbf{R}_{yy}^{-1} \tag{4.16}$$

For more details on the above optimal precoder and equaliser as well as their derivation, please refer to the appendix A.2.

In the next subsection, some state-of-the-art designs in the literature, which are taken as benchmark for the proposed designs, will be addressed.

4.1.4 Existing BDFE Systems with Optimal Linear Precoding

A BDFE which can work in the presence of remaining IBI has been proposed by Stamoulis *et. al* in [68], which is referred to as IBI-BDFE and classified into zero-forcing (ZF-) IBI-BDFE and MMSE-IBI-BDFE. On the transmitter side, a precoder can be operated. Below the (locally) optimal ZF and MMSE linear precoders as proposed in [25] are utilised. These precoders are similar to those used by [68] except for an additional power constraint in order to be compatible with the approach developed in subsection 4.1.3.

4.1.4.1 ZF-IBI-BDFE

The ZF-IBI-BDFE system in [68] has a structure similar to the one in Figure 4.1(b), where the first feedback loop with a filter bank $\mathbf{G} = \mathbf{G}_1 = \mathbf{H}_1\mathbf{F}$ aims to cancel the remaining IBI. The feed-forward and feedback filter banks are designed to satisfy the ZF requirement

$$\mathbf{W}_0\mathbf{H}_0\mathbf{F} = \mathbf{B}_0 + \mathbf{I} \tag{4.17}$$

and the noise-whitening requirement

$$\mathbf{W}_0\mathbf{R}_{vv}\mathbf{W}_0^{\mathrm{H}} = \mathbf{\Sigma}\ , \tag{4.18}$$

where $\mathbf{\Sigma}$ is diagonal matrix and $\mathbf{B}_0$ is an upper-triangular matrix in order to permit sequential detection. Based on the Cholesky decomposition

$$(\mathbf{H}_0\mathbf{F})^{\mathrm{H}}\mathbf{R}_{vv}^{-1}(\mathbf{H}_0\mathbf{F}) = \mathbf{A}^{\mathrm{H}}\mathbf{\Sigma}\mathbf{A}\ \ , \tag{4.19}$$

where $\mathbf{A}$ is an upper triangular matrix with a unit diagonal, one can write [68]

$$\mathbf{B}_0 = \mathbf{A} - \mathbf{I} \tag{4.20}$$

$$\mathbf{W}_0 = \mathbf{\Sigma}^{-1}\mathbf{A}^{-H}(\mathbf{H}_0\mathbf{F})^{\mathrm{H}}\mathbf{R}_{vv}^{-1}\ \ . \tag{4.21}$$

4.1.4.2 MMSE-IBI-BDFE

Instead of using a separate feedback loop to remove ISI, the MMSE-IBI-BDFE system sets $\mathbf{G}(z) = \mathbf{0}$, and uses more complex feed-forward and feedback filter banks $\mathbf{W}(z)$ and $\mathbf{B}(z)$ to combat the inter-block interference, intra-block interference and noise. With $P \geq L$, the feed-forward filter bank in [68] is proposed to have three taps $\mathbf{W}_{-1}$, $\mathbf{W}_0$, $\mathbf{W}_1$ and the feedback filter bank also to have three taps $\mathbf{B}_{-1}$, $\mathbf{B}_0$ and $\mathbf{B}_1$. Equation (4.2) now is replaced by

$$\boldsymbol{y}[i] = \mathbf{H}_0\mathbf{F}\boldsymbol{s}[i] + \mathbf{H}_1\mathbf{F}\boldsymbol{s}[i-1] + \boldsymbol{v}[i] \ , \tag{4.22}$$

and the signal before the decision device $\tilde{\boldsymbol{s}}[i]$ is given by

$$\begin{aligned} \tilde{\boldsymbol{s}}[i] = \mathbf{W}_{-1}\,\boldsymbol{y}[i+1] + \mathbf{W}_0\,\boldsymbol{y}[i] + \mathbf{W}_1\,\boldsymbol{y}[i-1] - \\ - \mathbf{B}_{-1}\hat{\boldsymbol{s}}[i+1] - \mathbf{B}_0\hat{\boldsymbol{s}}[i] - \mathbf{B}_1\hat{\boldsymbol{s}}[i-1] \ . \end{aligned} \tag{4.23}$$

Assuming the input signal is white with unit variance, one can define the following matrices

$$\mathbf{S} = \begin{bmatrix} \mathbf{H}_0\mathbf{F} & \mathbf{H}_1\mathbf{F} & \mathbf{0} \\ \mathbf{0} & \mathbf{H}_0\mathbf{F} & \mathbf{H}_1\mathbf{F} \\ \mathbf{0} & \mathbf{0} & \mathbf{H}_0\mathbf{F} \end{bmatrix} \tag{4.24}$$

$$\mathbf{R}_{\bar{v}\bar{v}} = \begin{bmatrix} \mathbf{R}_{vv} & \mathbf{0} & \mathbf{0} \\ \mathbf{0} & \mathbf{R}_{vv} & \mathbf{0} \\ \mathbf{0} & \mathbf{0} & \mathbf{R}_{vv} + \mathbf{H}_1\mathbf{F}(\mathbf{H}_1\mathbf{F})^{\mathrm{H}} \end{bmatrix} \tag{4.25}$$

$$\mathbf{R}_{\bar{y}\bar{y}} = \mathbf{S}\mathbf{S}^{\mathrm{H}} + \mathbf{R}_{\bar{v}\bar{v}} \ . \tag{4.26}$$

The tap weights of the feed-forward and feedback filter banks of the IBI-MMSE-BDFE are given by [68]

$$[\mathbf{W}_{-1}\ \mathbf{W}_0\ \mathbf{W}_1] = [\mathbf{0}_{N\times N}\ \mathbf{Q}_{22}\ \mathbf{Q}_{23}]\,\mathbf{S}^{\mathrm{H}}\mathbf{R}_{\bar{y}\bar{y}}^{-1} \tag{4.27}$$

$$\mathbf{B}_{-1} = \mathbf{0} \tag{4.28}$$

$$\mathbf{B}_0 = \mathbf{Q}_{22} - \mathbf{I} \tag{4.29}$$

$$\mathbf{B}_1 = \mathbf{Q}_{23} \ , \tag{4.30}$$

where $\mathbf{Q}_{22}$ and $\mathbf{Q}_{23}$ are sub-matrices of the matrix $\mathbf{Q} \in \mathbb{C}^{(3N \times 3N)}$ which is derived from the following Cholesky decomposition

$$\mathbf{I} + \mathbf{S}^{\mathrm{H}} \mathbf{R}_{\bar{v}\bar{v}}^{-1} \mathbf{S} = \mathbf{Q}^{\mathrm{H}} \mathbf{\Sigma} \mathbf{Q} \tag{4.31}$$

and

$$\mathbf{Q} = \begin{bmatrix} \mathbf{Q}_{11} & \mathbf{Q}_{12} & \mathbf{Q}_{13} \\ \mathbf{0}_{N \times N} & \mathbf{Q}_{22} & \mathbf{Q}_{23} \\ \mathbf{0}_{N \times N} & \mathbf{0}_{N \times N} & \mathbf{Q}_{33} \end{bmatrix} \quad . \tag{4.32}$$

4.1.4.3 ZF Optimal Linear Precoder

A ZF optimal linear precoder has been proposed in [25], which is designed in conjunction with a linear equaliser such that the signal-to-noise ratio at the receiver output is maximised. Linear equalisation is however only viable in the absence of IBI, hence we replace the linear equaliser and combine the precoder with the ZF-IBI-BDFE to form a benchmarker for the ZF case. The precoder design is accomplished via the EVD in (A.9), whereby the ZF linear precoder is given by [25]

$$\mathbf{F}_{0,\mathrm{ZF}} = \mathbf{V}_N \mathbf{\Phi} \quad , \tag{4.33}$$

where $\mathbf{\Phi}$ is a $N \times N$ diagonal matrix with on-diagonal elements equal to

$$|\phi_{ii}|^2 = \frac{P_0}{\sum_k^N \lambda_{kk}^{-1}} \frac{1}{\lambda_{ii}} \quad . \tag{4.34}$$

4.1.4.4 MMSE Optimal Linear Precoder

Similar to the ZF linear precoder, the MMSE linear precoder proposed in [25] is meant to operate with a linear equaliser in the absence of IBI, but here it is combined as a locally optimised precoder with the MMSE-IBI-BDFE of Section 4.1.4.2. Similar to the design reviewed in Section 2.4, the MMSE precoder is also given by

$$\mathbf{F}_{0,\mathrm{MMSE}} = \mathbf{V}_N \mathbf{\Phi} \quad , \tag{4.35}$$

where the diagonal elements of the diagonal $N \times N$ matrix $\mathbf{\Phi}$ are given by

$$|\phi_{ii}|^2 = \max\left(\frac{P_0 + \sum_{k=1}^{\bar{M}} \lambda_{kk}^{-1}}{\sum_{k=1}^{\bar{M}} \lambda_{kk}^{-1/2}} \lambda_{ii}^{-1/2} - \lambda_{ii}^{-1} \ , \ 0\right) \tag{4.36}$$

with $\bar{M}$ the number of $|\phi_{ii}|^2 > 0$.

4.1.5 Simulation and Results

In order to assess and compare the performance of the proposed design, consider a channel of order $L = 5$ with coefficients drawn from a complex Gaussian distribution with zero mean and unit variance. With a transmit block length of $P = 18$, the input block length of $N = M = 16$ admits a very limited amount of redundancy that is insufficient to permit the suppression of IBI by design of the precoder/equalisation system. The transmit power is constrained to $P_0 = 10$.

The results in terms of BER performance for QPSK transmision over the proposed jointly optimal system comprising a linear precoder and a BDFE for the ZF and MMSE case are shown in Figure 4.2, averaged over 50 randomised channel realisations. Jointly optimised linear precoding and linear equalisation is unsuitable, since linear equalisation such as in [25] offers no capability to combat IBI. Therefore, the two composite schemes outlined in subsection 4.1.4 have been considered as a benchmark:

1. optimal ZF linear precoding [25] combined with ZF-IBI-BDFE [68], and
2. optimal MMSE linear precoding [25] combined with MMSE-IBI-BDFE [68].

Although ZF and MMSE precoders are referred to as optimal, these are locally, i.e. with view of the transmitter only, optimised components. Considering the benchmark results in Figure 4.2, it is evident that the proposed design can achieve a considerably lower BER performance than the BER of benchmark systems. For example, at the SNR = 10 dB, the proposed designs can achieve a BER of about

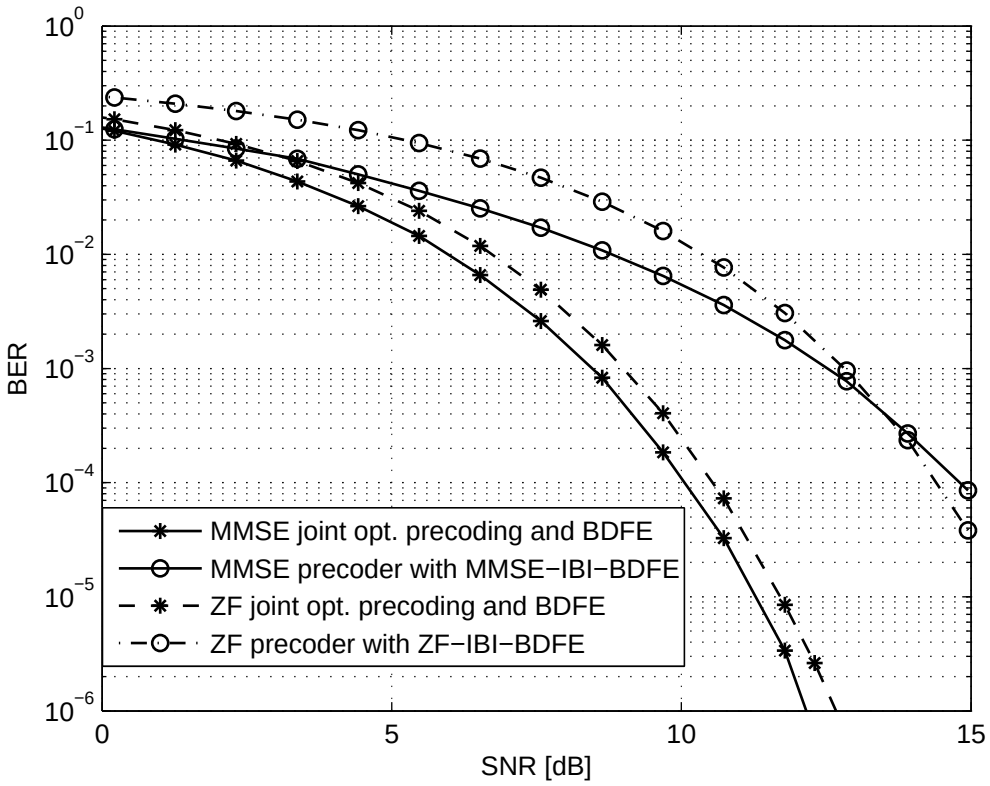

Figure 4.2: BER performance of the proposed IBI joint precoding and BDFE equalisation designs and benchmark designs.

10^{-4} while the benchmark designs can only achieve a BER of $4 \cdot 10^{-3}$ for the case of MMSE precoder and MMSE-IBI-BDFE and 10^{-2} for the case of ZF precoder and ZF-IBI-BDFE.

4.2 An Approach for Block Transmission Based Precoding and Equalisation with Improved Performance

Although block transmission is a very effective method to combat ISI, the way it uses the guard intervals reduces the spectral efficiency of the system. In this section, a

new approach to block transmission based precoding and equalisation for frequency selective channels is proposed. Different from standard block transmission schemes, the proposed method employs redundancy in a different way so that the channel energy can be better employed, thus leading to improved performance under the same code rate.

4.2.1 Motivation

It is well known that block transmission is an attractive method for wired and wireless broadband communications as it can efficiently combat ISI caused by the frequency selectivity of dispersive channels. In a number of designs for block transmission based precoding and equalisation, guard intervals in form of zero padding intervals [26, 27, 25] or cyclic prefix [69] are used to eliminate the IBI. The use of guard intervals helps to effectively remove IBI, however it creates some loss in channel energy as will be analysed later. Moreover, as it can be seen in [25] or [70], after IBI removal by using guard intervals, one has to use an additional amount of redundancy so that the system performance can be improved.

Therefore, this section will analyse the loss in channel energy due to the use of guard intervals and then propose a method to exploit the channel resource more efficiently. Several designs are proposed and the simulation results show that they outperform the systems using guard intervals proposed in [26]. For simplicity, the SISO scenario is concerned, but the proposed designs here can also be applied for the MIMO scenarios with appropriate modification.

In subsection 4.2.2, the overall channel and conventional system setup are set out. Then the analysis of the loss due to the use of guard intervals and the proposed designs are addressed. Simulation results are provided in subsection 4.2.3.

4.2.2 System Model and Proposed Designs

First, consider a system model of block transmission based linear precoding and equalisation, which is illustrated in Figure 4.3. The model here is similar to the one in section 3.2 and is actually a general form of the design proposed in [26]. The channel is also assumed to be frequency selective with finite impulse response of order L. The input symbol stream is demultiplexed into N substreams which compose the sequence of symbol blocks $\boldsymbol{s}[n] = [s[nN], s[nN+1], ..., s[nN+N-1]]^{\mathrm{T}}$. These blocks are passed through the precoder $\mathbf{F} \in \mathbb{C}^{P \times N}$, which maps the input blocks into output blocks $\boldsymbol{x}[n] = [x[nP], x[nP+1], ..., x[nP+P-1]]^{\mathrm{T}}$. At the channel output, the filtered transmitted symbols mixed with noise are again demultiplexed into P substreams that compose symbol blocks $\boldsymbol{y}[n] = [y[nP], y[nP+1], ..., y[nP+P-1]]^{\mathrm{T}}$ which are mapped back to output blocks $\hat{\boldsymbol{s}}[n] = [\hat{s}[nN], \hat{s}[nN+1], ..., \hat{s}[nN+N-1]]^{\mathrm{T}}$ by the equaliser $\mathbf{G} \in \mathbb{C}^{N \times P}$.

As it has been reviewed in Section 2.2, when $P > L$ the system operation can be described by

$$\hat{\boldsymbol{s}}[n] = \mathbf{G}\mathbf{H}_0\mathbf{F}\boldsymbol{s}[n] + \mathbf{G}\mathbf{H}_1\mathbf{F}\boldsymbol{s}[n-1] + \mathbf{G}\boldsymbol{v}[n] \tag{4.37}$$

where $\boldsymbol{v}[n]$ contains a block of noise samples of length P similar to $\boldsymbol{y}[n]$, and $\mathbf{H}_0$ and $\mathbf{H}_1$ are given by (2.13) and (2.14), respectively.

For optimal linear precoding and equalisation in [26] and [27], the authors assume that $P = M+L$, $(N \leq M)$ and that IBI can be eliminated either by the TZ approach where the last L rows of the precoder $\mathbf{F}$ are set to zero or the LZ approach where

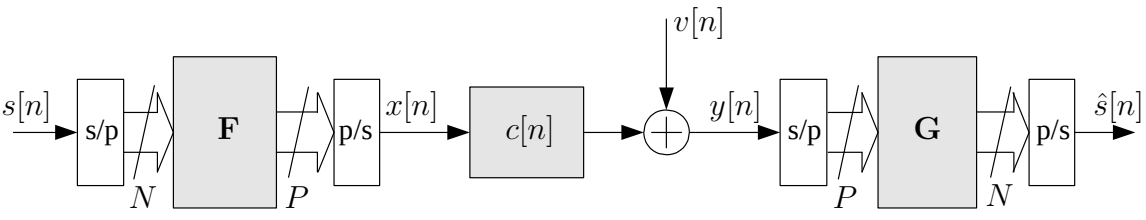

Figure 4.3: System model for linear precoding and equalisation.

the first L columns of $\mathbf{G}$ are set to zero.

For simplicity, the TZ case is considered. The precoder then has the form

$$\mathbf{F} = \begin{bmatrix} \hat{\mathbf{F}}_0 \\ \mathbf{0}_{L\times N} \end{bmatrix} \quad , \tag{4.38}$$

where $\hat{\mathbf{F}}_0 \in \mathbb{C}^{M\times N}$ will be jointly designed with the equaliser $\mathbf{G}$ under either ZF or MMSE criteria.

With IBI being eliminated, equation (4.37) can be written as

$$\hat{\boldsymbol{s}}[n] = \mathbf{G}\mathbf{H}\hat{\mathbf{F}}_0\boldsymbol{s}[n] + \mathbf{G}\boldsymbol{v}[n] \tag{4.39}$$

where $\mathbf{H}$ contains the first M columns of $\mathbf{H}_0$,

$$\mathbf{H} = \begin{bmatrix} c[0] & 0 & \cdots & 0 \\ \vdots & \ddots & \ddots & \vdots \\ c[L] & \ddots & \ddots & 0 \\ 0 & \ddots & \ddots & c[0] \\ \vdots & \ddots & \ddots & \vdots \\ 0 & \cdots & 0 & c[L] \end{bmatrix} . \tag{4.40}$$

With the transmit power to be constrained to P_0, the MMSE optimal precoder and equaliser are given by

$$\hat{\mathbf{F}}_0 = \mathbf{V}\boldsymbol{\Phi}\mathbf{U}^{\mathrm{H}} \tag{4.41}$$

$$\mathbf{G} = \mathbf{R}_{ss}\hat{\mathbf{F}}_0^{\mathrm{H}}\mathbf{H}^{\mathrm{H}}(\mathbf{R}_{vv} + \mathbf{H}\hat{\mathbf{F}}_0\mathbf{R}_{ss}\hat{\mathbf{F}}_0^{\mathrm{H}}\mathbf{H}^{\mathrm{H}})^{-1} \tag{4.42}$$

where $\mathbf{U}$ and $\mathbf{V}$ are unitary matrices derived from the EVD

$$\begin{aligned} \mathbf{R}_{ss} &= \mathbf{U}\boldsymbol{\Delta}\mathbf{U}^{\mathrm{H}} \\ \mathbf{H}^{\mathrm{H}}\mathbf{R}_{vv}^{-1}\mathbf{H} &= \mathbf{V}\boldsymbol{\Lambda}\mathbf{V}^{\mathrm{H}} \ , \end{aligned} \tag{4.43}$$

and $\boldsymbol{\Phi}$ is a diagonal matrix with main diagonal elements obtained from a water-filling algorithm over diagonal elements of $\boldsymbol{\Lambda}$ as explained in Section 2.2, $\mathbf{R}_{ss}$ is the covariance matrix of the input signal and $\mathbf{R}_{vv}$ is the noise covariance matrix.

As it has been shown in [26], the optimal precoder and equaliser render a frequency selective SISO channel into a maximum of $M = P - L$ flat subchannels with SNRs proportional to the eigenvalues of $\mathbf{H}^{\mathrm{H}}\mathbf{R}_{vv}^{-1}\mathbf{H}$. It can also be seen that the sum of these eigenvalues is proportional to the square of the Frobenius norm of $\mathbf{H}$ and therefore, if the Frobenius norm of $\mathbf{H}$ is increased, these eigenvalues and thus the SNRs on the flat subchannels will be increased as well. From (4.40), one can see that $\mathbf{H}$ contains the first M columns of $\mathbf{H_0}$ (in the LZ case, $\mathbf{H}$ contains the last M rows of $\mathbf{H_0}$) and therefore as M is getting closer to P, the Frobenius norm of $\mathbf{H}$ will be increased, thus the EVD in (4.43) will result in some increased eigenvalues [1] and therefore the SNRs on the corresponding flat subchannels can be improved.

From equation (2.8), we can write the structure of the TZ precoder as

$$\mathbf{F} = \begin{bmatrix} \hat{f}_0[0] & \hat{f}_1[0] & \cdots & \hat{f}_{N-1}[0] \\ \vdots & \vdots & \vdots & \vdots \\ \hat{f}_0[M-1] & \hat{f}_1[M-1] & \cdots & \hat{f}_{N-1}[M-1] \\ 0 & 0 & \cdots & 0 \\ \vdots & \vdots & \vdots & \vdots \\ 0 & 0 & \cdots & 0 \end{bmatrix}, \tag{4.44}$$

one can see that the columns of $\mathbf{F}$ correspond to the impulse responses of transmit filters with length of M, thus increasing M in this case also means increasing the length of the transmit filters.

From the above observations, it can be concluded that by increasing the length of the transmit filters, one can increase the SNRs of the decoupled flat subchannels, and thus the system performance can be improved. However, there are two issues

[1] Note that the Jacobian transform in the EVD decomposition always assigns more energy to some "strong" eigenmodes and less energy to some "weak" eigenmodes thus resulting in unequal eigenvalues. When M is increased, the Frobenius norm of $\mathbf{H}$ is increased but the number of eigenvalues is also increased. However due to the above property of the Jacobian transform, a part of the increased amount in the Frobenius norm of $\mathbf{H}$ will be given to some "strong" eigenmodes resulting in some increased eigenvalues.

that we have to consider. First, since the eigenvalues obtained from (4.43) are not equal, the SNRs on the decoupled flat subchannels will be different from each other and the system error performance will be dominated by the performance of the subchannels with lowest SNRs. In order to improve the system BER, one should discard the subchannels with low SNR as it has been shown in [25]. Therefore, in our approach, although we are going to increase $M \geq N$, we still keep the input block size N unchanged and set $N = P - L$. Thus, we use the redundancy not to eliminate the IBI but to discard the subchannels with low SNRs and retain only the subchannels with high SNRs. Second, as M is increased, the amount of IBI will increase and the question now is how to eliminate the IBI when $M > P - L$. In order to do so, we proposed several designs as below.

4.2.2.1 Linear Precoding and Equalisation with Shared Guard Interval (LPE-SGI).

In this design we combine the ideas reported in [71] and [26] and propose an optimal design of linear precoding and equalisation which can provide a better performance than the design in [26]. The design is based on the solutions in [26], but the guard interval now is shared between the transmitter and the receiver, namely instead of setting last L rows of the precoder matrix to zero, we only set last $K = \lfloor \frac{L}{2} \rfloor$ rows to zero, at the receiver, the first $L - K$ columns of $\mathbf{G}$ are also set to zero. Thus the precoder and equaliser have the following form

$$\mathbf{F} = \begin{bmatrix} \hat{\mathbf{F}}_0 \\ \mathbf{0}_{K \times N} \end{bmatrix} \tag{4.45}$$

$$\mathbf{G} = \begin{bmatrix} \mathbf{0}_{N \times (L-K)} & \hat{\mathbf{G}}_0 \end{bmatrix} \tag{4.46}$$

where $\hat{\mathbf{F}}_0 \in \mathbb{C}^{P-K \times N}$ and $\hat{\mathbf{G}}_0 \in \mathbb{C}^{N \times (P-L+K)}$. Such a pair of precoder and equaliser will drive the second term in (4.37) to zero. Thus the IBI is completely eliminated, but now one can see that the transmit filters have the length of $M = P - K$ which

is larger than $P - L$. Equation (4.37) can be re-written as

$$\hat{\boldsymbol{s}}[n] = \hat{\mathbf{G}}_0 \hat{\mathbf{H}} \hat{\mathbf{F}}_0 \boldsymbol{s}[n] + \hat{\mathbf{G}}_0 \boldsymbol{v}'[n] \tag{4.47}$$

where by $\hat{\mathbf{H}} \in \mathbb{C}^{(P-L+K)\times(P-K)}$ is given by

$$\hat{\mathbf{H}} = \begin{bmatrix} c[L-K] & \cdots & c[0] & 0 & \cdots & 0 \\ \vdots & & & \ddots & \ddots & \vdots \\ c[L] & & & & \ddots & 0 \\ 0 & \ddots & & & & c[0] \\ \vdots & \ddots & \ddots & & & \vdots \\ 0 & \cdots & 0 & c[L] & \cdots & c[K] \end{bmatrix} \tag{4.48}$$

and $\boldsymbol{v}'[n]$ is the block of noise samples of length $P - L + K$.

Figure 4.4 compares the loss in $\mathbf{H}_0$, which directly contributes to the transmission of signal $\boldsymbol{s}[n]$ as illustrated in equation (4.37), of the proposed approach and the loss of the TZ or LZ case in [26]. From equation (4.40), one can see that in the TZ case the last L columns of $\mathbf{H}_0$ are discarded by the TZ precoder, thus the elements in the shaded triangular in Figure 4.4.(a) will be lost resulting in a reduction in channel energy. In the LZ case, we can easily verify that the system bears exactly the same loss. When the guard interval is shared between transmitter and receiver, the first $L - K$ rows of $\mathbf{H}_0$ are discarded by the equaliser and the last K columns of $\mathbf{H}_0$ are discarded by the precoder. The loss in $\mathbf{H}_0$ now can be described by the two shaded triangles as illustrated in Figure 4.4.(b) where the triangle at the top-left corner corresponds to the loss caused by the equaliser and the triangular at the bottom-right corner corresponds to the loss caused by the precoder. We can shift the triangular at the top-left corner and compare the loss in two cases as illustrated in Figure 4.4.(c), here it is obvious that the loss of $\mathbf{H}_0$ in the proposed approach is smaller than the loss in the TZ or LZ cases, as the elements of $\mathbf{H}_0$ lying in the shaded rectangular area are retained within $\hat{\mathbf{H}}$ and will contribute to the SNR increase after eigenvalue decomposition.

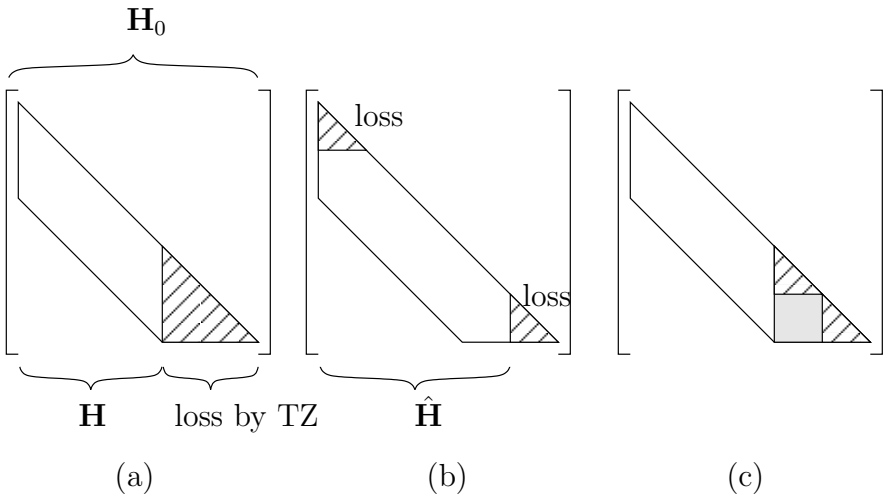

Figure 4.4: Comparison of the loss in $\mathbf{H}_0$ in two approaches.

The input block size is still kept to be $N = P - L$ so that the flat subchannels with low SNR can be discarded as we have mentioned above.

The precoder and equaliser matrices $\hat{\mathbf{F}}_0$ and $\hat{\mathbf{G}}_0$ can then be derived under the same optimal criteria as in [26, 27]. For example, the MMSE precoder and equaliser can be calculated as in equations (4.41), (4.42) with matrix $\mathbf{H}$ replaced by $\hat{\mathbf{H}}$ and $\mathbf{R}_{vv}$ resized accordingly.

4.2.2.2 Combined Linear Precoding and Equalisation with Decision Feedback Equalisation (LPE-DFE).

The LPE-SGI design still experiences a certain amount of loss in the matrix $\mathbf{H}_0$. To fully exploit $\mathbf{H}_0$ for transmission, we will combine the ideas reported in [26] and [68] and proposed the use of optimal linear precoders and equalisers in [26] with a decision feedback loop. Different from the previous design, the precoder $\mathbf{F}$ and equaliser $\mathbf{G}$ now do not contain any zero row or column and therefore the IBI elimination in the system will entirely rely on the feedback loop containing a feedback filterbank

$$\mathbf{B} = \mathbf{H}_1\mathbf{F} \; . \tag{4.49}$$

In the next step, the linear precoder and equaliser will be jointly optimised as in [26] with matrix $\mathbf{H}$ in equation (4.43) replaced with $\mathbf{H}_0$ from (2.13). The system model of this approach is illustrated in Figure 4.5 where with the assumtion that $P > L$ the matrix $\mathbf{H}(z) = \mathbf{H}_0 + \mathbf{H}_1 z^{-1}$ represents the channel transfer function. Due to limited space, we do not show the serial-to-parallel and parallel-to-serial converters.

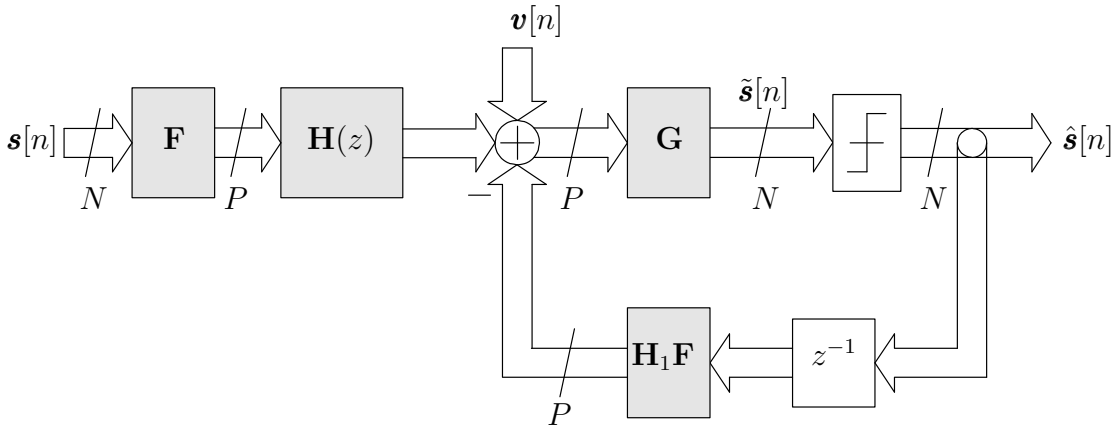

Figure 4.5: System model for combination of linear precoding and equalisation and decision-feedback equalisation.

The relation between the input and output signals can be written as

$$\tilde{\boldsymbol{s}}[n] = \mathbf{G}\{\mathbf{H}_0\mathbf{F}\boldsymbol{s}[n] + \mathbf{H}_1\mathbf{F}\boldsymbol{s}[n-1] - \mathbf{H}_1\mathbf{F}\hat{\boldsymbol{s}}[n-1] + \boldsymbol{v}[n]\} \,. \tag{4.50}$$

Assuming $\hat{\boldsymbol{s}}[n] = \boldsymbol{s}[n]$, the IBI can be eliminated and the above equation can be re-written as

$$\tilde{\boldsymbol{s}}[n] = \mathbf{G}\mathbf{H}_0\mathbf{F}\boldsymbol{s}[n] + \mathbf{G}\boldsymbol{v}[n] \tag{4.51}$$

which is now similar to equation (4.37).

Although here the IBI elimination is performed by the feedback loop, we still keep the input block size to be $N = P - L$ so that the flat subchannels with low SNRs resulting from linear precoding and equalisation can be discarded. Thus we do use redundancy but in a different way compared with the standard approach, and this leads to a significant improvement in system BER performance as one can see later in simulation results. Note that keeping $N = P - L$ also results in a certain

loss in channel energy which corresponds to the power gain of the discarded flat subchannels.

4.2.2.3 Modified Linear Precoder and Block Decision Feedback Equaliser (MLP-BDFE)

In this design, we suggest the use of a modified optimal MMSE linear precoder proposed in the previous subsection with the MMSE block decision feedback equaliser (MMSE-IBI-BDFE) proposed in [68]. The system model is illustrated in Figure 4.6.

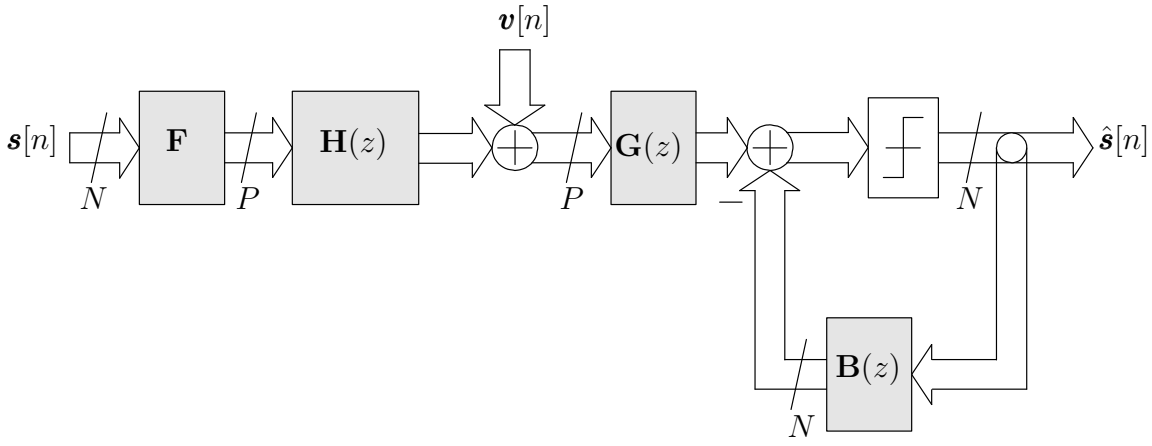

Figure 4.6: System model for proposed linear precoding and block decision-feedback equalisation.

The transmit filters have the length of P so that the whole matrix $\mathbf{H}_0$ in (2.13) can be exploited for transmission. The elimination of IBI will be performed by the MMSE-IBI-BDFE. As it is explained in [68], the MMSE-IBI-BDFE contains a three-tap feedforward filter bank and a two-tap feedback filter bank.

The precoder in this case is calculated similarly to the one in the LPE-DFE design. The MMSE-IBI-BDFE is then calculated as a function of the precoder. One can refer to [68] for more details on the derivation of the filter banks for the MMSE-IBI-BDFE.

Similarly to the previous subsection, we keep $N = P - L$ and thus the precoder does introduce some redundancy, but this redundancy is used for subchannel selection rather than for IBI elimination.

4.2.2.4 Modified Joint Optimal Precoder and Block Decision Feedback Equaliser (MJPR-BDFE)

In the previous section, we have combined the ideas reported in [68] and [32] and proposed a design of joint optimal precoding and BDFE equalisation with low redundancy. The system model is illustrated in Figure 4.1 where the precoder contains zero-padding intervals which are shorter than the channel order and therefore the IBI is removed partly. The remaining IBI is then removed by the outer feedback loop. The precoder and the inner block decision feedback equaliser are then jointly optimised so that the system mean square error can achieve its minimised lower bound.

In this section we focus on the system performance improvement rather than on saving the redundancy for long channels, therefore we propose the use of design in Figure 4.1 but the precoder now does not contain any zero-padding interval so that matrix $\mathbf{H}_0$ can be exploited for transmission as in LPE-DFE design and the IBI elimination will be performed by the outer feedback loop. Then the precoder and the inner BDFE are jointly optimised according to the idea in [32]. Similar to the previous designs, the input block size is also $N = P - L$ to ensure the selection of the flat subchannels with high SNRs.

4.2.3 Simulation and Results

To highlight the advantage of our proposed designs, we compare their BER performance with the performance of standard approaches in [26] and [32] where the guard intervals of length L are used for IBI elimination. The channel is assumed to be FIR with a length of $L + 1 = 11$, the components of the CIR are assumed

to be i.i.d Gaussian complex numbers with zero mean and unit variance. Channel CIR is normalised to have unit energy. The result is averaged over 100 channel realisations. In all designs, the input block size is $N = 22$, the transmit block size $P = N + L = 32$. Gray coded 4-QAM modulation is used for all designs.

The linear optimal precoders and equalisers used in our proposed LPE-SGI, LPE-DFE, MLP-BDFE designs as well as in the benchmark design from [26] are calculated under the MMSE criterion given by equations (4.41), (4.42) with matrix $\mathbf{H}$ replaced by $\hat{\mathbf{H}}$ or $\mathbf{H}_0$ accordingly. The joint optimal precoder and BDFE in the MJPR-BDFE design and the benchmark design from [32] are also derived under the MMSE criterion.

Figure 4.7 compares the BER performance of the MMSE optimal linear precoding and equalisation scheme in [26] with the performance of the LPE-SGI, LPE-DFE, MLP-BDFE designs. One can see, for example, from Figure 4.7 that under the same code rate at the BER of 10^{-4} the MLP-BDFE and the LPE-DFE designs can achieve a gain of about nearly 3 dB in SNR compared with the benchmark design and the LPE-SGI design can achieve a gain of about 1 dB compared with the benchmark design.

The result in Figure 4.8 shows the comparison of BER performance of the proposed MJPR-BDFE design in subsection 4.2.2.4 with the performance of the MMSE joint optimal precoder and BDFE proposed in [32] applied for the frequency selective channel with redundancy of L. As we can note from the figure, our proposed design also can achieve a gain of about 1.5 dB in its SNR at the BER of 10^{-4} compared with the benchmark design which uses guard intervals of length L.

The above results show that our proposed designs can better exploit the channel resource. Although the system design in our proposed approaches has a slightly higher complexity compared with the standard designs, this appears easily justified given the gain in performance that can be achieved.

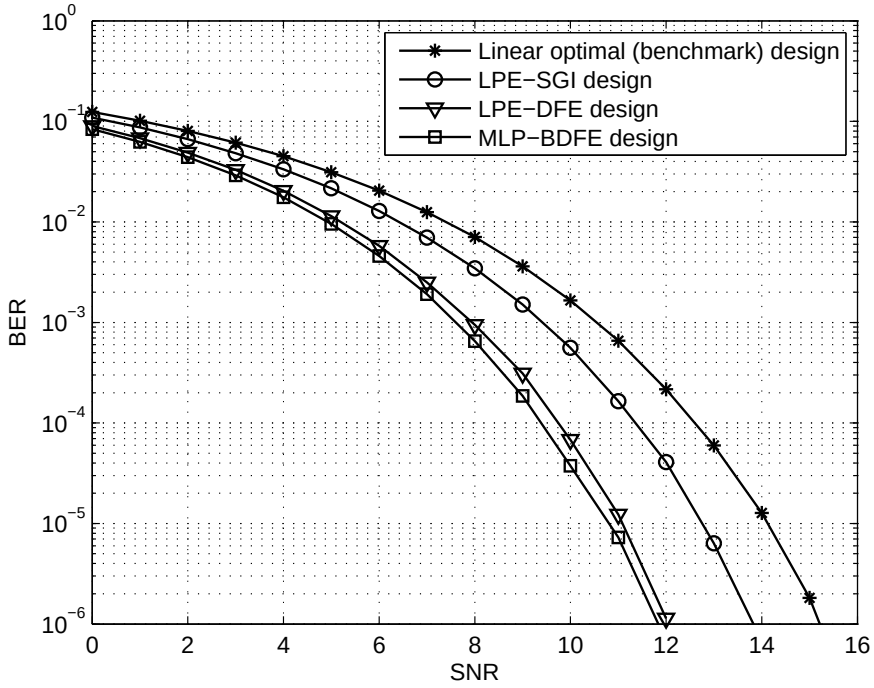

Figure 4.7: BER performance of the proposed designs and the optimal linear design in [26].

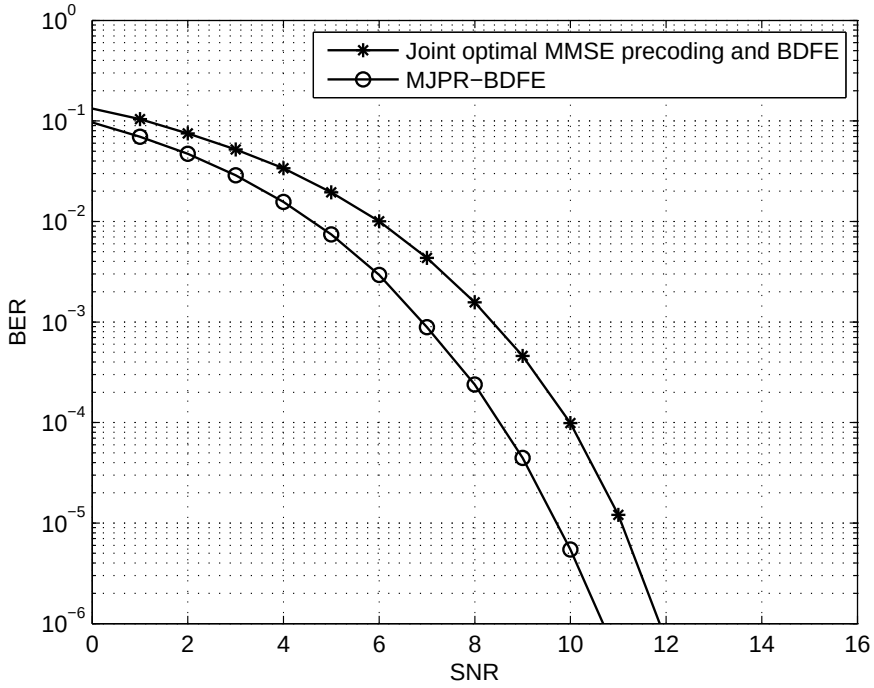

Figure 4.8: BER performance of the MJPR-BDFE design and the MMSE joint optimal precoder and BDFE in [32].

4.3 Precoding and Equalisation for Broadband MIMO Systems with Improved Performance

As it has been mentioned, all the proposed designs in the previous section can be extended to the MIMO case. We can also see that the LPE-DFE approach can help to significantly improve the system performance while the system complexity is just slightly higher than that of the linear design. In this section, we will apply the LPE-DFE approach for the decoupled SISO FS subchannels resulted from the BSVD in Chapter 3. The resulting system is referred to as LPE-DFE-BSVD design. At the same time, we also extend the LPE-DFE design for broadband MIMO case and form the LPE-DFE-MIMO design. The BER performance of the two aforementioned designs will be investigated and compared.

4.3.1 System Model

The system model of the LPE-DFE-BSVD design is obvious from sections 3.4 and 4.2.2. This means that firstly, the BSVD is applied to decompose the broadband MIMO channel into independent FS SISO channels as explained in Section 3.2.3, then the LPE-DFE design proposed in the previous subsection is applied to remove the remaining ISI on the decoupled FS SISO subchannels resulted from the first step. Similar to the design in Section 3.4, the input symbol block of length N is divided into sub-blocks of length N_i. We give higher priority for some first FS subchannels which have high gain due to the spectral majorisation and write

$$N_i = P_i - L_i \ . \tag{4.52}$$

For the last subchannel, the input block length is given by

$$N_K = N - \sum_{i=1}^{K-1} N_i \ , \tag{4.53}$$

where K is the number of FS subchannels which are selected for transmission.

The transmit power P_0 is allocated with the help of the water-filling algorithm as explained in equation (2.26). Similar to the design proposed in Chapter 3, the water-filling algorithm is performed simultaneously for all FS SISO subchannels.

The LPE-DFE-MIMO design has a similar structure to the one illustrated in Figure 4.5, with the channel matrix $\mathbf{H}(z)$ now being of size $PR \times PT$, the precoder $\mathbf{F} \in \mathbb{C}^{PT \times N}$ and the equaliser $\mathbf{G} \in \mathbb{C}^{N \times PR}$. Similar to the design in Section 2.4, with matrix $\mathbf{H}_0$ given by (2.46), consider the EVD

$$\mathbf{H}_0^{\mathrm{H}} \mathbf{R}_{vv}^{-1} \mathbf{H}_0 = \hat{\mathbf{V}} \hat{\mathbf{\Lambda}} \hat{\mathbf{V}}^{\mathrm{H}} \, . \tag{4.54}$$

The optimal precoder and equaliser in LPE-DFE-MIMO design are given by

$$\mathbf{F} = \mathbf{V} \mathbf{\Phi} \tag{4.55}$$

$$\mathbf{G} = \mathbf{R}_{ss} \mathbf{F}^{\mathrm{H}} \mathbf{H}_0^{\mathrm{H}} \left(\mathbf{H}_0 \mathbf{F} \mathbf{R}_{ss} \mathbf{F}^{\mathrm{H}} \mathbf{H}_0^{\mathrm{H}} + \mathbf{R}_{vv} \right)^{-1} \, , \tag{4.56}$$

where the diagonal elements of matrix $\mathbf{\Phi}$ are given by the MMSE water-filling algorithm in (2.56), $\mathbf{V}$ contains the first N columns of $\hat{\mathbf{V}}$. The IBI is eliminated by the feedback filter bank $\mathbf{B} = \mathbf{H}_1 \mathbf{F}$ with matrix $\mathbf{H}_1$ given by (2.47).

4.3.2 Simulation Results

In this section, we will investigate the BER performance of our proposed designs in the previous subsection and compare it with the BER performance of the standard MMSE design in [25] (Lemma 2) and of the design based on the combination of MMSE/CP linear optimal precoding and equalisation and BSVD in Chapter 3, where guard intervals of a length of the channel order are used for IBI elimination. For convenience, the last two designs are referred to as MMSE-LPE-MIMO and MMSE-LPE-BSVD designs, respectively.

We consider a 4×4 broadband MIMO channel which is generated from the Saleh-Valenzuela channel model in [61]. Similar to the channel model in Section 3.5, the parameters of the model considered here are also chosen to be $1/\Lambda = 300$ ns, $1/\lambda =$

5 ns, $\Gamma = 60$ ns, $\gamma = 20$ ns, and the observation time is 800 ns. Similar to the case in Section 3.5, the channel length is also limited to $L+1 = 11$ as the components of the CIR after 11 are statistically very small and can be neglected. The simulation is performed over 50 channel realisations.

We also choose BPSK modulation for all the designs being considered. The length of input symbol block and the length of the transmitted block in all designs considered in this section are chosen similar to those in Section 3.5, leading to a code rate of 0.57.

Figure 4.9 illustrates the average BER of the designs for broadband MIMO case mentioned above as well as the average BER of the MMSE-LPE-BSVD design in Chapter 3 and the MMSE-LPE-MIMO design in [25]. The SNR used here is also de-

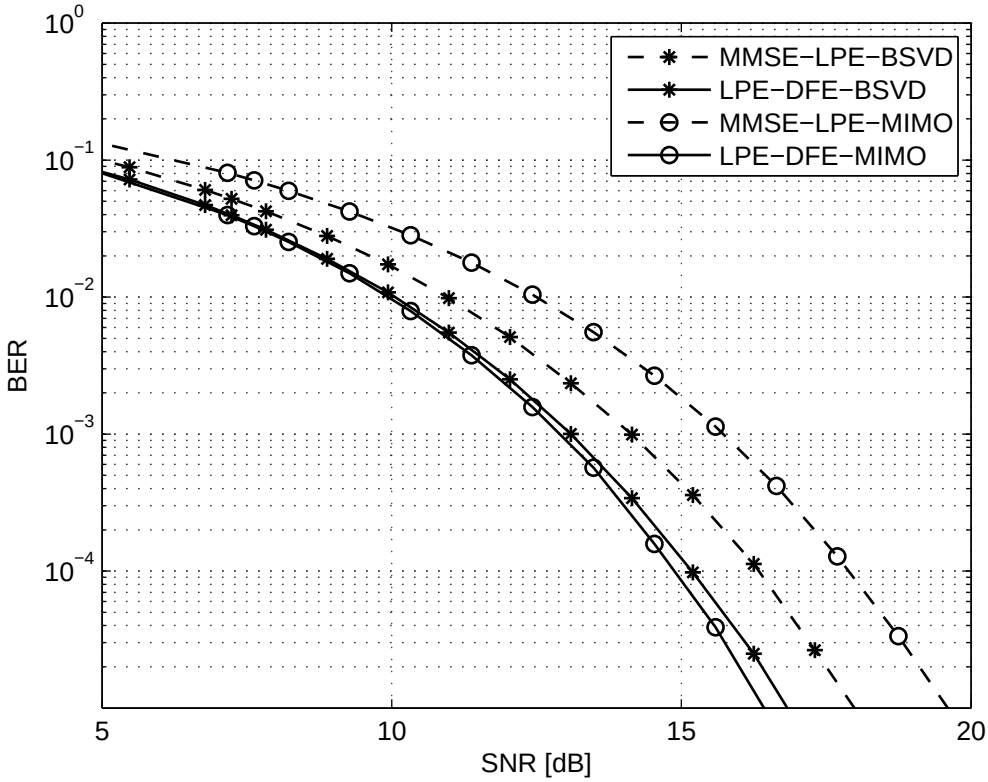

Figure 4.9: BER performance comparison for broadband MIMO case.

fined as the one in (3.47). From the figure, one can see that the LPE-DFE approach helps to achieve significant improvement when it is applied directly to broadband MIMO channels. However, in case of combination with BSVD, the improvement in BER by the LPE-DFE design is not very high. This is because among the FS SISO subchannels resulting from the BSVD, the subchannels with high gain are less dynamic and have lower order while the subchannels with low gain are more dynamic and have higher order. Furthermore, we can see that the higher the channel order is, the larger the amount of channel energy that can be saved by the LPE-DFE design. Thus the amount of channel energy saved by the LPE-DFE approach when it is applied to the FS subchannels resulting from the BSVD is less than in the case of the LPE-DFE-MIMO design where the LPE-DFE approach is applied directly to broadband MIMO channels.

One can also see from Figure 4.9 that the BER performance of the LPE-DFE-MIMO design is slightly better than the BER performance of the LPE-DFE-BSVD design. This is because in the LPE-DFE-BSVD design, the BSVD cannot achieve a perfect diagonalisation and therefore there always exists a certain amount of CCI that slightly deteriorates the BER performance.

4.4 Concluding Remarks

In this chapter, we have proposed several approaches for block transmission based joint optimal precoding and equalisation schemes that can either work with low redundancy or can provide an improved performance at the same redundancy compared with the standard block transmission based linear approaches.

In Section 4.1, we have proposed a design which can work with low levels of redundancy where linear block transmission schemes such as in [25] will suffer from IBI. The proposed approach utilises a non-linear block decision feedback equaliser suggested in [68]. We have used this receiver structure to create a jointly optimal de-

sign of both precoder and BDFE, overcoming the required absence of IBI in previous work [32].

Simulation results have demonstrated the advantage of the system in terms of BER when compared to a design akin to [68] where precoder and equaliser are locally optimised at the transmitter and receiver.

In Section 4.2, we have disscused the efficiency of the standard block transmission method and proposed some designs which can better exploit the channel resource. In the LPE-SGI design, the guard interval is shared between transmitter and receiver so that the IBI can be eliminated while the length of the transmit filter can be increased to reduce the loss in channel energy. The input code rate is kept unchanged so that we can have an additional amount of redundancy to discard the flat subchannels with low SNRs. In all other proposed designs, the length of the transmit filters is set equal to the transmit block size P so that the channel energy can be better utilised and the IBI elimination is performed by the receiver only. Again in these designs the redundancy introduced by the precoder is used for the selection of the flat subchannels with the highest SNRs.

The simulation results show that our proposed designs can achieve better performance than state-of-the-art approaches.

Finally, in Section 4.3 we applied the LPE-DFE approach for the broadband MIMO channels in two cases, with BSVD and without BSVD and formed two designs, LPE-DFE-BSVD and LPE-DFE-MIMO. The simulation results in this section also show that the LPE-DFE approach helps to better exploit the channel resource and thus leads to a better BER performance than that of the linear designs which use guard intervals for IBI elimination only. The result in Section 4.3 also shows that the LPE-DFE is more effective when applied directly to broadband MIMO channels that in combination with BSVD.

Analysing the complexity of the various approaches is difficult, as the proposed methods generally depend on the number of steps required by SBR2 to converge, as

well as the resulting channel lengths of the SISO subsystems. Beyond the analysis of the SBR2-related part of the design, it was qualitatively found that DFE-based methods are expensive due to the requirement of inverting a $3P \times 3P$ matrix at a cost of $\mathcal{O}(P^3)$ operations, which is higher than the linear designs. The MJPR-DFE and the LPE-DFE designs have generally been seen to have a slightly lower complexity due to $P \times P$ covariance matrices, while the LPE-SGI design's complexity is of the same order of complexity as linear designs. To curb the high impact of SBR2 on the system complexity, Chapter 5 will explore methods to shorten the SISO responses and paraunitary filter banks in an attempt to drastically reduce the computational complexity of proposed transceiver systems that are based on the BSVD.

In the previous chapters, we have investigated the applicability of the BSVD algorithm to communication over broadband MIMO channels. The results have shown that the BSVD can help to remove a part of ISI in the system at very small loss in channel power gain. In the next chapter, we will take a deeper look at the BSVD algorithm and consider an approach to simplify the paraunitary matrices resulting from this algorithm, namely we will try to shorten the order of these paraunitary matrices and therefore simplify the precoder and equaliser filterbanks that help to decompose our boradband MIMO channels. We also evaluate the influence of non-perfect CSI onto the system performance.

Chapter 5

Performance Studies

In Chapter 3 we have seen that generally the BSVD is effective in diagonalising the broadband MIMO channel matrix and therefore suppressing CCI. We have also demonstrated that the BSVD helps to remove a part of the ISI in the system at only a very small loss in channel power gain or channel energy. Both the methods as well as the performed simulations have assumed perfect knowledge of the channel.

In this chapter, firstly we will discuss some issues related to the computational complexity of the paraunitary filterbanks that are based on the paraunitary matrices resulting from the BEVD computation algorithm, since the BEVD is the key component of BSVD as shown in Section 3.3.1. Therefore, shortening the order of the matrices implementing the BSVD will be considered in Section 5.1. Secondly, the performance of the proposed BSVD based precoding and equalisation design in the case when the CSI is not perfect will also be evaluated in Section 5.2.

5.1 Shortening the Order of Paraunitary Matrices in BEVD Computation Algorithm

In order to compute a BEVD, an algorithm has recently been proposed as an effective tool in decomposing a para-Hermitian polynomial matrix $\mathbf{R}(z)$ into a diagonal polynomial matrix $\mathbf{\Gamma}(z)$ and a paraunitary matrix $\mathbf{B}(z)$, extending the eigenvalue decomposition to polynomial matrices, $\mathbf{R}(z) = \mathbf{B}(z)\mathbf{\Gamma}(z)\tilde{\mathbf{B}}(z)$. However, the algorithm can result in polynomials of very high order, which may limit its applicability. Therefore, in this section we evaluate approaches to reduce the order of the paraunitary matrices, either within each step of the BEVD computation algorithm, or after its convergence. The paraunitary matrix $\mathbf{B}(z)$ is replaced by a near-paraunitary quantity $\mathbf{B}_N(z)$, whose error will be assessed. Simulation results show that the proposed truncation can greatly reduce the polynomial order while retaining good near-paraunitariness of $\mathbf{B}_N(z)$.

5.1.1 Introduction

An algorithm to compute the BEVD, originally referred to as second order sequential best rotation (SBR2) algorithm, was proposed by McWhirter et al. in [58, 57]. It is an iterative algorithm which aims to decompose a polynomial para-Hermitian matrix $\mathbf{R}(z) \in \mathbb{C}^{Q\times Q}(z)$ into a diagonal polynomial matrix $\mathbf{\Gamma}(z)$ and a polynomial paraunitary matrix $\mathbf{B}(z)$, such that matrix $\mathbf{R}(z) = \mathbf{B}(z)\mathbf{\Gamma}(z)\tilde{\mathbf{B}}(z)$ can be regarded as a generalisation of the standard eigenvalue decomposition to the broadband case [57]. Different from conventional methods which often perform the diagonalisation of polynomial matrices in the frequency domain, the SBR2 algorithm diagonalises para-Hermitian matrices in the time domain by applying a sequence of suitably chosen delays and Givens rotations.

The algorithm has been demonstrated to be rather effective in diagonalising $\mathbf{R}(z)$

such that ideally

$$\mathbf{\Gamma}(z) = \mathrm{diag}\{\Gamma_0(z), \Gamma_1(z), \cdots \Gamma_{Q-1}(z)\} \tag{5.1}$$

with on-diagonal elements $\Gamma_i(z)$, which are generally spectrally majorised, i.e. their power spectral densities fulfil

$$\left|\Gamma_i(e^{j\Omega})\right| \geq \left|\Gamma_{i+1}(e^{j\Omega})\right| \quad \forall\Omega \quad , \quad i \in [0, \ldots, Q-2] \, . \tag{5.2}$$

BEVDs based on SBR2 have been applied to a number of problems, such as source separation of array data [57], subband-based source coding [59], subspace-based channel coding in the presence of structured noise [72], precoding and equalisation for broadband MIMO systems [35], or beamforming for broadband MIMO systems [73]. However, the iterative SBR2 algorithm often results in matrices of rather high polynomial order, which for many applications leads to filter banks of considerable delay and computational complexity.

In [74, 57], the authors address the truncation of the para-Hermitian matrix during the diagonalisation process and show that with a small loss in its Frobenius norm, the order of the para-Hermitian matrix can be significantly reduced. The truncation of the extracted paraunitary matrix $\mathbf{B}(z)$ is not considered there, although the matrix is utilised for a number of applications [72, 35, 73]. As one can see later, the order of $\mathbf{B}(z)$ can be prohibitively high, although generally the coefficient matrices corresponding to high and low powers of z in $\mathbf{B}(z)$, which will be referred to as outer coefficient matrices, can be observed to tail off to very small values.

In this section we will propose a method to shorten the order of the paraunitary matrix $\mathbf{B}(z)$. This method will discard the outer coefficient matrices which have the smallest Frobenius norm, thus replacing the paraunitary matrix $\mathbf{B}(z)$ with $\mathbf{B}(z)\tilde{\mathbf{B}}(z) = \mathbf{I}$ by a near-paraunitary matrix $\mathbf{B}_N(z)$ such that $\mathbf{B}_N(z)\tilde{\mathbf{B}}_N(z) \approx \mathbf{I}$. We aim to keep the loss in paraunitariness bounded, with simulation results showing that the order of $\mathbf{B}_N(z)$ can be significantly reduced even with a low error threshold.

The remaining part of this section is organised as follow. In subsection 5.1.2, a brief description of the SBR2 algorithm will be laid out. Subsection 5.1.3 addresses

the proposed method for shortening the order of paraunitary matrices and simulation results are given in subsection 5.1.4.

5.1.2 SBR2 Algorithm [57]

The SBR2 algorithm is an iterative eigenvalue decomposition technique for the broadband case. In each step the algorithm eliminates the largest off-diagonal element at a specific lag value of $\mathbf{R}[\tau] \circ\!\!-\!\!\bullet\, \mathbf{R}(z)$,

$$\mathbf{R}(z) = \sum_{\tau=-L}^{L} z^{-\tau}\mathbf{R}[\tau] \tag{5.3}$$

where L is maximum lag for which cross-correlation coeffcients are non-zero, by means of an elementary paraunitary operation. After a sufficient amount of iterations, the algorithm converges to a diagonalised version of the para-Hermitian matrix $\mathbf{R}(z)$. Note that since $\mathbf{R}(z)$ is a para-Hermitian polynomial matrix, the elements of its coefficient matrices $\mathbf{R}[\tau]$ satisfy

$$r_{ij}[\tau] = r_{ji}^{*}[-\tau] \quad . \tag{5.4}$$

The algorithm commences its operation on the original para-Hermitian matrix, $\mathbf{\Gamma}^{(0)}(z) = \mathbf{R}(z)$ with $\mathbf{B}^{(0)}(z) = \mathbf{I}$, and the gradually diagonalised matrix after the ith iteration is denoted as $\mathbf{\Gamma}^{(i)}(z)$ with coefficient $r_{kl}^{(i)}[\tau]$.

At the ith iteration, the algorithm finds the two largest off-diagonal polynomial coefficients - suppose one is $r_{lk}^{(i-1)}[T_d]$ which belongs to the coefficient matrix $\mathbf{\Gamma}^{(i-1)}[T_d]$ then according to (5.4) the other should be $r_{kl}^{(i-1)}[-T_d]$ which belongs to $\mathbf{\Gamma}^{(i-1)}[-T_d]$. A delay of T_d then will be applied to the kth column of $\mathbf{\Gamma}^{(i-1)}(z)$ by means of

$$\mathbf{\Lambda}_i(z) = \mathbf{I}_{Q\times Q} - \mathbf{v}_k\mathbf{v}_k^H + z^{-T_d}\mathbf{v}_k\mathbf{v}_k^H \tag{5.5}$$

with $\mathbf{v}_k = [0\ \cdots 0\ 1\ 0\ \cdots\ 0]^{\mathrm{T}}$ containing zeros except for a unit element in the kth position. Thus $\mathbf{\Lambda}_i(z)$ is an identity matrix with the kth diagonal element replaced by a delay z^{-T_d}. In conjunction with advancing the kth row of $\mathbf{\Gamma}^{(i-1)}(z)$ by T_d sampling

periods, the power of z associated with $r_{lk}^{(i-1)}[T_d]$ and $r_{kl}^{(i-1)}[-T_d]$ will become zero. In other words, the maximum off-diagonal elements at lags T_d and $-T_d$ are now brought to lag zero of $\mathbf{\Lambda}_i(z)\mathbf{\Gamma}^{(i-1)}(z)\tilde{\mathbf{\Lambda}}_i(z)$.

In the same ith step, the above mentioned maximum elements now in lag zero are eliminated by a Givens rotation $\mathbf{Q}_i$, which is an identity matrix with elements at the intersections of the kth and lth rows and the kth and lth columns given by

$$\begin{bmatrix} q_{ll}^{(i)} & q_{lk}^{(i)} \\ q_{kl}^{(i)} & q_{kk}^{(i)} \end{bmatrix} = \begin{bmatrix} \cos(\theta) & \sin(\theta)e^{i\phi} \\ -\sin(\theta)e^{-i\phi} & \cos(\theta) \end{bmatrix} \tag{5.6}$$

where

$$\phi = \arg\{r_{lk}^{(i-1)}[-T_d]\} \tag{5.7}$$

$$\theta = \frac{1}{2}\arctan\left\{\frac{2|r_{lk}^{(i-1)}[-T_d]|}{r_{ll}^{(i-1)}[0] - r_{kk}^{(i-1)}[0]}\right\} \quad . \tag{5.8}$$

Therefore, the overall operation in the ith step is characterised by

$$\mathbf{\Gamma}^{(i)}(z) = \mathbf{Q}_i\mathbf{\Lambda}_i(z)\mathbf{\Gamma}^{(i-1)}(z)\tilde{\mathbf{\Lambda}}_i(z)\mathbf{Q}_i^H \tag{5.9}$$

$$= \tilde{\mathbf{B}}^{(i)}(z)\mathbf{R}(z)\mathbf{B}^{(i)}(z) \tag{5.10}$$

$$\mathbf{B}^{(i)}(z) = \mathbf{Q}_i\mathbf{\Lambda}_i(z)\mathbf{B}^{(i-1)}(z) = \prod_{j=1}^{i}\mathbf{Q}_j\mathbf{\Lambda}_j(z) \quad . \tag{5.11}$$

It is shown in [57] that in order to ensure a strong spectral majorisation of the BEVD algorithm, the angle θ in equation (5.8) should be calculated using the fourquadrant arctangent function which gives the value of θ in the range of $(-\pi, \pi]$.

The operations described above can be visualised as in Figure 5.1 where all the coefficient matrices of $\mathbf{\Gamma}^{(i-1)}(z)$ are placed next to each other and ordered according to their time indicies. Figure 5.1.a shows the coefficient matrices of para-Hermitian matrix $\mathbf{\Gamma}^{(i-1)}(z)$ with the two dominant elements $r_{lk}^{(i-1)}[T_d]$ and $r_{kl}^{(i-1)}[-T_d]$. Figure 5.1.b shows the application of a delay of T_d to kth column of $\mathbf{\Gamma}^{(i-1)}(z)$ which actually "shifts" all the kth columns, which are lying in the plane surrounded by the dotted lines in the figure, in the coefficient matrices to the left, such that $r_{lk}^{(i-1)}[T_d]$ is

brought to the central lag. The application of an advance of T_d to the kth row of $\mathbf{\Lambda}_i(z)\mathbf{\Gamma}^{(i-1)}(z)$ is shown in Figure 5.1.c where we can see all the kth rows of the coefficient matrices are shifted to the right, such that $r_{kl}^{(i-1)}[-T_d]$ is also brought to the central lag. The coefficient matrices of the resulting $\mathbf{\Gamma}^{(i)}(z)$ after the ith step are shown in Figure 5.1.d where the dashed circles illustrate the dominant off-diagonal elements that have been nullified by the Given rotations. One can also see from the figure that due to the application of the delay and advance, the order of the para-Hermitian matrix becomes higher.

The algorithm is stopped either after reaching a certain measure for suppressing off-diagonal terms or after exceeding a specified number of iterations [58, 57].

After N iterations, the original matrix is decomposed as

$$\mathbf{R}(z) = \mathbf{B}^{(N)}(z)\mathbf{\Gamma}^{(N)}(z)\tilde{\mathbf{B}}^{(N)}(z) \tag{5.12}$$

where $\mathbf{\Gamma}^{(N)}(z)$ is an approximately diagonalised polynomial matrix and $\mathbf{B}^{(N)}(z)$ is the paraunitary matrix given by

$$\mathbf{B}^{(N)}(z) = \prod_{i=1}^{N} \mathbf{Q}_i\mathbf{\Lambda}_i(z) \quad . \tag{5.13}$$

Example. Figure 5.2 characterises a para-Hermitian matrix $\mathbf{R}(z) \in \mathbb{C}^{4\times4}(z)$ of order 20. This matrix may, for example, emerge from a signal vector $\mathbf{x}[n] \in \mathbb{C}^4$ obtained from a 4-element sensor array, by correlating

$$\mathbf{R}(z) \bullet\!\!-\!\!\circ\, \mathbf{R}[\tau] = \mathcal{E}\{\mathbf{x}[n]\mathbf{x}^H[n-\tau]\} \ ,$$

whereby $\mathcal{E}\{\cdot\}$ is the expectation operator. In this case, the responses on the main diagonal of figure 5.2 are the auto-correlation sequences of each sensor signal, while off-diagonal responses are the cross-correlation sequences between the various sensors. Figure 5.2 shows the moduli of the - potentially complex valued - elements in the para-Hermitian matrix.

Figure 5.3 depicts the moduli of the elements of the resulting

$$\mathbf{\Gamma}^{(N)}(z) = \tilde{\mathbf{B}}^{(N)}(z)\mathbf{R}(z)\mathbf{B}^{(N)}(z) \tag{5.14}$$

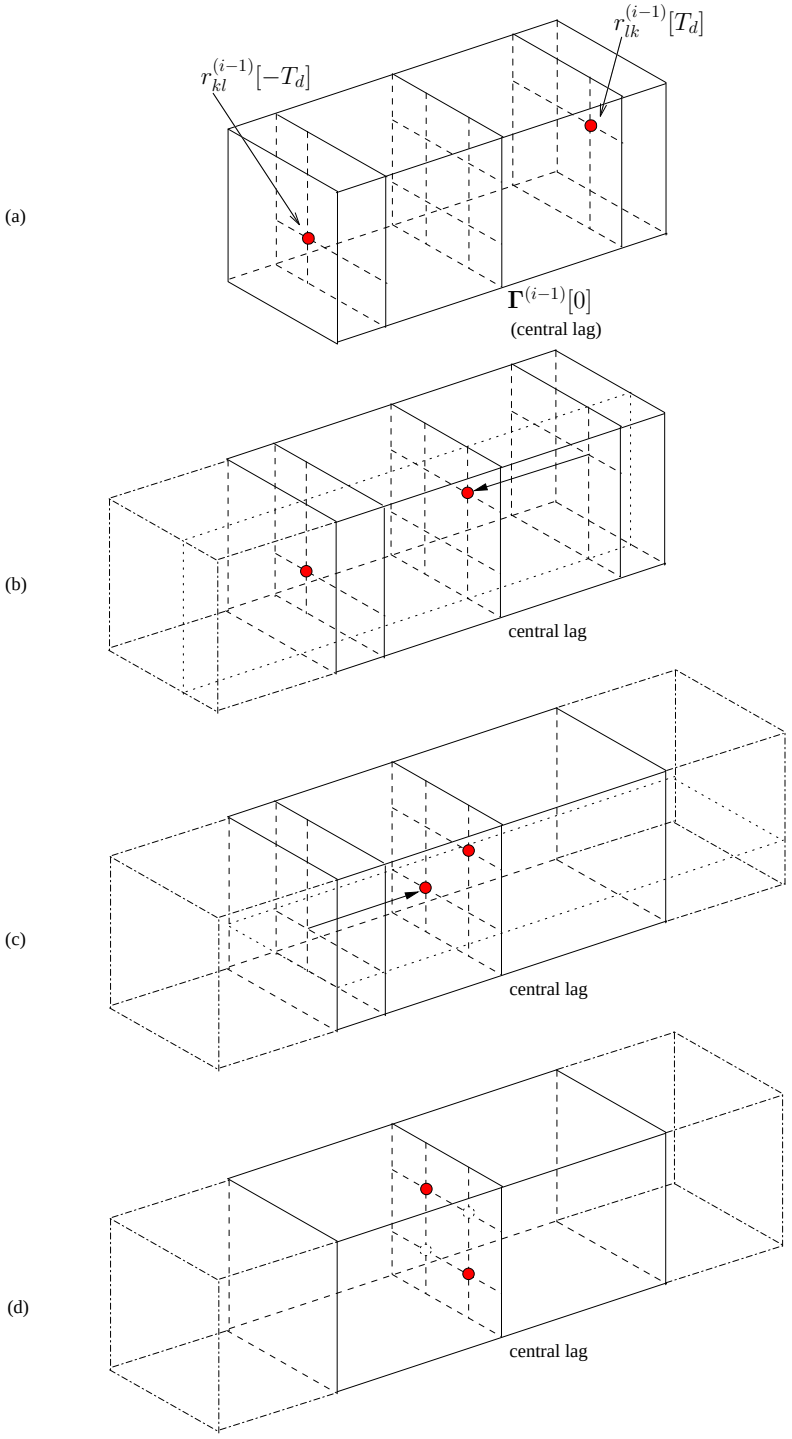

Figure 5.1: Visualisation of the ith iteration in the SBR2 algorithm: (a) coefficient matrices of para-Hermitian matrix $\mathbf{\Gamma}^{(i-1)}(z)$; (b) applying a delay of T_d to the kth column of $\mathbf{\Gamma}^{(i-1)}(z)$; (c) applying an advance of T_d to the kth raw of $\mathbf{\Gamma}^{(i-1)}(z)$; (d) coefficient matrices of the para-Hermitian matrix $\mathbf{\Gamma}^{(i)}(z)$.

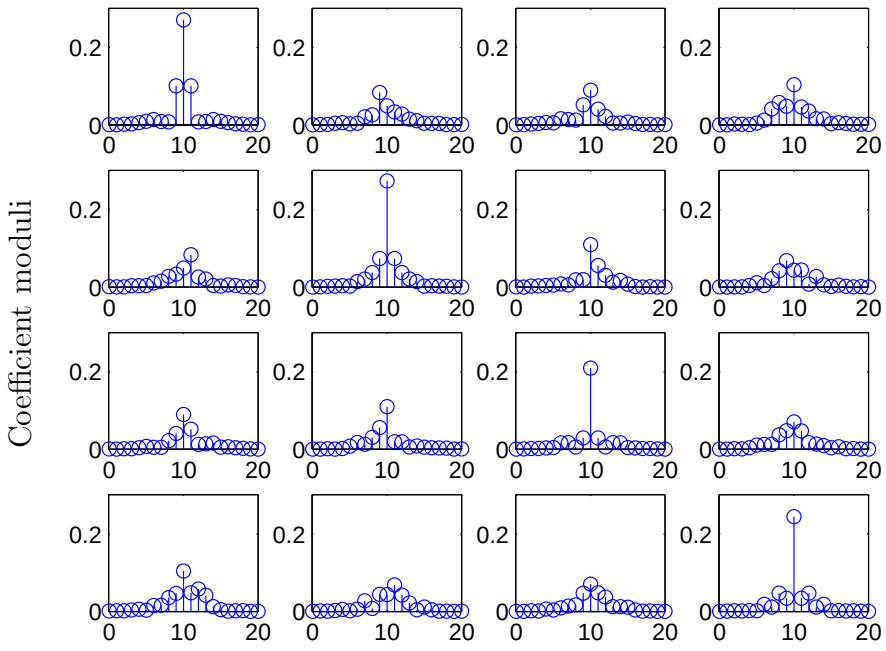

Figure 5.2: Moduli of coefficients of a para-Hermitian matrix $\mathbf{R}(z) \in \mathbb{C}^{4\times4}(z)$.

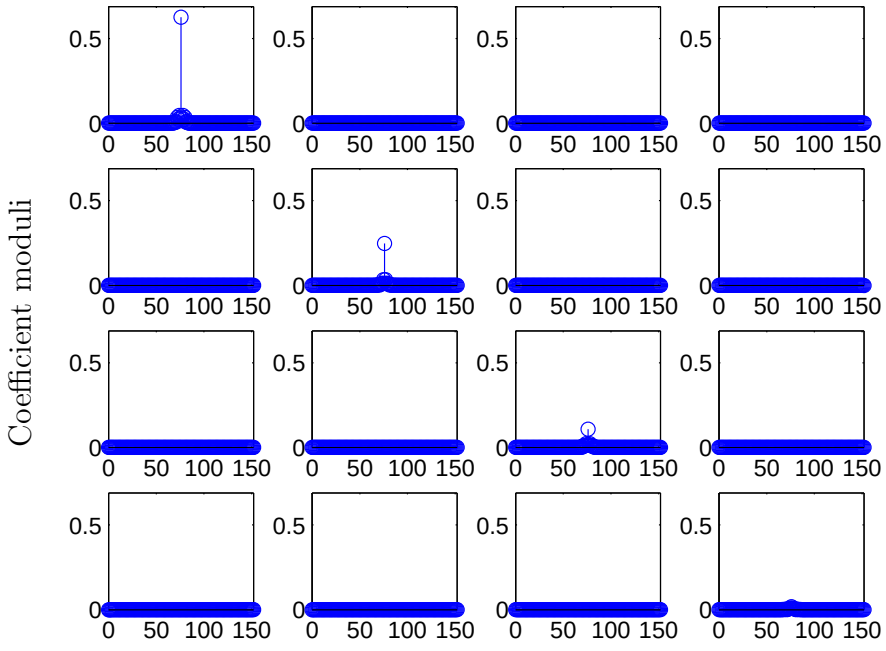

Figure 5.3: Moduli of coefficients of the para-Hermitian matrix $\mathbf{\Gamma}^{(N)}(z)$ after applying the SBR2 algorithm.

obtained by applying the SBR2 algorithm as described above. A windowed version of $\mathbf{\Gamma}^{(N)}(z)$ which contains 21 central coefficients is shown in Figure 5.4. It is evident from Figures 5.3 and 5.4 that off-diagonal elements have been largely suppressed, and only on-diagonal components remain. Note however that the order of the matrix $\mathbf{\Gamma}^{(N)}(z)$ has significantly increased as compared to $\mathbf{R}(z)$ in Figure 5.2.

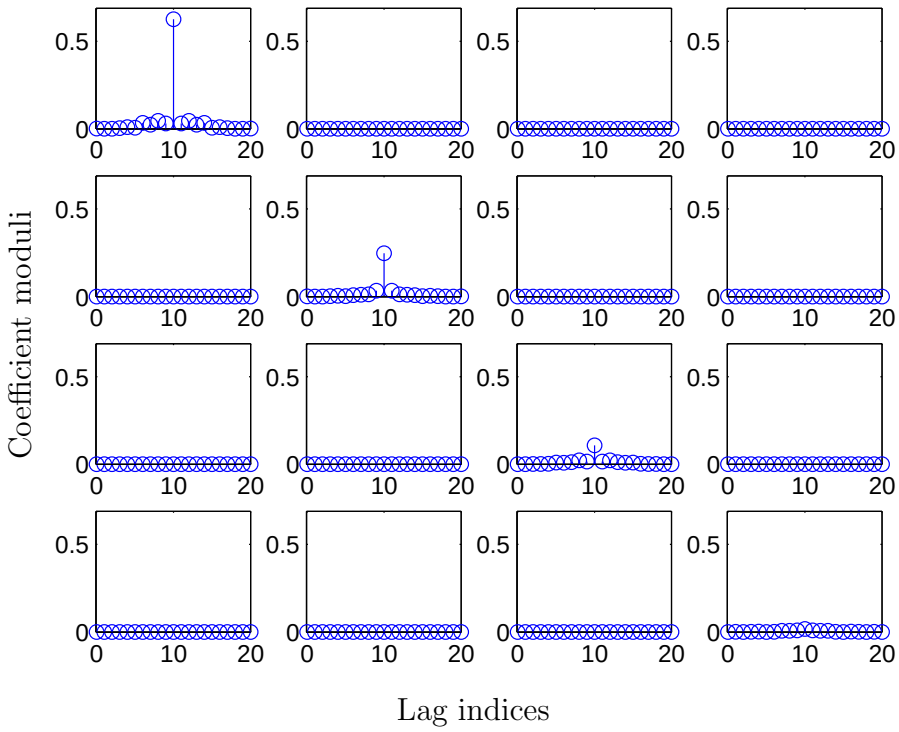

Figure 5.4: Moduli of coefficients of a windowed version of $\mathbf{\Gamma}^{(N)}(z)$.

The effect of spectral majorisation is highlighted in Figure 5.5, where the power spectral densities along the diagonal of $\mathbf{\Gamma}^{(N)}(z)$ are shown. As we can see, these frequency responses are ordered in descending values, which shows that the spectral majorisation according to (5.2) has been achieved along with the diagonalisation of $\mathbf{R}(z)$.

Since in each iteration the SBR2 algorithm eliminates only a pair of the maximum off-diagonal elements, the resulting matrix $\mathbf{\Gamma}^{(N)}(z)$ after N iterations is only approximately diagonal. The higher the number of iterations, the closer $\mathbf{\Gamma}^{(N)}(z)$

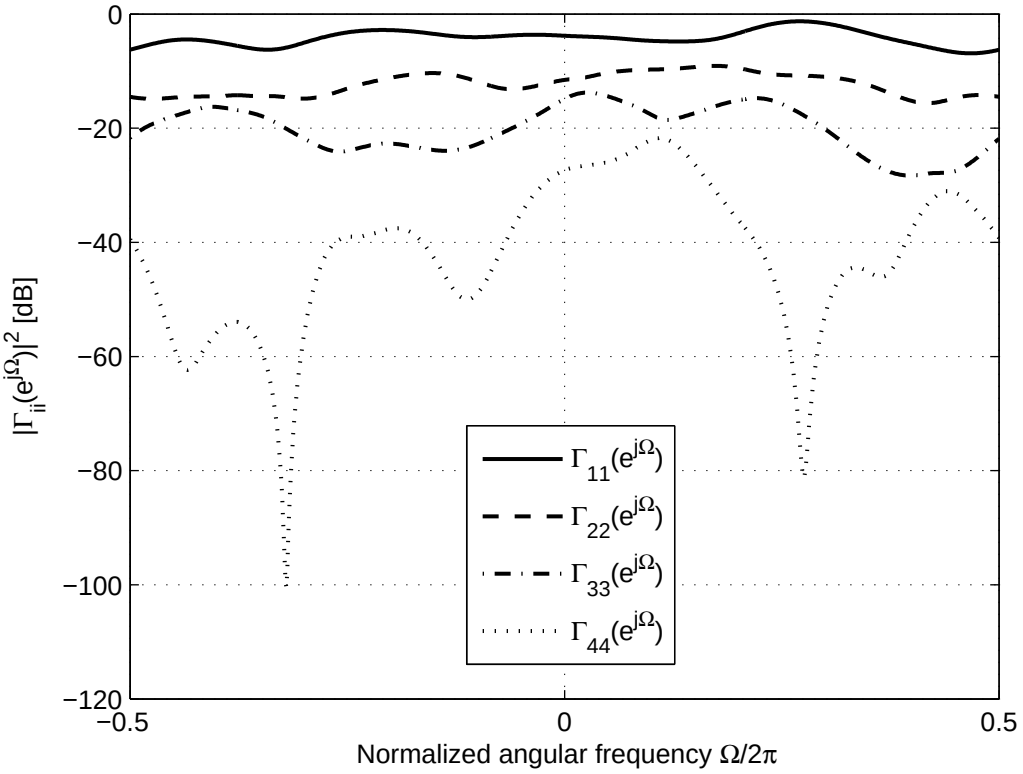

Figure 5.5: Power spectral densities $\Gamma_i^{(N)}(e^{j\Omega})$ along the main diagonal of $\mathbf{\Gamma}^{(N)}(z)$ in Figure 5.3.

approaches a diagonal matrix.

SBR2 and pseudo-circulant matrices. Section 3.5 indicated that spectral majorisation and diagonalisation are not performed well when SBR2 is applied to pseudo-circulant matrices. Here a deeper investigation on the convergence of the SBR2 algorithm applied to a para-Hermitian matrix $\mathbf{R}(z)$ constructed from a pseudo-circulant matrix $\mathbf{H}(z)$ by $\mathbf{R}(z) = \mathbf{H}(z)\tilde{\mathbf{H}}(z)$ will be provided.

Defining a function which reflects the diagonality of matrix $\mathbf{\Gamma}^{(i)}(z)$ as

$$\kappa = \frac{\left\| \mathbf{\Gamma}^{(i)}(z) - \mathbf{D}_{\Gamma}^{(i)}(z) \right\|_F^2}{\left\| \mathbf{D}_{\Gamma}^{(i)}(z) \right\|_F^2} \quad , \tag{5.15}$$

where $\mathbf{D}_{\Gamma}^{(i)}(z)$ is a diagonal polynomial matrix with the main diagonal elements equal to those of $\mathbf{\Gamma}^{(i)}(z)$, we consider the diagonalisation of the para-Hermitian

matrix $\mathbf{R}(z) = \mathbf{H}(z)\tilde{\mathbf{H}}(z)$ where $\mathbf{H}(z)$ is a pseudo-circulant matrix derived from a MIMO channel transfer function $\mathbf{C}(z)$ given P according to (2.3). As a reference, we compare $\mathbf{R}(z)$ to another para-Hermitian matrix $\mathbf{\Phi}(z) = \mathbf{H}'(z)\tilde{\mathbf{H}}'(z)$, where $\mathbf{H}'(z)$ has the same dimension of $\mathbf{H}(z)$ and the same statistics for matrix entries.

Example. We assume $\mathbf{H}(z)$ to be constructed from a 2×2 channel matrix $\mathbf{C}(z)$ of order 3 and complex Gaussian random numbers with zero mean and unit variance elements. Figure 5.6 shows the ensemble-averaged value of κ during the diagonalisation of the matrices $\mathbf{R}(z)$ and $\mathbf{\Phi}(z)$ with different numbers of polyphase components. Note that the number of iterations is chosen to be only 500 since from this value onward, the convergence of $\mathbf{R}(z)$ becomes very slow. It is clear from Figure 5.6 that for the matrix $\mathbf{\Phi}(z)$, SBR2 converges much faster than for $\mathbf{R}(z)$ although both matrices have exactly the same size, order and number of non-zero elements. For example, in the case that the number of polyphase components $P = 2$, one can see from Figure 5.6 that the value of κ in case of diagonalising $\mathbf{R}(z)$ (labelled as "$\mathbf{R}(z),\ P = 2$") is considerably higher than for the corresponding matrix $\mathbf{\Phi}(z)$ (labelled as "$4 \times 4\ \mathbf{\Phi}(z)$"). Similar observations can be made for the cases $P = 3, 4, 5$.

Thus we can see that for pseudo-circulant matrices the SBR2 algorithm converges slower than for polynomial matrices without this structure and therefore requires a higher number of iterations to approximate a BSVD.

As one can note from Figures 5.1 and 5.3, the order of the para-Hermitian matrix $\mathbf{\Gamma}^{(i)}(z)$ along with the order of paraunitary matrix $\mathbf{B}^{(i)}(z)$ is growing with each iteration. In the next subsection, we will consider the problem of shortening the order of the paraunitary matrix, in order to simplify the structure of the paraunitary filterbank based on this matrix.

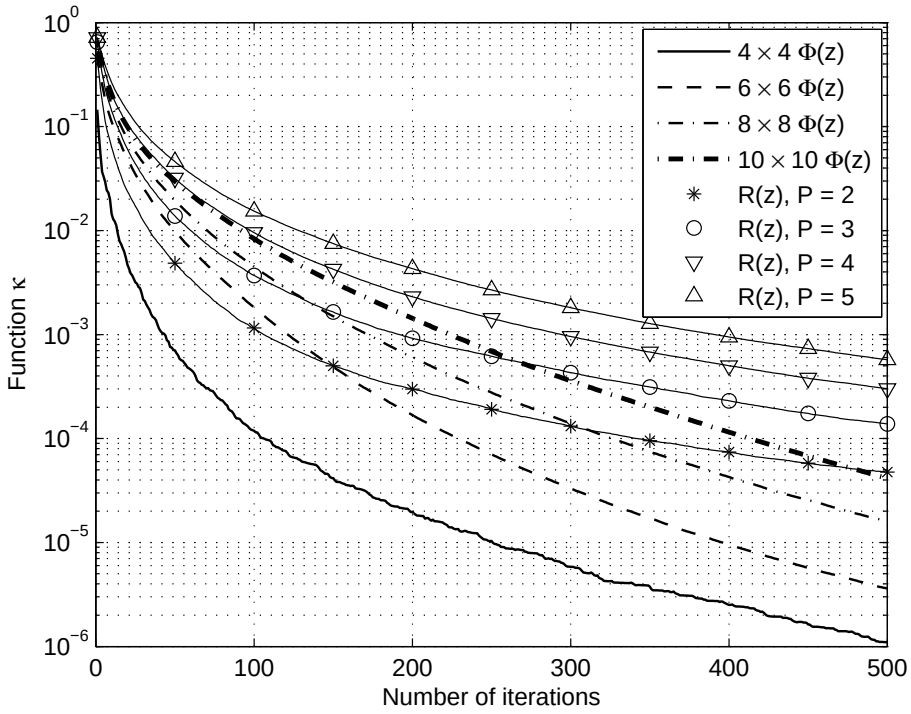

Figure 5.6: Convergence of SBR2 algorithm with different $\mathbf{R}(z)$ and $\mathbf{\Phi}(z)$ matrices.

5.1.3 Truncation of Paraunitary Matrix

Due to the delays and advances applied in the diagonalisation process, the order of the polynomial matrix $\mathbf{\Gamma}^{(N)}(z)$ as well as the order of the paraunitary matrix $\mathbf{B}^{(N)}(z)$ grow as the number of iterations increases [58, 74]. This growth requires large memory to accommodate a record of both the para-Hermitian $\mathbf{\Gamma}^{(i)}(z)$ and the paraunitary $\mathbf{B}^{(i)}(z)$ within SBR2. Also, the computational complexity to perform one iteration step increases with the iteration number. In order to avoid this, in [74] the authors have proposed to discard the outer coefficient matrices of $\mathbf{\Gamma}^{(i)}(z)$ while allowing an acceptable small loss in its Frobenius norm [1]. This approach can help to significantly reduce the order of the para-Hermitian matrix, while the

[1]The Frobenius norm of a polynomial matrix $\mathbf{A}(z)$ is defined as $\|\mathbf{A}(z)\|_F = \sqrt{\sum_{\tau=-\infty}^{+\infty} \|\mathbf{A}[\tau]\|_F^2}$ where $\mathbf{A}[\tau]$ are the coefficient matrices of $\mathbf{A}(z)$

order of the paraunitary matrix remains unaltered. Note that despite of truncation, $\mathbf{\Gamma}^{(i)}(z)$ will retain its para-Hermitian property. However, the order of the paraunitary matrix $\mathbf{B}^{(N)}(z)$ remains very high, which affects the speed of convergence for SBR2 and is likely to inhibit the application of $\mathbf{B}^{(N)}(z)$ in practical senarios where long paraunitary filter banks with large delay and complexity are undesired. Therefore it is important to consider the problem of lowering the order of the paraunitary matrix $\mathbf{B}^{(N)}(z)$ or $\mathbf{B}^{(i)}(z)$ for the more general case.

Similar to the approach in [74], we also consider the approach which discards the outer coefficient matrices of $\mathbf{B}^{(i)}(z)$ with smallest Frobenius norm. The truncation of $\mathbf{B}^{(i)}(z)$ to a matrix $\mathbf{B}_{\mathrm{T}}^{(i)}(z)$ of lower order in the course of SBR2 leads to a loss of paraunitarity. We therefore refer to $\mathbf{B}_{\mathrm{T}}^{(i)}(z)$ as a *near-paraunitary* matrix, provided that the deviation from a paraunitary matrix can be kept small. In order to quantify how close $\mathbf{B}_{\mathrm{T}}^{(i)}(z)$ is to a paraunitary matrix, we therefore define a cost function

$$\xi = \frac{1}{P} \sum_{\tau=-\infty}^{\infty} \|\mathbf{Q}[\tau]\|_F^2 \tag{5.16}$$

where

$$\mathbf{Q}[\tau] \circ\!\!-\!\!\bullet\, \mathbf{Q}(z) = \mathbf{I}_{P\times P} - \mathbf{B}_{\mathrm{T}}^{(i)}(z)\tilde{\mathbf{B}}_{\mathrm{T}}^{(i)}(z) \; . \tag{5.17}$$

In the case of no truncation, $\mathbf{B}_{\mathrm{T}}^{(i)}(z) = \mathbf{B}_{N}^{(i)}(z)$ and ξ equals to zero. Truncation of $\mathbf{B}^{(i)}(z)$ will lead to a positive error. The truncation of $\mathbf{B}^{(i)}(z)$, either during each SBR2 step or after convergence, can be performed under the condition

$$\xi \leq \epsilon \quad . \tag{5.18}$$

where ϵ is a given upper bound of the cost function.

A second measure evaluates by how much the matrix $\mathbf{R}'(z) = \tilde{\mathbf{B}}_{\mathrm{T}}^{(i)}(z)\mathbf{\Gamma}^{(i)}(z)\mathbf{B}_{\mathrm{T}}^{(i)}(z)$ deviates from the original para-Hermitian matrix $\mathbf{R}(z)$ due to truncation of $\mathbf{B}^{(i)}(z)$, for which we consider the normalised error

$$\chi = \frac{\|\mathbf{R}'(z) - \mathbf{R}(z)\|_F^2}{\|\mathbf{R}(z)\|_F^2} \quad . \tag{5.19}$$

Again, this error depends on whether $\mathbf{B}^{(i)}(z)$ is truncated only after convergence, i.e. for $i = N$, or as an ongoing operation in each step of SBR2. Unlike ξ, the error

χ is not a design parameter which permits control, but a true output to assess the impact of truncation. Note that if we perform the truncation of $\mathbf{\Gamma}^{(i)}(z)$ in each step of SBR2 as proposed in [74], it causes another deviation in addition to the deviation caused by the truncation of $\mathbf{B}^{(i)}(z)$. Thus, in such case the error χ has two sources, whereby one is from the truncation of $\mathbf{\Gamma}^{(i)}(z)$ and the other is from the truncation of $\mathbf{B}^{(i)}(z)$.

5.1.4 Simulations and Results

To highlight the advantage of the proposed truncation scheme, we consider the diagonalisation of a covariance matrix $\mathbf{R}(z)$, which is generated from a 4×4 polynomial MIMO channel matrix $\mathbf{C}(z)$ based on the Saleh-Valenzuela indoor statistical channel model in [61]. The parameters of this channel model are chosen to be similar to that of the MIMO channel in Section 3.5, thus the channel order is also 10 leading to $\mathbf{R}(z) = \mathbf{C}(z)\tilde{\mathbf{C}}(z)$ to be of order 21. Simulation is performed over an ensemble of 50 randomly generated MIMO channels. The MIMO channel matrices are normalised such that they all have unit Frobenius norm.

First we consider the truncation of the paraunitary matrix when there is no truncation of the para-Hermitian matrix $\mathbf{\Gamma}^{(i)}(z)$ in the diagonalisation process. The truncation of the paraunitary matrix is performed after the convergence of SBR2. The ensemble-averaged length of the resulting near-paraunitary matrix $\mathbf{B}_T^{(N)}(z)$ as a function of the number of iterations in case $\epsilon = 10^{-6}$ and $\epsilon = 10^{-5}$ is compared with the length of the untruncated paraunitary matrix $\mathbf{B}^{(N)}(z)$ in Figure 5.7. As one can see from the figure, without truncation the length of the paraunitary matrix is rather high. However, this length can be significantly (more than 5 times) reduced by truncating the matrix with a very small loss in its paraunitarity, namely the cost function defined in (5.16) for the truncated cases has been chosen to be upper bounded by $\epsilon = 10^{-6}$ or $\epsilon = 10^{-5}$ such that $\xi \leq 10^{-6}$ and $\xi \leq 10^{-5}$.

Figure 5.8 shows the dependence of the cost function on the number of iterations

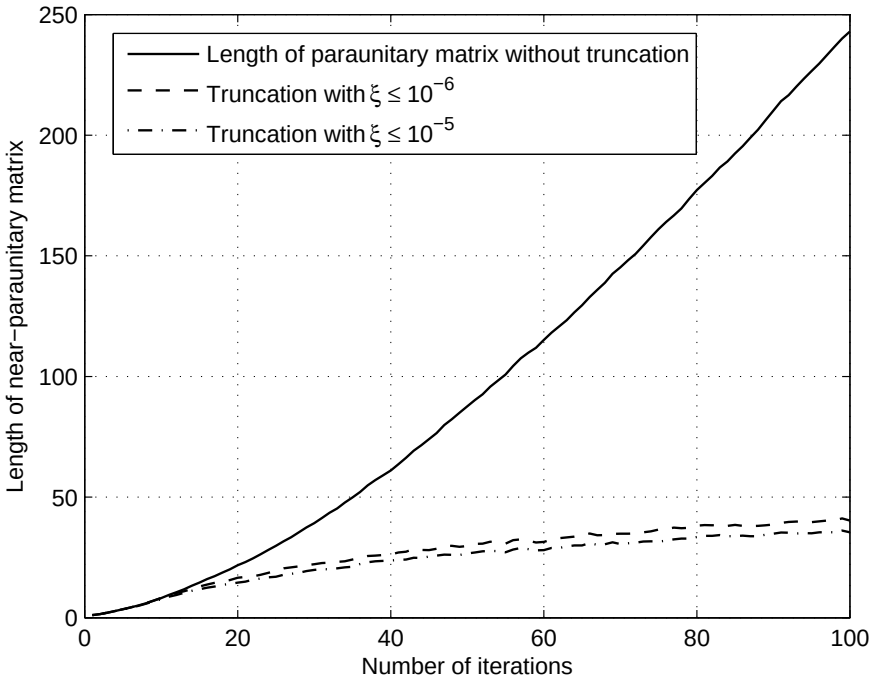

Figure 5.7: Ensemble-averaged length of the paraunitary matrix with and without truncation.

with the upper bound to be 10^{-6} and 10^{-5}.

We see from the figure that the cost function is always kept under the given upper bound. The dependence of the error funtion χ on the number of iterations is illustrated in Figure 5.9. From the figure, one can see that the distortion caused by the truncation of the paraunitary matrix is very small.

Figure 5.10 and Figure 5.11 show the averaged length of the near-paraunitary matrix and the ensemble-averaged error function in two cases where the truncation of the paraunitary matrix is performed (i) after and (ii) during the diagonalisation. One can see from the figures that performing the truncation during the diagonalisation process results in a higher order of the truncated near-paraunitary matrix under the same upper error bound. The error caused by truncation in this case is also higher but more stable than in the case of truncation after the diagonalisation process. This can be explained as in the case of performing the truncation in the diagonalisation

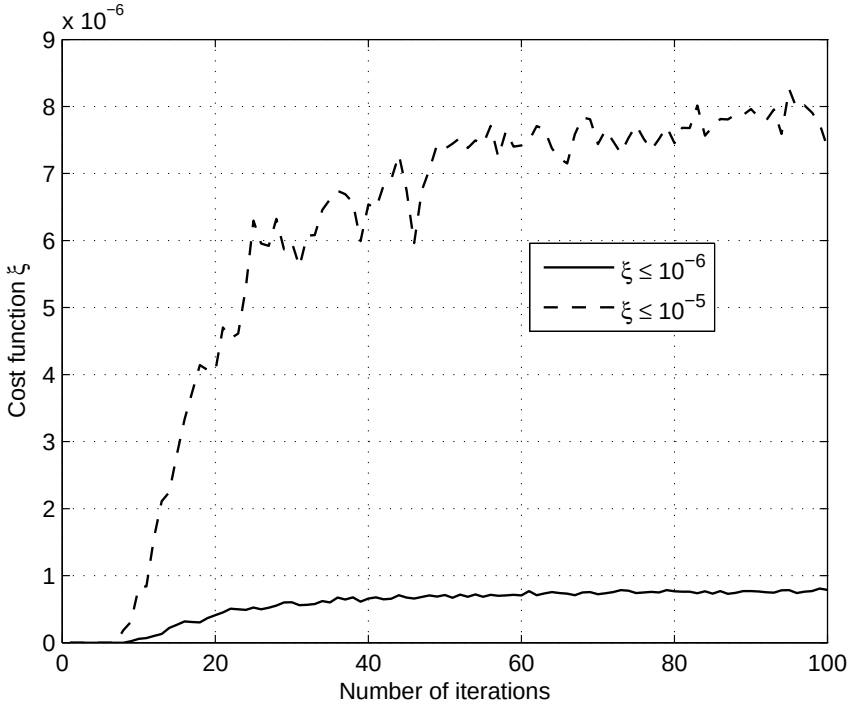

Figure 5.8: Ensemble-averaged value of the cost function for the truncated cases in Figure 5.7.

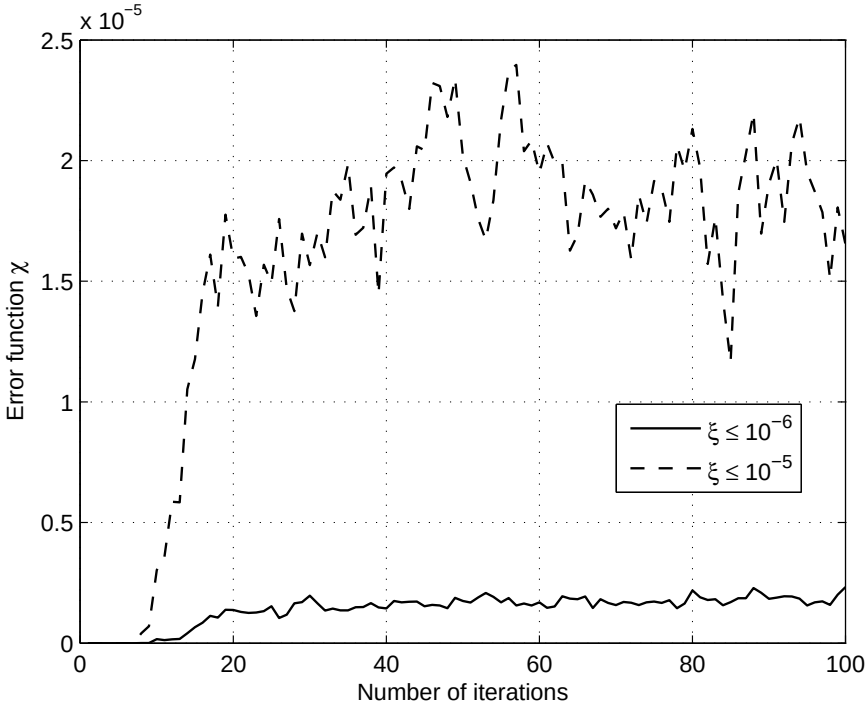

Figure 5.9: Ensemble-averaged distortion caused by truncation of $\mathbf{B}^{(N)}(z)$.

process, due to the accumulated error caused by the truncation, the near-paraunitary matrix might not satisfy the condition (5.18) in some iterations and therefore it is not truncated in those steps, this leads to a higher order of the near-paraunitary matrix $\mathbf{B}_T^{(i)}(z)$ and more stable error function as well.

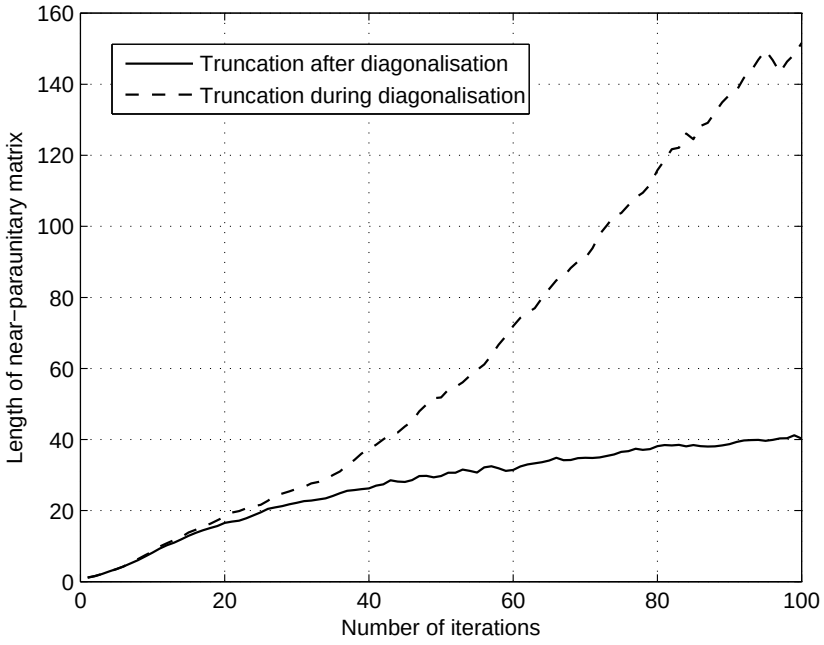

Figure 5.10: Ensemble-averaged length of the near-paraunitary matrices truncated after and during diagonalisation.

Next we consider the case where the truncation of the para-Hermitian matrix $\mathbf{\Gamma}^{(i)}(z)$ is performed during the diagonalisation process as proposed in [74] with a loss of 10^{-5} in Frobenius norm of $\mathbf{\Gamma}^{(i)}(z)$ after each iteration. As one can see from Figure 5.12, the truncation of $\mathbf{\Gamma}^{(i)}(z)$ does not have a significant effect on the length of near-paraunitary matrix, but it results in the error function increasing with the number of iterations, which means the error function χ is dominated by the error component caused by the truncation of para-Hermitian matrix.

This section has demonstrated that the order of the paraunitary matrices obtained from the SBR2 algorithm can be significantly reduced by truncating $\mathbf{B}^{(N)}(z)$. The loss in paraunitarity of $\mathbf{B}_{\mathrm{T}}^{(N)}(z)$ can be controlled by an error bound and the deviation

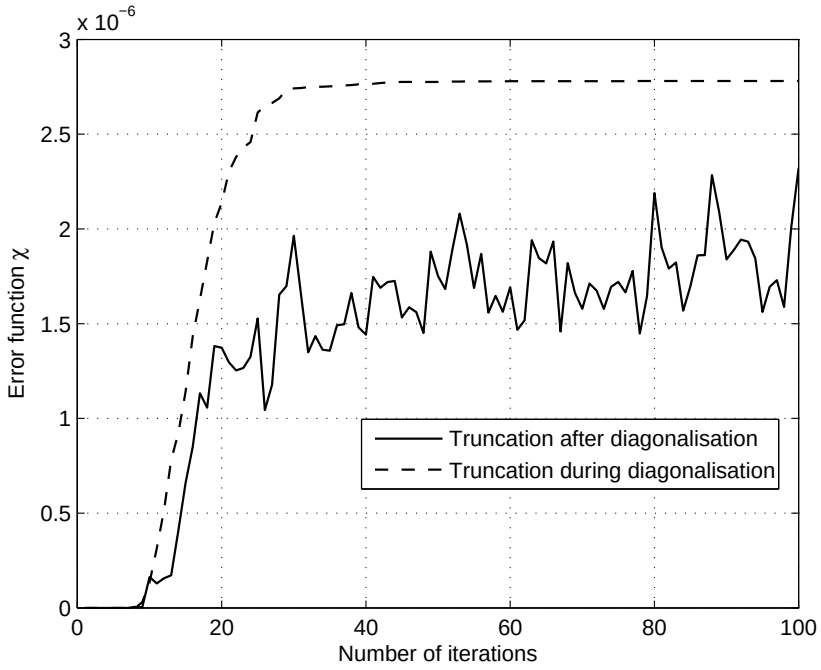

Figure 5.11: Ensemble-averaged error function in two cases of truncation (after and during the diagonalisation).

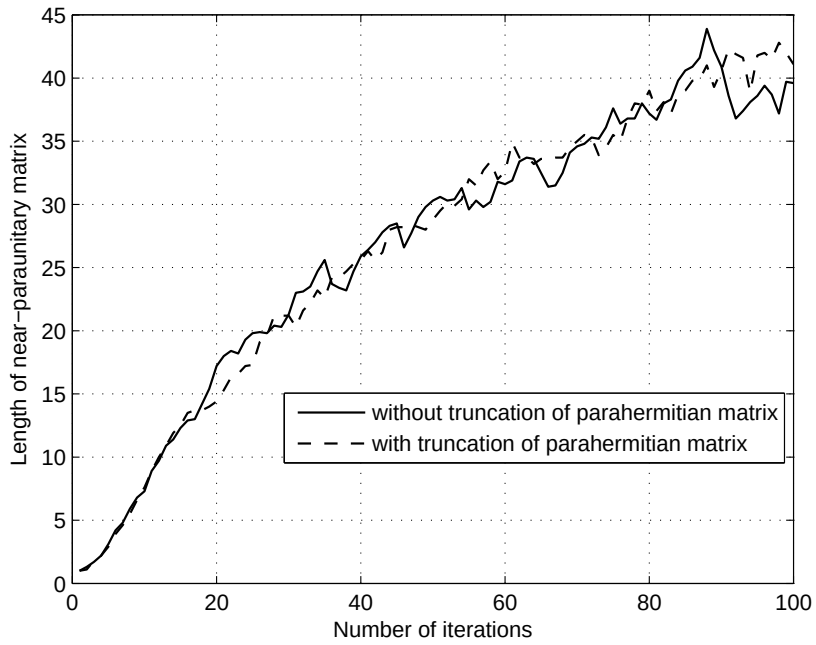

Figure 5.12: Ensemble-averaged length of the near-paraunitary matrices with and without truncation of para-Hermitian matrix.

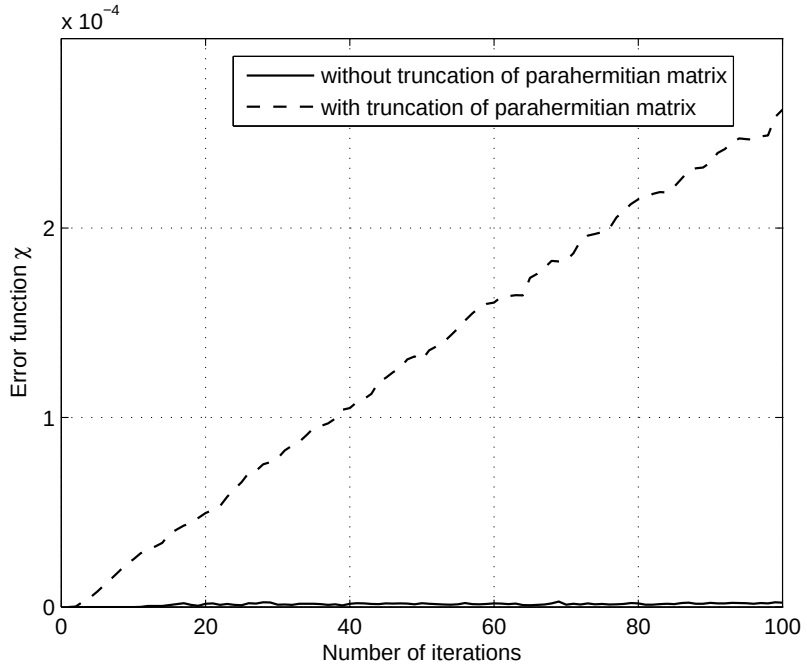

Figure 5.13: Ensemble-averaged error function with and without truncation of para-Hermitian matrix.

of $\mathbf{R}'(z) = \tilde{\mathbf{B}}_{\mathrm{T}}^{(N)}(z)\mathbf{\Gamma}^{(N)}(z)\mathbf{B}_{\mathrm{T}}^{(N)}(z)$ from the original para-Hermitian matrix $\mathbf{R}(z)$ is very small.

5.2 Performance of Recent Precoding and Equalisation Schemes with Non-Perfect CSI

In the previous chapters, we have considered different precoding and equalisation designs which can to some extent avoid the disadvantage of standard block transmission systems and cause a smaller loss in channel power gain, leading to better BER performance as well as higher data throughput. However, all the designs considered in previous chapters are based on the assumption that perfect CSI is available at both the transmitter and receiver. In practice, CSI has to be estimated, which may be prone to some estimation errors [75] unless very long data windows are available. Even then, in a realistic environment the channel may be time varying, such that a trade-off arises in the identification of the channel between an inconsistent estimate due to too short a time window, and a tracking error if the estimation error is too long. Therefore, although in the designs considered in Chapter 3, we have assumed that the channel is stationary, perfect CSI cannot be obtained due to channel estimation errors and thus an evaluation of the influence of non-perfect CSI on the performance of the considered designs is necessary.

Generally, CSI is obtained at the receiver either by means of a training sequence sent by the transmitter or identified blindly. In the former case, the training sequence, which is also referred to as pilot sequence, is known to the receiver beforehand. The receiver will, based on the knowledge of the training sequence and the received signal, attempt to estimate the CSI. In the later case, instead of using a training sequence, the receiver will utilise a specific structure of the transmitted signal or of the channel to estimate the CSI.

If the channel is estimated at the receiver end, CSI may be shared with the transmitter via a feedback channel. In 3G LTE [76], where OFDM is employed, a codebook entry to a very coarsely quantised version of the precoding matrix is fed back to the transmitter side.

Alternatively, the reciprocity of the channel may be exploited to employ a channel estimate for the reversed link. This is often considered practical for TDD systems, provided that the channel can be assumed stationary, i.e. the duration of a time slot should be sufficiently shorter than the coherence time of the channel.

For FDD systems, where the reverse link often occurs over neighbouring a frequency band, narrowband MIMO systems may use channel reciprocity if the coherence bandwidth of the channel is larger than the total bandwidth of both the up- and downlink. For the broadband MIMO systems considered in this thesis, this is not fullfilled and FDD cannot be used to obtain CSI via reciprocity.

The problem of designing transceivers under non-perfect CSI has been considered in a number of papers where the approaches generally assume flat-fading or OFDM based MIMO channels and can be classified into Bayesian techniques and worst-case techniques (see [77, 78] and references therein). In this section, we only consider the evaluation of the effect of non-perfect CSI on the system performance of our proposed design in Chapter 3. The problem of designing robust precoding and equalisation schemes for our design will be left opened for the future research.

In Section 5.2.1, we will first introduce our model for channel estimation errors. The influence of non-perfect CSI on the performance of the precoding and equalisation designs discussed in Chapter 3 will be examined through simulations in Section 5.2.2.

5.2.1 Channel Error Model

Consider a broadband MIMO channel with T transmit and R receive antennas as described in Section 2.1. Assuming that the channel transfer function is $\mathbf{C}(z) \in \mathbb{C}^{R\times T}(z)$ while the estimated channel transfer function is $\hat{\mathbf{C}}(z) \in \mathbb{C}^{R\times T}(z)$, we can write

$$\hat{\mathbf{C}}(z) = \mathbf{C}(z) + \mathbf{\Delta}(z) \tag{5.20}$$

where $\mathbf{\Delta}(z)$ is the channel estimation error, whose elements are assumed to be complex Gaussian random numbers with variance σ_E^2. We define an inverse SNR of estimation as

$$\epsilon_E = \frac{\|\mathbf{\Delta}(z)\|_F^2}{\|\mathbf{C}(z)\|_F^2} \,. \tag{5.21}$$

In some literature, the estimation error of the channel noise statistics is also considered in the design of robust precoders and/or equalisers. However, since this error has no influence on the BSVD operation in our proposed design in Chapter 3, we will not consider it here and assume that the noise is white with perfectly known variance σ_n^2.

5.2.2 Effect of Non-Perfect CSI on Precoding and Equalisation Performance - Simulation Results

In this subsection, we will investigate the effect of non-perfect CSI on the performance of the precoding and equalisation designs considered in Chapter 3. We take the same broadband MIMO channel model as described in Section 3.5 with the error model described in the previous subsection being taken into account. Similar to the error model in [75], the variance σ_E^2 of the error is choosen to be $\sigma_E^2 = 0.01$. The error matrix $\mathbf{\Delta}(z)$ is normalised such that the inverse SNR of estimation $\epsilon_E = \{0.02, 0.05, 0.1, 0.15\}$.

The number of polyphase components is choosen to be $P = 1$. The transmit block size for all the SISO FS subchannels resulting from the BSVD is choosen to be $P_1 = P_2 = P_3 = P_4$. These block sizes and the input block length N are choosen similar to those in Section 3.5, leading to a code rate of 0.57. The benchmark design, which is the MMSE optimal linear precoding and equalisation scheme proposed in [25], utilises the same sizes of its transmit as well as its input blocks.

In order to evaluate the influence of non-perfect CSI on the performance of our proposed design and the benchmark, we measure the average BER of the two designs

under various values of ϵ_E. To highlight the influence of the channel estimation error only, we keep the channel matrix $\mathbf{C}(z)$ in (5.20) fixed and randomise the error matrix $\mathbf{\Delta}(z)$.

Figure 5.14 compares the BER performace of our proposed MMSE-LPE-BSVD design and of the benchmark design (MMSE-LPE-MIMO design). From the figure, one can see that at a BER of 10^{-4} when the channel error is small ($\epsilon_E = 0.02; \epsilon_E = 0.05$) our proposed design experiences a loss of nearly 1 dB for $\epsilon_E = 0.02$, and of nearly 3 dB for $\epsilon_E = 0.05$ while the benchmark design bears a loss of more than 1 dB for $\epsilon_E = 0.02$ and nearly 4 dB for $\epsilon_E = 0.05$. Thus under small channel estimation error, our proposed design is less sensitive to channel error than the benckmark design. However, when the channel estimation errors become larger, namely in case $\epsilon_E = 0.1$ or $\epsilon_E = 0.15$, one can see from the figures that the BER performance of our proposed design becomes much poorer and closer to the BER performance of the benckmark design. This shows that under strong channel error, the proposed design approaches the BER performance of the benchmark design.

5.3 Concluding Remarks

In this chapter, several issues relating to the performance of our proposed design have been addressed. First, after reviewing the BEVD computation algorithm, we have proposed an approach to shorten the order of the paraunitary matrix obtained from the BEVD. The algorithm tries to reduce the order of a paraunitary matrix while still keeping the loss in its paraunitarity below a given upper bound. The simulation results show that our proposed approach can significantly reduce the order of the paraunitary matrix while the upper bound of the loss in paraunitarity can still be controlled and the error introduced by the truncation of the paraunitary matrix to the diagonalisation process is very small. Performing the truncation of the paraunitary matrix after the diagonalisation process has been shown to result in a lower order of the near-paraunitary matrix as compared to when performing the

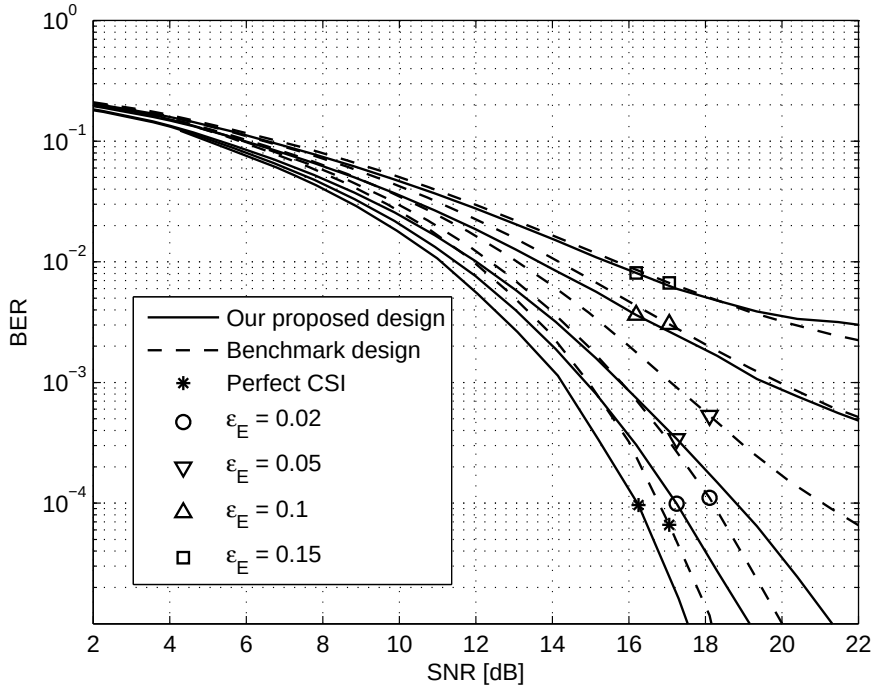

Figure 5.14: Comparison of the BER performance of the proposed MMSE-LPE-BSVD design and the benchmark with non-perfect CSI.

truncation during the diagonalisation process.

Second, the influence of non-perfect CSI on the BER performance of the proposed design in Chapter 3 has been investigated and compared with that of a benchmark design based on block transmission. The simulation results show that the proposed design has a better performance in the case of perfect CSI and is less sensitive to small errors compared to the benchmark design, however under stronger channel errors our proposed design becomes less robust and its BER performance approaches that of the benchmark design. This can be explained as follow. The effect of the channel error on the system performance depends on how much error is "transferred" from the estimated channel matrix to the FS SISO subchannels resulting from the BSVD operation. Since the SBR2 is looking for maximum off-diagonal elements to be eliminated during its iteration process, after a certain number of iterations, there is always a number of off-diagonal elements that are small enough so that they are not eliminated by the BEVD. The value of those small elements depends on the

number of iterations as well as the criterion terminating the iteration: the higher the number of iteration is, the smaller off-diagonal elements are. Thus when the channel error is small, by setting an appropriate number of iterations, we discard a part of the channel error occupying those small off-diagonal elements and therefore reduce the amount of channel error that is "transferred" to the design of the precoders and equalisers of the FS SISO subchannels. Meanwhile, the benchmark design relies entirely on the EVD of the channel matrix as shown in (2.52) which can entirely eliminate the off-diagonal elements and may therefore suffer from a higher amount of channel error.

Chapter 6

Conclusions and Future Works

In this thesis, several approaches for precoding and equalisation for broadband MIMO channels have been addressed. Standard techniques for broadband MIMO utilise block transmission schemes, such as OFDM, which require the introduction of a guard interval. The main focus of this thesis has rested on achieving a higher spectral efficiency by reducing or circumventing the use of a guard interval in block transmission. In the following, we first summarise the main outcomes of this thesis before providing thoughts for future work.

6.1 Summary

In Chapter 3 we have proposed a design for precoding and equalisation for broadband MIMO channels. First, based on the recently proposed BSVD algorithm, we have derived a pair of precoders and equalisers that decompose a broadband MIMO channel into a number of independent FS SISO subchannels. Second, we have applied conventional block transmission based approaches to design second-tier pairs of linear joint optimal precoders and equalisers to remove the remaining ISI on each SISO subchannel. The use of BSVD based precoders and equalisers not only removes the CCI in the MIMO channels, but also helps to indirectly suppress part of the

ISI caused by the channel's frequency selectivity. This aids in reducing the loss in channel energy due to elimination of ISI and also helps to direct more power towards strong eigenmodes when a water-filling algorithm is performed following the second step. Overall, it has been shown that the proposed system can achieve a better BER performance or higher data throughput under a quality of service constraint compared to a benchmark system.

The first part of Chapter 4 has focused on the reduction of the redundancy used for ISI cancellation in block transmission systems and proposed an approach to joint precoding and block decision feedback equalisation. The proposed design has emerged from two recently reported methods: first, IBI is removed by a decision-feedback equaliser, then a joint optimal linear precoder and non-linear BDFE is designed for the remaining fading MIMO channel. With the help of the decision-feedback equaliser in the first step, the precoder can use guard intervals that are much shorter than the channel order. It is the optimality inherited from the design in the second step that provides an enhanced BER performance compared to other analogous designs in the literature.

The second part of Chapter 4 has focused on the improving the performance of block transmission systems. Based on an analysis of the loss in channel energy caused by the conventional use of guard intervals, we have proposed several designs to reduce this loss. In the first design, although the guard interval is used for IBI elimination, it is shared between the precoder and the equaliser. In all the other designs, the IBI elimination entirely relies on a DFE at the receiver, and the redundancy introduced by the precoder is used to discard the weak subchannels. Our proposed designs have been shown to outperform conventional block transmission designs. The proposed designs can also be applied to broadband MIMO scenarios.

In order to further improve the applicability of the BSVD algorithm for communications scenarios, Chapter 5 has been dedicated to reduce the order of the paraunitary matrices as well as the SISO subchannels obtained from the BSVD algorithm. This allows near-paraunitary filterbanks based with a reduced imple-

mentation cost. From the simulation results, it has been evident that it is possible to significantly reduce the order of the parauniraty matrices while keeping the loss in paraunitarity below a given threshold.

Finally, the second part of Chapter 5, has considered the situation where the only non-perfect CSI is available to both transmitter and receiver. The simulation results in this part have shown that our proposed design in Chapter 3 is more robust than the standard linear joint optimal precoding and equalisation design when the channel error is small. For larger estimation errors, the proposed design and the benchmark system showed similar performance. Thus, overall it appears advantageous to utilise the proposed system.

6.2 Future Work

Beyond the research summarised in Sec. 6.1 a number of issues have been identified as relevant, but are beyond the scope of this thesis and are recommended for future investigation:

Combination of BSVD with non-linear precoding methods. The combination of BSVD based precoding and equalisation with non-linear precoding methods, such as Tomlinson-Harashima precoding (THP) [79, 80, 81], can help to avoid the problem of error propagation in a DFE and may offer performance advantages over the BDFE designs presented in Chapter 4. For both DFE and THP, the detection order is critical and will require optimisation. If these techniques are combined with the BSVD MIMO decoupling, spectral majorisation would help to determine a suitable detection order, whereby the data streams are detected in order of their subchannel gain and subsequently their SNR.

Combination of BSVD with robust precoding and equalisation schemes. Robust designs of precoding and equalisation proposed in the literature, such as

[77, 75], require the knowledge of an upper bound for the channel estimation error. This could be utilised to achieve a more robust design with enhanced performance, if, after decoupling the MIMO channel using the BSVD, the channel estimation error of the SISO subchannels was known. The known error bounds that are imposed on the system as part of the truncation of the precoding, equalisation, as well as the para-Hermitian matrices within SBR2 during the BSVD calculation could contribute to such an improved robust design.

Hardware implementation issues of the SBR2 algorithm. The effect of quantisation noise and rounding errors when using fixed point arithmetic, such as found on many hardware platforms, should be investigated for the SBR2 algorithm. Some numerical techniques may be more robust and less prone to error propagation than others, and the aim would be to identify a suitable computational scheme and quantify any performance loss compared to a floating point calculation.

Channel coding. In addition to precoding and equalisation, paraunitary filter banks can also be used for channel coding. Discarded subchannels can form a syndrom vector, which should have a zero output in the receiver. Deviations may be used to detect impulse noise [82] in order to increase the robustness of a transmission system. In an impulse noise environment, filter bank based precoding and equalisation already adds robustness, as information is spread over time and therefore less affected by impulsive interference. If additionally decoded symbols in the presence of a detected noise impulse are labelled as erasures, the error correction capability of some codes, such as Reed-Solomon, may be increased. Preliminary work on using paraunitary filter banks designed by SBR2 for channel coding has been performed in a power line communications scenario [72, 83], but combination of such coding techniques with the precoding and equalisation techniques for broadband MIMO systems as presented in this thesis appear very attractive.

Appendix A

Derivation of Joint Optimal Precoders and BDFEs

This appendix will provide a brief description of the derivation of the joint optimal precoders and BDFEs in subsections 4.1.3.1 and 4.1.3.2. The derivations in this section are based on the work by Xu et. al in [32]. Since these design problems are central to this thesis, the problem formulations, derivations, and solutions for the ZF and MMSE design case are set out below.

A.1 Derivation of ZF Joint Optimal Precoding and BDFE

The design problem for ZF joint optimal precoding and BDFE is stated as [32]

$$\begin{aligned} \min_{\mathbf{F}_0,\mathbf{W}_0,\mathbf{B}_0} \quad & \text{trace}(\mathbf{R}_{ee}) \\ \text{subject to} \quad & \text{trace}(\mathbf{F}_0\mathbf{F}_0^{\text{H}}) = P_0 \\ & \mathbf{W}_0\mathbf{H}_M\mathbf{F}_0 = \mathbf{B}_0 + \mathbf{I} \\ & \mathbf{B}_0 \text{ is strictly upper triangular,} \end{aligned}$$

where P_0 is the transmit power.

With the ZF constraint $\mathbf{W}_0\mathbf{H}_M\mathbf{F}_0 = \mathbf{B}_0 + \mathbf{I}$, the error covariance matrix in (4.6) can be written as

$$\begin{aligned}\mathbf{R}_{ee} &= \mathbf{W}_0\mathbf{R}_{vv}\mathbf{W}_0^H \\ &= (\mathbf{B}_0 + \mathbf{I})\,(\mathbf{H}_M\mathbf{F}_0)^\dagger\,\mathbf{R}_{vv}\left[(\mathbf{H}_M\mathbf{F}_0)^\dagger\right]^{\mathrm{H}}(\mathbf{B}_0 + \mathbf{I})^{\mathrm{H}}\,.\end{aligned} \tag{A.1}$$

Setting $\mathbf{H}_R = \mathbf{R}_{vv}^{-1/2}\mathbf{H}_M$, one can write

$$\mathbf{R}_{ee} = (\mathbf{B}_0 + \mathbf{I})\,(\mathbf{H}_R\mathbf{F}_0)^\dagger\left[(\mathbf{H}_R\mathbf{F}_0)^\dagger\right]^{\mathrm{H}}(\mathbf{B}_0 + \mathbf{I})^{\mathrm{H}}\,. \tag{A.2}$$

If $\mathbf{F}_0$ is selected such that $\mathrm{rank}(\mathbf{F}_0) = N$ then $\mathrm{rank}(\mathbf{H}_R\mathbf{F}_0) = N$ and therefore the matrix $\left(\mathbf{F}_0^{\mathrm{H}}\mathbf{H}_R^{\mathrm{H}}\mathbf{H}_R\mathbf{F}_0\right)$ is invertible and one can write

$$(\mathbf{H}_R\mathbf{F}_0)^\dagger = \left(\mathbf{F}_0^{\mathrm{H}}\mathbf{H}_R^{\mathrm{H}}\mathbf{H}_R\mathbf{F}_0\right)^{-1}\mathbf{F}_0^{\mathrm{H}}\mathbf{H}_R^{\mathrm{H}}\,. \tag{A.3}$$

Applying this result to the equation (A.2), one can have

$$\mathbf{R}_{ee} = (\mathbf{B}_0 + \mathbf{I})\left(\mathbf{F}_0^{\mathrm{H}}\mathbf{H}_R^{\mathrm{H}}\mathbf{H}_R\mathbf{F}_0\right)^{-1}(\mathbf{B}_0 + \mathbf{I})^{\mathrm{H}}\,. \tag{A.4}$$

Based on the trace-determinant inequality [32] [1], one can now write

$$\frac{\mathrm{trace}(\mathbf{R}_{ee})}{N} \geq \left|(\mathbf{B}_0 + \mathbf{I})\left(\mathbf{F}_0^{\mathrm{H}}\mathbf{H}_R^{\mathrm{H}}\mathbf{H}_R\mathbf{F}_0\right)^{-1}(\mathbf{B}_0 + \mathbf{I})^{\mathrm{H}}\right|^{1/N}\,. \tag{A.6}$$

Since $|\mathbf{B}_0 + \mathbf{I}| = 1$ as $\mathbf{B}_0$ is a strictly upper triangular matrix, the above inequality can be rewritten as

$$\frac{\mathrm{trace}(\mathbf{R}_{ee})}{N} \geq \left|\mathbf{F}_0^{\mathrm{H}}\mathbf{H}_R^{\mathrm{H}}\mathbf{H}_R\mathbf{F}_0\right|^{-1/N} \tag{A.7}$$

or

$$\frac{\mathrm{trace}(\mathbf{R}_{ee})}{N} \geq \left|\mathbf{F}_0^{\mathrm{H}}\mathbf{H}_M^{\mathrm{H}}\mathbf{R}_{vv}^{-1}\mathbf{H}_M\mathbf{F}_0\right|^{-1/N}\,. \tag{A.8}$$

[1] This inequality is a consequence of the arithmetic-geometric mean inequality [84] and is formulated as: for an $N \times N$ positive semidefinite matrix $\mathbf{A}$

$$\frac{\mathrm{trace}(\mathbf{A})}{N} \geq |\mathbf{A}|^{1/N} \tag{A.5}$$

with equality holds if and only if $\mathbf{A} = \alpha\mathbf{I}$ for some $\alpha \geq 0$.

This inequality shows that the system arithmetic MSE trace($\mathbf{R}_{ee}$)/N has a lower bound of $\left|\mathbf{F}_0^{\mathrm{H}}\mathbf{H}_M^{\mathrm{H}}\mathbf{R}_{vv}^{-1}\mathbf{H}_M\mathbf{F}_0\right|^{-1/N}$. Thus, the minimisation of the lower bound of the arithmtic MSE is the minimisation of $\left|\mathbf{F}_0^{\mathrm{H}}\mathbf{H}_M^{\mathrm{H}}\mathbf{R}_{vv}^{-1}\mathbf{H}_M\mathbf{F}_0\right|^{-1/N}$ which in turn is equivalent to the maximisation of $\left|\mathbf{F}_0^{\mathrm{H}}\mathbf{H}_M^{\mathrm{H}}\mathbf{R}_{vv}^{-1}\mathbf{H}_M\mathbf{F}_0\right|$. Therefore one now has to find a precoder $\mathbf{F}_0$ which maximises the aforementioned determinant subject to the transmit power constraint.

To calculate $\mathbf{F}_0$, from the EVD

$$\mathbf{H}_M^{\mathrm{H}}\mathbf{R}_{vv}^{-1}\mathbf{H}_M = \mathbf{V}\mathbf{\Lambda}\mathbf{V}^{\mathrm{H}} \quad , \tag{A.9}$$

let $\mathbf{V}_N$ contain the first N columns of $\mathbf{V}$, $\mathbf{\Lambda}_N$ to be the upper left $N \times N$ block of the diagonal matrix $\mathbf{\Lambda}$ holding the eigenvalues λ_{ii}, $i = 1 \cdots N$, and let $\mathbf{\Gamma} = \sqrt{\mathbf{\Lambda}_N}$. Since rank($\mathbf{F}_0$) = N, it can be decomposed as

$$\mathbf{F}_0 = \mathbf{U}_F\mathbf{\Phi}\mathbf{V}_F \tag{A.10}$$

where $\mathbf{U}_F \in \mathbb{C}^{M\times N}$ and $\mathbf{V}_F \in \mathbb{C}^{N\times N}$ are unitary matrices, $\mathbf{\Phi}$ is an $N \times N$ diagonal positive definite matrix. With the above decompositions and notations and again based on the trace-determinant inequality in (A.5) one can write

$$\left|\mathbf{F}_0^{\mathrm{H}}\mathbf{H}_M^{\mathrm{H}}\mathbf{R}_{vv}^{-1}\mathbf{H}_M\mathbf{F}_0\right| = \left|\mathbf{\Phi}^2\right| \ \left|\mathbf{U}_F^{\mathrm{H}}\mathbf{V}\mathbf{\Lambda}\mathbf{V}^{\mathrm{H}}\mathbf{U}_F\right| \ , \tag{A.11}$$

$$\left|\mathbf{\Phi}^2\right| \ \left|\mathbf{U}_F^{\mathrm{H}}\mathbf{V}\mathbf{\Lambda}\mathbf{V}^{\mathrm{H}}\mathbf{U}_F\right| \leq \left[\frac{\mathrm{trace}(\mathbf{\Phi}^2)}{N}\right]^N \prod_{j=1}^{N}\lambda_{jj} = \left(\frac{P_0}{N}\right)^N \prod_{j=1}^{N}\lambda_{jj} \ , \tag{A.12}$$

as trace($\mathbf{F}_0\mathbf{F}_0^{\mathrm{H}}$) = trace($\mathbf{\Phi}^2$) = P_0. Therefore

$$\left|\mathbf{F}_0^{\mathrm{H}}\mathbf{H}_M^{\mathrm{H}}\mathbf{R}_{vv}^{-1}\mathbf{H}_M\mathbf{F}_0\right| \leq \left(\frac{P_0}{N}\right)^N \prod_{j=1}^{N}\lambda_{jj} \ . \tag{A.13}$$

From (A.8) and the above inequality, it can be seen that the MSE lower bound can be minimised to $(N/P_0)(\prod_{j=1}^{N}\lambda_{jj})^{-1/N}$. In order for the first equality in (A.12) to hold, which also means that the MSE lower bound is then minimised, it is required that $\mathbf{\Phi} = \alpha\mathbf{I}$ for some $\alpha > 0$ and $\mathbf{U}_F = \mathbf{V}_N$. Therefore it can be derived from the transmit power constraint that $\alpha = \sqrt{P_0/N}$ and $\mathbf{F}_0$ now has the form $\mathbf{F}_0 = \sqrt{P_0/N}\mathbf{V}_N\mathbf{V}_F$.

One now has to find $\mathbf{V}_F$ and $\mathbf{B}_0$ such that the system MSE can achieve its minimised lower bound. For this, it is required that the equality in (A.6) to hold, which in turn requires that $\mathbf{R}_{ee} = \alpha\mathbf{I}$ for some $\alpha > 0$. From the value of the minimised lower bound of MSE found above, one can see that now

$$\mathbf{R}_{ee} = \frac{N}{P_0}\left(\prod_{j=1}^{N}\lambda_{jj}\right)^{-1/N}\mathbf{I}\,. \tag{A.14}$$

Replacing the $\mathbf{F}_0$ found above into the the product in the right hand side of (A.6) gives

$$(\mathbf{B}_0+\mathbf{I})\mathbf{V}_F^{\mathrm{H}}\mathbf{\Lambda}_N^{-1}\mathbf{V}_F(\mathbf{B}_0+\mathbf{I})^{\mathrm{H}} = \left(\prod_{j=1}^{N}\lambda_{jj}\right)^{-1/N}\mathbf{I} \tag{A.15}$$

Based on the geometric mean decomposition [31], which decomposes the matrix $\mathbf{\Gamma}$ such that

$$\mathbf{\Gamma} = \mathbf{U}\mathbf{R}\mathbf{\Theta}^{\mathrm{H}} \quad , \tag{A.16}$$

whereby $\mathbf{U}$ and $\mathbf{\Theta}$ are unitary matrices and $\mathbf{R}$ is an upper-triangular matrix with equal diagonal elements identical to the geometric mean of the diagonal elements of $\mathbf{\Gamma}$

$$r_{ii} = \left(\prod_{j=1}^{N}\gamma_{jj}\right)^{1/N} = \left(\prod_{j=1}^{N}\lambda_{jj}\right)^{1/(2N)} \quad , \tag{A.17}$$

one can see that by choosing

$$\mathbf{V}_F = \mathbf{\Theta} \tag{A.18}$$

$$\mathbf{B}_0+\mathbf{I} = \left(\prod_{i=1}^{N}\lambda_{ii}\right)^{-\frac{1}{2N}}\mathbf{R}\,, \tag{A.19}$$

the condition in (A.15) will be satisfied. Thus the optimal precoder matrix has the form

$$\mathbf{F}_0 = \sqrt{P_0/N}\,\mathbf{V}_N\mathbf{\Theta} \quad . \tag{A.20}$$

The feedback and feedforward matrices are then given by

$$\mathbf{B}_0 = \left(\prod_{i=1}^{N}\lambda_{ii}\right)^{-\frac{1}{2N}}\mathbf{R}-\mathbf{I} \tag{A.21}$$

$$\mathbf{W}_0 = (\mathbf{B}_0+\mathbf{I})(\mathbf{H}_M\mathbf{F}_0)^{\dagger} \quad . \tag{A.22}$$

A.2 Derivation of MMSE Joint Optimal Precoding and BDFE

The design problem of a precoder and BDFE equaliser for the case of joint optimality in the MMSE sense is stated as [32]:

$$\begin{aligned} \min_{\mathbf{F}_0,\mathbf{W}_0,\mathbf{B}_0} \quad & \text{trace}(\mathbf{R}_{ee}) \\ \text{subject to} \quad & \text{trace}(\mathbf{F}_0\mathbf{F}_0^{\text{H}}) = P_0 \\ & \mathbf{W}_0 = (\mathbf{B}_0 + \mathbf{I})\mathbf{R}_{sy}\mathbf{R}_{yy}^{-1} \\ & \mathbf{B}_0 \text{ is strictly upper triangular.} \end{aligned}$$

where

$$\mathbf{R}_{sy} = (\mathbf{H}_M\mathbf{F}_0)^{\text{H}} \tag{A.23}$$

$$\mathbf{R}_{yy} = (\mathbf{H}_M\mathbf{F}_0)(\mathbf{H}_M\mathbf{F}_0)^{\text{H}} + \mathbf{R}_{vv} \quad . \tag{A.24}$$

In this case, the error covariance matrix in (4.6) can be re-written as [32]

$$\mathbf{R}_{ee} = (\mathbf{B}_0 + \mathbf{I})(\mathbf{I} + \mathbf{F}_0^{\text{H}}\mathbf{H}_M^{\text{H}}\mathbf{R}_{vv}^{-1}\mathbf{H}_M\mathbf{F}_0)^{-1}(\mathbf{B}_0 + \mathbf{I})^{\text{H}} \, . \tag{A.25}$$

Based on the trace-determinant inequality, it can be seen that

$$\begin{aligned} \frac{\text{trace}(\mathbf{R}_{ee})}{N} &\geq \left|(\mathbf{B}_0 + \mathbf{I})(\mathbf{I} + \mathbf{F}_0^{\text{H}}\mathbf{H}_M^{\text{H}}\mathbf{R}_{vv}^{-1}\mathbf{H}_M\mathbf{F}_0)^{-1}(\mathbf{B}_0 + \mathbf{I})^{\text{H}}\right|^{1/N} && \text{(A.26)} \\ &= \left|\mathbf{I} + \mathbf{F}_0^{\text{H}}\mathbf{H}_M^{\text{H}}\mathbf{R}_{vv}^{-1}\mathbf{H}_M\mathbf{F}_0\right|^{-1/N} \, . && \text{(A.27)} \end{aligned}$$

Therefore the problem of minimising the lower bound of the system MSE is equivalent to the problem of maximising the value of $\left|\mathbf{I} + \mathbf{F}_0^{\text{H}}\mathbf{H}_M^{\text{H}}\mathbf{R}_{vv}^{-1}\mathbf{H}_M\mathbf{F}_0\right|$, which represents the mutual information of the system with Gaussian input, subject to the transmit power constraint. This requires that the singular values of the precoder matrix $\mathbf{F}_0$ [2] are derived from a water-filling algorithm with single water level which

[2]The precoder matrix $\mathbf{F}_0$ is assumed to have the form $\mathbf{F}_0 = \mathbf{V}_q \begin{bmatrix} \mathbf{\Phi} & \mathbf{0}_{q\times(N-q)} \end{bmatrix} \mathbf{U}_F$ where $\mathbf{V}_q$ contains q first columns of $\mathbf{V}$ in (A.9), $\mathbf{\Phi}$ is a $q \times q$ diagonal matrix and $\mathbf{U}_F$ is an $N \times N$ unitary matrix.

is applied to the diagonal elements of $\mathbf{\Lambda}$ as in (A.9). Thus the singular values of $\mathbf{F}_0$ belong to a $q \times q$ diagonal matrix $\mathbf{\Phi}$ and are given by

$$|\phi_{ii}|^2 = \frac{P_0 + \sum_{j=1}^{q} \frac{1}{\lambda_{jj}}}{q} - \frac{1}{\lambda_{ii}} \quad , \tag{A.28}$$

whereby $q = \min\{\bar{N}, N\}$, and $\bar{N}$ is the maximum integer satisfying

$$\frac{1}{\lambda_{\bar{N}\bar{N}}} < \frac{P_0 + \sum_{j=1}^{\bar{N}} \frac{1}{\lambda_{jj}}}{\bar{N}} \, . \tag{A.29}$$

With the singular values of the precoder matrix described above, the inequality (A.26) can be re-written as

$$\frac{\text{trace}(\mathbf{R}_{ee})}{N} \geq q^{q/N} \left(P_0 + \sum_{j=1}^{q} \frac{1}{\lambda_{jj}} \right)^{-q/N} \prod_{i=1}^{q} \lambda_{ii}^{-1/N} \, . \tag{A.30}$$

For the system MSE to achieve its lower bound, it is required that $\mathbf{R}_{ee} = \alpha \mathbf{I}$ for some $\alpha > 0$. Thus similar to the case of ZF design, the right-singular vectors of the precoder matrix $\mathbf{F}_0$ must be the columns of the matrix $\mathbf{\Theta}$ which is a unitary matrix derived from the following geometric mean decomposition [31]

$$\left(\mathbf{I}_N + \mathbf{\Phi}'^T \mathbf{\Lambda}_q \mathbf{\Phi}' \right)^{1/2} = \mathbf{U}\mathbf{R}\mathbf{\Theta}^{\text{H}} \tag{A.31}$$

whereby $\mathbf{\Phi}' = [\mathbf{\Phi} \quad \mathbf{0}_{q \times (N-q)}]$, $\mathbf{\Lambda}_q$ is the upper left $q \times q$ block of $\mathbf{\Lambda}$ in (A.9), $\mathbf{U}$ is a unitary and $\mathbf{R}$ an upper-triangular matrix with equal diagonal elements.

The optimal precoder that helps to minimise the MSE lower bound and to achieve that bound is then given by

$$\mathbf{F}_0 = \mathbf{V}_q \mathbf{\Phi}' \mathbf{\Theta} \, , \tag{A.32}$$

where matrix $\mathbf{V}_q$ contains the first columns of $\mathbf{V}$.

The feedback filter bank that helps to achieve the minimised MSE lower bound under the MMSE criterion is given by

$$\mathbf{B}_0 = \mathbf{R} - \mathbf{I} \tag{A.33}$$

and the feedforward filter bank under the MMSE criterion is given by

$$\mathbf{W}_0 = \sigma_e \mathbf{R}\mathbf{R}_{sy}\mathbf{R}_{yy}^{-1} \tag{A.34}$$

where

$$\sigma_e^2 = q^{q/N}\left(P_0 + \sum_{j=1}^{q}\frac{1}{\lambda_{jj}}\right)^{-q/N}\prod_{j=1}^{q}\lambda_{jj}^{-1/N} \quad . \tag{A.35}$$

List of Figures

Glossary

3G-LTE	3rd generation long term evolution
BDFE	block decision feedback equaliser/equalisation
BER	bit error rate
BEVD	broadband eigenvalue decomposition
BPSK	binary phase shift keying
BSVD	broadband singularvalue decomposition
CCI	co-channel interference
CIR	channel impulse response
CSI	channel state information
CSIR	channel state information at the receiver
CSIT	channel state information at the transmitter
DFE	decision feedback equaliser
DOF	degree of freedom
EVD	eigenvalue decomposition
FDD	frequency division duplex
FIR	finite impulse response
FS	frequency selective
ISI	inter-symbol interference
IBI	inter-block interference
LPE-DFE	combined linear precoding and equalisation with DFE
LPE-SGI	linear precoding and equalisation with shared guard interval
LZ	leading zero

MaxIR	maximum information rate
MaxSNR	maximum output SNR
MIMO	multi-input multi-output
MJPR	modified joint optimal precoder
MMSE	minimum mean square error
MMSE/CP	minimum mean square error under constrained transmit power
MLP	modified linear precoder
MSE	mean square error
MUI	multiuser interference
QAM	quadrature amplitude modulation
QPSK	quadrature phase shift keying
OFDM	orthogonal frequency-division multiplexing
QoS	quality of service
SBR2	second order sequential best rotation algorithm
SNR	signal-to-noise ratio
SVD	singular value decomposition
TDD	time division duplex
TZ	trailing zero
ZF	zero-forcing

Mathematical Notations

General Notations

h	scalar quantity
$\mathbf{h}$ or $\underline{H}$	vector quantity
$\mathbf{H}$	matrix quantity
$h(t)$	function of a continuous variable t
$h[n]$	function of a discrete variable n
$H(e^{j\omega})$	periodic Fourier spectrum of a discrete function $h[n]$
$H(z)$	z-transform of a discrete function $h[n]$

Relations and Operators

$\bullet\!\!-\!\!\circ$	transform pair, e.g. $h[n] \bullet\!\!-\!\!\circ H(e^{j\Omega})$ or $h[n] \bullet\!\!-\!\!\circ H(z)$
$(\cdot)^*$	complex conjugate
$(\cdot)^H$	Hermitian (conjugate transpose)
$\tilde{(\cdot)}$	Parahermitian ($\tilde{\mathbf{A}}(z) = \mathbf{A}^{\mathrm{H}}(z^{-1})$)
$(\cdot)^T$	transpose
$(\cdot)^+$	pseudo-inversion
$\mathcal{E}\{\cdot\}$	expectation operator
$\lceil\cdot\rceil$	ceiling operator
$\lfloor\cdot\rfloor$	flooring operator
$\lvert\mathbf{A}\rvert$	determinant of $\mathbf{A}$

$\|\mathbf{A}\|_F$	Frobenius norm of $\mathbf{A}$
$\text{diag}(\cdot)$	diagonal matrix with as diagonal elements equal to $(\cdot)$
$\max(\cdot)$	select the maximum value
$\text{trace}(\cdot)$	trace of a matrix
$\text{rank}(\mathbf{A})$	rank of $\mathbf{A}$ (number of linearly independent rows)

Sets and Spaces

$\mathbb{C}$	set of complex numbers
$\mathbb{C}^{M\times N}$	set of $M \times N$ matrices with complex entries
$\mathbb{R}$	set of real numbers
$\mathbb{R}^{M\times N}$	set of $M \times N$ matrices with real entries
$\mathbb{Z}$	set of integers

Symbols and Variables

$\mathbf{\Gamma}$	majorised diagonal matrix
λ	eigenvalue
Ω or ω	(angular) frequency
σ^2	variance
τ	delay / lag
$\mathbf{C}(z)$	MIMO channel matrix
$\mathbf{H}(z)$	time-multiplexed MIMO channel matrix
$\mathbf{R}(z)$	para-Hermitian matrix
$\mathbf{I}$	identity matrix
L	channel order
P	number of polyphase components
R	number of receive antennas
T	number of transmit antennas

Bibliography

[1] T. Virki, "Global cellphone penetration reaches 50 pct," Reuters, November 2006, available online at http://investing.reuters.co.uk/news.

[2] Qi Bi, G.L. Zysman, and H. Menkes, "Wireless Mobile Communications at the Start of the 21st Century," *IEEE Communications Magazine*, vol. 39, no. 1, pp. 110 – 116, January 2001.

[3] A.J. Paulraj, D.A. Gore, R.U. Nabar, and H. Bolcskei, "An overview of MIMO communications - A key to gigabit wireless," *Proceedings of the IEEE*, vol. 92, no. 2, pp. 198 – 218, 2 2004.

[4] J. H. Winters, "Optimum combining in digital mobile radio with cochannel interference," *IEEE Journal on Selected Areas in Communications*, vol. 2, no. 4, pp. 528–539, July 1984.

[5] A. Wittneben, "A new bandwith efficient transmit antenna modulation diversity scheme for linear digital modulation," in *Proc. IEEE International Conference on Communications*, Geneva, Switzerland, May 1993, pp. 1630–1634.

[6] P.B. Wong and D.C. Cox, "Low-complexity diversity combining algorithms and circuit architectures for co-channel interference cancellation and frequency-selective fading mitigation," *IEEE Transactions on Communications*, vol. 44, no. 9, pp. 1107–1116, September 1996.

[7] A.J. Paulraj and C.B. Papadias, "Space-time processing for wireless communications," *IEEE Signal Processing Magazine*, vol. 14, no. 6, pp. 49 – 83, Novermber 1997.

[8] S. M. Alamouti, "A Simple Transmit Diversity Technique for Wireless Communications," *IEEE Journal on Selected Areas in Communications*, vol. 16, no. 8, pp. 1451 – 1458, October 1998.

[9] V. Tarokh, N. Shesadri, and A. R. Calderbank, "Space-time Codes for High Data Rate Wireless Communications: Performance Criterion and Code Construction," *IEEE Transactions on Information Theory*, vol. 44, no. 2, pp. 744–765, March 1998.

[10] H. Bölcskei and A.J. Paulraj, "Multiple-Input Multiple-Output (MIMO) Wireless Systems," in *The Communications Handbook*, 2nd Edition, J. Gibson, Ed. CRC Press, 2002, pp. 90.1–90.14.

[11] K. Higuchi and H. Taoka, "Field Experiments of 2.5 Gbit/s High-Speed Packet Transmission Using MIMO OFDM Broadband Packet Radio Access," *NTT DoCoMo Technical Journal*, vol. 8, no. 1, pp. 19–24, Jun 2006.

[12] K. Higuchi and H. Taoka, "Field Experiment on 5-Gbit/s Ultra-High-Speed Packet Transmission Using MIMO Multiplexing in Broadband Packet Radio Access," *NTT DoCoMo Technical Journal*, vol. 9, no. 2, Sep 2007.

[13] R. Janaswamy, "Spatial Diversity for Wireless Communications," in *Handbook of Antennas in Wireless Communications*, L.C. Godara, Ed. CRC Press, 2001.

[14] L. C. Godara, "Application of Antenna Arrays to Mobile Communications, Part II: Beam-Forming and Direction-of-Arrival Estimation," *Proceedings of the IEEE*, vol. 85, no. 8, pp. 1195–1245, August 1997.

[15] L. C. Godara, "Application of Antenna Arrays to Mobile Communications, Part I: Performance Improvement, Feasibility, and System Considerations," *Proceedings of the IEEE*, vol. 85, no. 7, pp. 1031–1060, July 1997.

[16] V. Tarokh, H. Jafarkhani, and A. R. Calderbank, "Space-Time Block Codes from Orthogonal Designs," *IEEE Transactions on Information Theory*, vol. 45, no. 5, pp. 1456–1467, July 1999.

[17] Mohinder Jankiraman, *Space-Time Codes and MIMO Systems*, Artech House, 2004.

[18] V. Tarokh, H. Jafarkhani, and A. R. Calderbank, "Space-Time Block Coding For Wireless Communications: Performance Results," *IEEE Journal on Selected Areas in Communications*, vol. 17, no. 3, pp. 451–460, March 1999.

[19] S. Sandhu and A. Paulraj, "Space-time block codes: a capacity perspective," *IEEE Communications Letters*, vol. 4, no. 12, pp. 384–386, December 2000.

[20] D. Wubben, R. Bohnke, V. Kuhn, and K.-D. Kammeyer, "Near-maximum-likelihood detection of MIMO systems using MMSE-based lattice reduction," in *Proc. IEEE International Conference on Communications*, Paris, France, June 2004, vol. 2, pp. 798–802.

[21] G. J. Foschini, "Layered Space-Time Architecture for Wireless Communication in a Fading Environment when using Multi-Element Antennas," *Bell Labs Technical Journal*, vol. 1, no. 2, pp. 41–59, 1996.

[22] G.J. Foschini, G.D. Golden, R.A. Valenzuela, and P.W. Wolniansky, "Simplified Processing for High Spectral Efficiency Wireless Communication Employing Multi-Element Arrays," *IEEE Journal on Selected Areas in Communications*, vol. 17, no. 11, pp. 1841–1852, November 1999.

[23] G.D. Golden, C.J. Foschini, R.A. Valenzuela, and P.W. Wolniansky, "Detection algorithm and initial laboratory results using V-BLAST," *Electronics Letters*, vol. 35, no. 1, pp. 14–15, 1999.

[24] H. Sampath, P. Stoica, and A. Paulraj, "Generalized Linear Precoder and Decoder Design for MIMO Channels Using the Weighted MMSE Criterion," *IEEE Transactions on Communications*, vol. 49, no. 12, pp. 2198–2206, December 2001.

[25] A. Scaglione, P. Stoica, S. Barbarossa, G. B. Giannakis, and H. Sampath, "Optimal designs for space-time linear precoders and decoders," *IEEE Transactions on Signal Processing*, vol. 50, no. 5, pp. 1051–1064, 2002.

[26] A. Scaglione, G. B. Giannakis, and S. Barbarossa, "Redundant Filterbank Precoders and Equalizers Part I: Unification and Optimal Designs," *IEEE Transactions on Signal Processing*, vol. 47, no. 7, pp. 1988–2006, 1999.

[27] A. Scaglione, S. Barbarossa, and G. B. Giannakis, "Filterbank transceivers optimizing information rate in block transmissions over dispersive channels," *IEEE Transactions on Information Theory*, vol. 45, no. 3, pp. 1019–1032, 1999.

[28] D.P. Palomar, M. Bengtsson, and B. Ottersten, "Minimum BER linear transceivers for MIMO channels via primal decomposition," *IEEE Transactions on Signal Processing*, vol. 53, no. 8, pp. 2866 – 2882, August 2005.

[29] Y. Ding, T.N. Davidson, Z.-Q. Luo, and K.M. Wong, "Minimum BER block precoders for zero-forcing equalization," *IEEE Transactions on Signal Processing*, vol. 51, no. 9, pp. 2410 – 2423, September 2003.

[30] J.-K. Zhang, A. Kavcic, and K. M. Wong, "Equal-diagonal QR decomposition and its application to precoder design for successive-cancellation detection," *IEEE Transactions on Information Theory*, vol. 51, no. 1, pp. 154–172, January 2005.

[31] Y. Jiang, J. Li, and W. W. Hager, "Joint Transceiver Design for MIMO Communications Using Geometric Mean Decomposition," *IEEE Transactions on Signal Processing*, vol. 53, no. 10, pp. 3791–3803, October 2005.

[32] F. Xu, N. T. Davidson, J. K. Zhang, and K. M. Wong, "Design of Block Transceivers With Decision Feedback Detection," *IEEE Transactions on Signal Processing*, vol. 54, no. 3, pp. 965–978, March 2006.

[33] M. Vu and A. Paulraj, "MIMO Wireless Linear Precoding," *IEEE Signal Processing Magazine*, vol. 24, no. 5, pp. 86–105, September 2007.

[34] C. H. Ta and S. Weiss, "Design of Precoding and Equalization for Broadband MIMO Transmission," in *Proc. 2nd IEE/EURASIP Conference on DSPenabledRadio*, Southampton, UK, September 2005.

[35] C. H. Ta and S. Weiss, "A Design of Precoding and Equalisation for Broadband MIMO Systems," in *Proc. 15th International Conference on Digital Signal Processing*, Cardiff, UK, July 2007.

[36] C. H. Ta and S. Weiss, "A Design of Precoding and Equalisation for Broadband MIMO Systems," in *Proc. 41st Asilomar Conference on Signals, Systems, and Computers*, Pacific Grove, CA, November 2007.

[37] C. H. Ta and S. Weiss, "A Jointly Optimal Precoder and Block Decision Feedback Equaliser Design with Low Redundancy," in *Proc. 15th European Signal Processing Conference (EUSIPCO)*, Poznan, Poland, September 2007.

[38] C. H. Ta, C. Liu, and S. Weiss, "An Approach for Block Transmission based Precoding and Equalisation with Improved Performance," in *Proc. 12th IEEE International Symposium on Power Line Communications and Its Applications (ISPLC)*, Jeju, Korea, April 2008.

[39] C. H. Ta and S. Weiss, "Shortening the Order of Paraunitary Matrices in SBR2 Algorithm," in *Proc. 6th International Conference on Information, Communications & Signal Processing*, Singapore, December 2007.

[40] T.M. Cover and J.A. Thomas, *Elements of Information Theory*, Wiley, New-Jersey, 2nd edition, 2006.

[41] C. Peel, Q. Spencer, A.L. Swindlehurst, and B. Hochwald, "Downlink transmit beamforming in multi-user MIMO systems," in *IEEE Sensor Array and Multichannel Signal Processing Workshop Proceedings*, Sitges, Spain, July 2004, vol. 1, pp. 43–51.

[42] Q. H. Spencer, A. L. Swindlehurst, and M. Haardt, "Zero-forcing methods for downlink spatial multiplexing in multiuser MIMO channels," *IEEE Transactions on Signal Processing*, vol. 52, no. 2, pp. 461–471, February 2004.

[43] G. J. Foschini and M. Gans, "On Limits of Wireless Communications in a Fading Environment when Using Multiple Antennas," *Wireless Personal Communications*, vol. 6, pp. 311–335, 1998.

[44] I. E. Telatar, "Capacity of Multi-Antenna Gaussian Channels," *European Transactions on Telecommunications*, vol. 10, no. 6, pp. 585–595, November 1999.

[45] A. Goldsmith, S. A. Jafar, N. Jindan, and S. Vishwanath, "Capacity limits of MIMO channels," *IEEE Journal on Selected Areas in Communications*, vol. 21, no. 5, pp. 684–702, 2003.

[46] H. Jafarkhani, *Space-Time Coding: Theory and Practice*, Cambridge University Press, New York, 2005.

[47] P. W. Wolniansky, G. J. Foschini, G. D. Golden, and R. A. Valenzuela, "V-BLAST: An Architecture for Realizing Very High Data Rates over The Rich-

Scattering Wireless Channel," in *Proc. URSI International Symposium on Signals, Systems and Electronics Conference*, New York, 1998, pp. 295–300.

[48] N. Al-Dhahir and A.H. Sayed, "The Finite-Length Multi-Input Multi-Output MMSE-DFE," *IEEE Transactions on Signal Processing*, vol. 48, no. 10, pp. 2921–2936, October 2000.

[49] X. Zhu and R. D. Murch, "Layered Space-Time Equalization for Wireless MIMO Systems," *IEEE Transactions on Wireless Communications*, vol. 2, no. 6, pp. 1189–1203, November 2003.

[50] K. D. Rao, "Equalization of a MIMO Channel Using FIR Inverses," *IEEE Transactions on Signal Processing*, vol. 54, no. 7, pp. 2844 – 2848, July 2006.

[51] J. Yang and S. Roy, "Joint Transmitter-Receiver Optimization for Multi-Input Multi-Output Systems with Decision Feedback," *IEEE Transactions on Information Theory*, vol. 40, no. 5, pp. 1334–1347, September 1994.

[52] J. Yang and S. Roy, "On Joint Transmitter and Receiver Optimization for Multiple-Input Multiple-Output (MIMO) Transmission Systems," *IEEE Transactions on Communications*, vol. 42, no. 12, pp. 3221–3231, December 1994.

[53] D.P. Palomar, J.M. Cioffi, and M.A. Lagunas, "Joint Tx-Rx beamforming design for multicarrier MIMO channels: a unified framework for convex optimization," *IEEE Transactions on Signal Processing*, vol. 51, no. 9, pp. 2381 – 2401, September 2003.

[54] A. Hjørungnes, Marcello L. R. de Campos, and Paulo S. R. Diniz, "Jointly Optimized Transmitter and Receiver FIR MIMO Filters in the Presence of Near-End Crosstalk," *IEEE Transactions on Signal Processing*, vol. 53, no. 1, pp. 346–359, January 2005.

[55] K. C. Hwang and K. B. Lee, "Joint Transmit and Receiver Filters Design for Multiple-Input Multiple-Output (MIMO) Systems," *IEEE Transactions on Wireless Communications*, vol. 4, no. 4, pp. 1635–1649, July 2005.

[56] A. Yasotharan, "Multirate Zero-Forcing Tx-Rx Design for MIMO Channel Under BER Constraints," *IEEE Transactions on Signal Processing*, vol. 54, no. 6, pp. 2288–2301, June 2006.

[57] J. G. McWhirter, P. D. Baxter, T. Cooper, S. Redif, and J. Foster, "An EVD Algorithm for Para-Hermitian Polynomial Matrices," *IEEE Transactions on Signal Processing*, vol. 55, no. 5, pp. 2158–2169, May 2007.

[58] J. G. McWhirter and P. D. Baxter, "A Novel Technique for Broadband SVD," in *12th Annual Workshop on Adaptive Sensor Array Processing*, MIT Lincoln Labs, Cambridge, MA, March 2004.

[59] S. Redif and T. Cooper, "Paraunitary Filter Bank Design via a Polynomial Singular Value Decomposition," in *Proc. IEEE International Conference on Acoustics, Speech, and Signal Processing*, Philadelphia, PA, March 2005, vol. IV, pp. 613 – 616.

[60] P. P. Vaidyanathan, "Theory of Optimal Orthonormal Subband Coders," *IEEE Transactions on Signal Processing*, vol. 46, no. 6, pp. 1528–1543, June 1998.

[61] A. Saleh and R. Valenzuela, "A statistical model for indoor multipath propagation," *IEEE Journal on Selected Areas in Communications*, vol. 5, no. 2, pp. 128–137, February 1987.

[62] W. Shi, *Frequency Division Multiple Access using Spectrally Overlapping Signals*, Ph.D. thesis, Churchill College, University of Cambridge, 2003.

[63] H. Mohamad, *Subband Adaptive Equalisation for Communication Transceivers*, Ph.D. thesis, School of Electronics and Computer Science, University of Southampton, 2003.

[64] C. Tibenderana, *A High-Performance, Efficient, and Reliable Receiver for Bluetooth Signals*, Ph.D. thesis, School of Electronics and Computer Science, University of Southampton, 2005.

[65] P. J. W. Melsa, R. C. Younce, and C. E. Rohrs, "Impulse Response Shortening for Discrete Multitone Transceivers," *IEEE Transactions on Communications*, vol. 44, no. 12, pp. 1662–1672, December 1996.

[66] C. Toker, S. Lambotharan, and J.A. Chambers, "Joint Transceiver Design for MIMO Channel Shortening," *IEEE Transactions on Signal Processing*, vol. 55, no. 7, pp. 3851–3866, July 2007.

[67] A. Mertins, "MMSE Design of Redundant FIR Precoders for Arbitrary Channel Lengths," *IEEE Transactions on Signal Processing*, vol. 51, no. 9, pp. 2402–2409, September 2003.

[68] A. Stamoulis, G. B. Giannakis, and A. Scaglione, "Block FIR Decision-Feedback Equalizers for Filterbank Precoded Transmission with Blind Channel Estimation Capabilities," *IEEE Transactions on Communications*, vol. 49, no. 1, pp. 69–83, January 2001.

[69] Z. Wang and G. B. Giannakis, "Wireless Multicarrier Communications: Where Fourier Meets Shannon," *IEEE Signal Processing Magazine*, vol. 17, no. 3, pp. 29–48, May 2000.

[70] K. Takeda, H. Tomeba, and F. Adachi, "Single-Carrier Transmission with Joint Tomlinson-Harashima Precoding and Frequency-Domain Equalization," in *Proc. 3rd IEEE VTS Asia Pacific Wireless Communications Symposium*, Daejon, Korea, August 2006.

[71] Y. P. Lin and S. M. Phoong, "Minimum Redundancy for ISI Free FIR Filterbank Transceivers," *IEEE Transactions on Signal Processing*, vol. 50, no. 4, pp. 842–853, April 2002.

[72] S. Weiss, S. Redif, T. Cooper, C. Liu, P. D. Baxter, and J. G. McWhirter, "Paraunitary Oversampled Filter Bank Design for Channel Coding," *EURASIP Journal on Applied Signal Processing*, vol. 2006, no. 1, January 2006.

[73] M. Davies, S. Lambotharan, J.A. Chambers, and J.G. McWhirter, "Broadband MIMO Beamforming for Frequency Selective Channels using the Sequential Best Rotation Algorithm," in *Proc. 67th IEEE Vehicular Technology Conference (VTC Spring 2008)*, 2008, pp. 1147–1151.

[74] J. Foster, J.G. McWhirter, and J. Chambers, "Limiting the Order of Polynomial Matrices Within the SBR2 Algorithm," in *IMA International Conference on Mathematics in Signal Processing*, Cirencester, UK, December 2006.

[75] M. Bengtsson and B. Ottersten, "Optimal and Suboptimal Transmit Beamforming," in *Handbook of Antennas in Wireless Communications*, L.C. Godara, Ed. CRC Press, 2001.

[76] H. Ekstrom, A. Furuskar, J. Karlsson, M. Meyer, S. Parkvall, J. Torsner, and M. Wahlqvist, "Technical solutions for the 3G long-term evolution," *IEEE Communications Magazine*, vol. 44, no. 3, pp. 38 – 45, March 2006.

[77] D. P. Palomar, *A Unified Framework for Communications through MIMO Channels*, Ph.D. thesis, Technical University of Catalonia (UPC), Barcelona, Spain, 2003.

[78] A. Pascual-Iserte, D.P. Palomar, A.I. Perez-Neira, and M.A. Lagunas, "A Robust Maximin Approach for MIMO Communications With Imperfect Channel State Information Based on Convex Optimization," *IEEE Transactions on Signal Processing*, vol. 54, no. 1, pp. 346 – 360, January 2006.

[79] M. Tomlinson, "A new automatic equalizer employing modulo arithmetic," *IEE Electronics Letters*, vol. 7, pp. 138–139, March 1971.

[80] H. Harashima and H. Miyakawa, "matched transmission technique for channel with intersymbol interference," *IEEE Transactions on Communications*, vol. COM-20, pp. 774–780, June 1972.

[81] M. Joham, D.A. Schmidt, J. Brehmer, and W. Utschick, "Finite-Length MMSE TomlinsonHarashima Precoding for Frequency Selective Vector Channels," *IEEE Transactions on Signal Processing*, vol. 55, no. 6, pp. 3073–3088, June 2007.

[82] F. Labeau, J. C. Chiang, M. Kieffer, P. Duhamel, L. Vandendorpe, and B. Macq, "Oversampled Filter Banks as Error Correcting Codes: Theory and Impulse Noise Correction," *IEEE Transactions on Signal Processing*, vol. 53, no. 12, pp. 4619–4630, December 2005.

[83] S. Weiss, C. H. Ta, and C. Liu, "A Wiener Filter Approach to the Design of Filter Bank Based Sigle-Carrier Precoding and Equalisation," in *Proc. IEEE International Symposium on Powerline Communications and Its Applications*, Pisa, Italy, March 2007.

[84] R. A. Horn and C. R. Johnson, *Matrix Analysis*, Cambridge University Press, Cambridge, UK, 1985.